Mitt. Österr. Geol. Ges.	ISSN 0251-7493	**90** (1997)	83-125	Wien, Dezember 1999

Keywords
Mongolia
continental sediments
Cenozoic
rodents
basalts
age dating

Oligocene-Miocene sediments, fossils and basalts from the Valley of Lakes (Central Mongolia) – An integrated study.

HÖCK, V.[1], DAXNER-HÖCK, G.[2], SCHMID, H. P.[3], BADAMGARAV, D.[5], FRANK, W.[4], FURTMÜLLER, G.[1a], MONTAG, O.[1], BARSBOLD, R.[5], KHAND, Y.[5], SODOV, J[5].

with 22 Figures, 4 Tables and 4 Supplements

Content

Address of the authors

[1] Inst. Geol. Pal., Univ. Salzburg, Hellbrunnerstr. 34, A-5020 Salzburg, Austria
[1a] Present address: Inst. Eng. Geology, Univ. Technol., Vienna, Karlsplatz 13, A-1040, Vienna, Austria
[2] Dept. Geol. Pal., Museum of Natural History, Vienna; Burgring 7, A-1014, Vienna, Austria
[3] Inst. Petrology, Univ. Vienna, Geozentrum, Althanstr. 14, A-1090 Vienna, Austria
[4] Inst. Geology, Univ. Vienna, Geozentrum, Althanstr. 14, A-1090 Vienna, Austria
[5] Paleontological Center, Mongolian Academy Sci., Ulaan Baatar, Mongolia

Oligozäne bis miozäne Sedimente, Fossilien und Basalte aus dem Tal der Seen (Zentrale Mongolei) – Eine integrative Studie.

Zusammenfassung

In der zentralen Mongolei wurde im „Tal der Seen" eine interdisziplinäre geowissenschaftliche Studie durchgeführt, die paläontologische Untersuchungen in kontinentalen Sedimenten, Sedimentologie, geologische Kartierung, das Studium der Petrologie und Geochemie der Basalte, die mit diesen Sedimenten wechsellagern, sowie deren Altersdatierung zum Inhalt hatte. Ziel der Studie war es, auf der Basis von Lithostratigraphie, Biostratigraphie und Geochronologie ein gesamtstratigraphisches Konzept zu entwerfen. Das Arbeitsgebiet liegt in einem ungefähr NW-SE bzw. NNW-SSE quer durch die Mongolei streichenden Korridor, in dem unter anderem paläogene und neogene Basalte, die als chronostratigraphische Marker fungieren, mit kontinentalen Sedimenten wechsellagern.

Diese Arbeit führte zu einer Neudefinition bisher benutzter lithostratigraphischer Begriffe, die formal eingeführt und verwendet werden. Die tiefste Einheit wird Tsagaan Ovoo-Formation genannt. Die darüberliegende Hsanda Gol-Formation wird auf ziegelrote Tone und Silte beschränkt. In dieser Formation liegt Basalt I. Hingegen wird die Loh-Formation über ihren bisherigen Geltungsbereich ausgeweitet und enthält alle klastischen Sedimente im Hangenden der Hsanda Gol-Formation. Die Basalte II und III liegen in der Loh-Formation. Auch wenn Basalt III häufig die höchste Lage der Loh-Formation bildet, reicht ihre stratigraphische Reichweite an manchen Stellen darüber hinaus.

Die Tsagaan Ovoo-Formation und die Loh-Formation beinhalten im wesentlichen fluviale Sedimente, die Hsanda Gol-Formation äolische. Die tiefere Tsagaan Ovoo-Formation zeigt Übergänge zwischen einem „debris flow dominated fan" und einem „braided fluvial fan", die höhere Tsagaan Ovoo-Formation hat nur Anzeichen des letzteren. Die Hsanda Gol-Formation besteht aus äolischen Ablagerungen mit gelegentlichen Linsen fluvialer und lakustriner Sedimente. Seichte Playas dürften bei der Bildung der Hsanda Gol Sedimente existiert haben. Die Loh-Formation hingegen kann als Übergang zwischen einem „braided fluvial fan" und einem „low sinuosity/meandering fluvial fan" betrachtet werden und beinhaltet Linsen und Lagen äolischer Silte. Das Klima dürfte während der Ablagerung der Loh-Formation etwas feuchter gewesen sein.

Alle drei Basaltlagen zeigen in ihrer Geochemie einen klaren Intraplattencharakter und stimmen recht gut mit Ozean Insel Basalten überein. Trotzdem sind signifikante geochemische und mineralogische Unterschiede zwischen Basalt I und II auf der einen Seite und Basalt III auf der anderen erkennbar. Das Vorkommen der Basalte gibt wichtige Hinweise auf das Alter der lithostratigraphischen Einheiten. $^{40}Ar/^{39}Ar$ Alter zeigen, daß die Basalte I um 31.5 Mio. Jahren, d. i. im Frühen Oligozän eruptierten. Basalt II stammt mit einem Alter von 27-28 Mio. Jahren aus dem Späten Oligozän und die Platznahme von Basalt III erfolgte im Mittleren Miozän zwischen 12.5 und 13 Mio. Jahren.

In der Mongolei wurden innerhalb der Hsanda Gol- und der Loh Formation sieben Biozonen (A, B, C, C1, D, D1, E) unterschieden. Sie sind durch bestimmte Nagetier-Arten charakterisiert und bilden von A bis E eine chronologische Abfolge. Ihr Alter wird durch ihre Lage zu den Basalten I bis III eingegrenzt. Nagetiere der Biozonen A und B finden sich in Hsanda Gol-Sedimenten im Liegenden und Hangenden von Basalt I. Das Alter ist Unter-Oligozän. Charakteristische Nagetiere der Biozonen C und C1 kommen in höheren Sedimenten der Hsanda Gol Formation und in Sedimenten der Loh Formation im unmittelbaren Liegenden und Hangenden von Basalt II vor. Das Alter ist Ober-Oligozän. Nagetiere der Biozonen D, D1 und E wurden ausschließlich innerhalb der Loh Formation vorgefunden. Fossilien der Biozone D1 kommen nur im Liegenden von Basalt III vor. Das Alter ist damit auf das Unter-Mittel-Miozän eingegrenzt. Die mongolischen Biozonen A und B können mit dem chinesischen Säugetier-Alter Ulantatalium und der Buran Svita in Kasachstan korreliert werden. Die Biozonen C und C1 werden mit dem Tabenbulukium in China korreliert. Fossilien der Biozonen C und C1 lassen eine vorläufige Korrelation mit der Altyn Chokysu Fauna von Kasachstan zu. Die Biozone D korreliert mit Teilen des chinesischen Xiejium, D1 mit Teilen des Shanwangium and Tunggurium, und E mit dem mittleren Baodium.

Abstract

An interdisciplinary study was carried out in the Valley of Lakes in Central Mongolia including paleontological investigations in continental sediments, sedimentology, geological mapping, petrological-geochemical studies of basalts interlayered with the sediments, and the accompanying age dating. The aim was to establish a stratigraphic concept by means of lithostratigraphy, biostratigraphy and geochronologic data. The study area was chosen in an approximately NW-SE to NNW-SSE striking corridor in which Paleogene and Neogene basalts, serving as chronostratigraphic markers, are interlayered with continental sediments.

This study led to the redefinition of hitherto used lithostratigraphic terms which were now formally established. The deepest unit was termed the Tsagaan Ovoo Formation. The overlying Hsanda Gol Formation is restricted to coherent red clays and silts. It contains basalt layer I. The Loh Formation in turn is extended to sometimes varied coarse-grained sediments above the Hsanda Gol silts and clays. It is interlayered in its lower part by basalt II and topped in some areas by basalt III. Nevertheless, the sedimentation of the Loh Formation reaches beyond basalt III.

The Tsagaan Ovoo and the Loh Formation reflect essentially fluvial deposits, whereas the Hsanda Gol Formation is primarily of aeolian origin. The lower Tsagaan Ovoo Fm. is transitional in its features between a debris-flow dominated fan and a braided fluvial fan, the upper part having characteristics of the latter only. The Hsanda Gol Fm. contains aeolian deposits with locally fluvial and lacustrine sediments as well as shallow playas. The Loh Fm. in turn is best described as a fan that is transitional between a braided fluvial fan and a low sinuosity/meandering fluvial fan interfingering with aeolian sediments. The climate was apparently more humid during the deposition of the Loh Formation.

All three basalt layers are typical intraplate basalts and show in their geochemical composition a fair agreement with Ocean-Island basalts. Nevertheless, there are significant geochemical differences between basalt I and II on one hand and basalt III on the other. The occurrence of basalt layers poses important time constraints on the lithostratigraphic formations. $^{40}Ar/^{39}Ar$ whole rock data showed that basalt I erupted around 31.5 Ma, i. e. Early Oligocene. Basalt II erupted in the Late Oligocene between 27 and 28 Ma. Basalt III, finally, was emplaced in the Middle Miocene between 12.5 and 13 Ma.

In Mongolia seven informal biozones (A, B, C, C1, D, D1, E) were established throughout the Hsanda Gol and Loh Formations. They are characterized by certain rodent species and represent from A to E a chronological sequence. The ages are controlled by the basalts I to III. Rodents of biozones A and B were recovered within the Hsanda Gol sediments below and above basalt I and are therefore of Early Oligocene age. Rodents which characterize the biozones C and C1 were found in Hsanda Gol sediments and in Loh sediments immediately below and above basalt II. The age is Late Oligocene. Rodents of biozone D, D1 and E are situated exclusively in Loh sediments. There is no age control by basalts for biozone D. Fossils indicating biozone D1 were recovered below basalt III; the age is Early to Middle Miocene. Based on characteristic rodents the biozones A and B are correlative with the Chinese mammal age Ulantatalian and the Buran Svita in Kasachstan. The biozones C and C1 can be correlated with parts of the Chinese Tabenbulukian. A tentative correlation with the Altyn Chokysu fauna from Kasachstan and fossils indicating the biozones C and C1 is possible. Biozone D correlates with parts of the Chinese Xiejian, D1 with parts of the Chinese Shanwangian and Tunggurian, and E with the middle part of the Chinese Baodean.

1. Introduction

Mongolia is not only a mountainous country, but also partly a highland with smooth topography. The elevation of most of the country is above 1000 m. In Western and Central Mongolia the prominent physiographic features are the Altai Mtns. in the W, SW and S (separated into the Mongolian Altai and the Gobi Altai) and the Khangai Mtns. in the north. Both mountain ranges are separated by a series of large depressions, the northwestern "Valley of Great Lakes" and the southeastern "Valley of Lakes" (BALJINNYAM et al. 1993). Their elevation ranges from 1000 to 1500 m.

The first comprehensive geological description of these depressions were already published in 1901 by E. SUESS (cum lit. cit.). His outline was mainly based on the reports by Obrutschew and Klemenz (see cit. in SUESS 1901). Among the first geoscientists doing systematic geological research such as mapping, describing, grouping and classifying the rocks within the Valley of Lakes were the geologists and paleontologists of the "Third Asiatic Expedition" of the American Museum of Natural History led by R. Ch. Andrews. Among many other places this group worked in the Tatal Gol and the Taatsiin-Tsagaan Noor area and called the same region "Mt. Uskuk-Tsagan Noor" area. They developed the first, later somewhat modified but still partly valid stratigraphic scheme for this region and recognized the basalts interlayered in the sediments (BERKEY and GRANGER 1923, BERKEY and MORRIS 1927, BERKEY et. al. 1929). On top of the crystalline basement which they assigned to the Late Proterozoic, a possibly Jurassic(?) sequence was found. The oldest fossil-bearing sediments are of Early Cretaceous age (Ondai Sair formation by BERKEY and MORRIS 1927) overlain by Cenozoic successions.

After World War II the geological research in the Valley of Lakes was dominated by the Joint Soviet – Mongolian Geological Expeditions and the Joint Soviet – Mongolian Paleontological Expeditions. The scientific results were published in special series (e.g.: BADAMGARAV et al. 1975, DEVYATKIN 1981, DEVYATKIN et al. 1973, LISKUN and BADAMGARAV 1977). In addition, during the 1960s a Polish-Mongolian Paleontological Expedition carried out field studies in the Valley of Lakes (GRADZINSKI et al. 1968, KIELAN-JAWOROWSKA and DOVCHIN 1968). The achievements of these expeditions led to a first systematic lithological and stratigraphic classification of the Cenozoic sediments of the Valley of Lakes, a petrographical and geochemical description of the basalts, the first radiometric age datings, fossil lists and a biostratigraphic scheme.

In 1993 a field conference took place in Mongolia in the course of the IGCP Project 326 entitled: "Oligocene-Miocene Transition in the Northern Hemisphere". Based on the hitherto available results (DEVYATKIN, 1993a, b and c, DEVYATKIN and BADAMGARAV, 1993) the Cenozoic continental sediments in Central Mongolia were studied for the purpose of correlation with similar sediments from Asia, Europe and North America. The findings and problems arising from this IGCP conference were the starting point of a joint Austrian-Mongolian project aiming at a detailed field study of the Cenozoic sequence in the Taatsiin Gol and the Taatsiin-Tsagaan Noor area, scientifically the most important part of the Valley of Lakes in Central Mongolia. The field work of this joint project was carried out during three field seasons from 1995 to 1997.

The goals are to establish a biochronology based on rodent assemblages and to develop an integrated stratigraphy using lithostratigraphic, biostratigraphic and geochronologic data. This will be the basis for correlations with Asian mammal ages and faunas. To achieve these goals an interdisciplinary program has been set up in an area outlined in Fig 1. Therefore, the field work included extensive geological mapping, mineralogical, petrological and geochemical studies of basalts interlayered with the sediments, and the respective age dating. Further investigations were carried out in sedimentology as well as paleontology. The mammal fossils were collected from carefully selected sections across the Cenozoic sequences. In this paper we will present results of three field seasons and the corresponding analytical investigations.

Abbreviations for the localities and profiles used throughout this paper, their Mongolian full transcriptions as well as some important Mongolian terms are given in Tab. 1. The exact location (GPS data) and the altitude can be taken from Tab. 2.

2. Methods

2.1 Geological and Paleontological Methods

During two field seasons (1996 & 1997), we mapped almost 1700 km^2. A topographic map in the scale 1:100000 and aerial photographs with a scale of approximately 1:45000 were used as the mapping basis. We obtained these items from the Mongolian Academy of Sciences. Although the combined usage of a topographic map and aerial photographs allows a reasonably exact location of the outcrops, we used a GPS. The GPS data give on the one hand accurate GPS positions of the sedimentological and paleontological profiles and sample locations (Tab. 2) and on the other hand they enable the reliability of the topographic map to be checked. The precision of the GPS measurements is in the range of 50 to 100 m horizontally. The geological map in suppl. 1 was generated in AutoCAD by digitising topographical features and geological boundaries.

The most important sedimentological investigations concentrated on the analysis of about thirty sections. The profiles were carefully selected, according to the occurrence of fossil-bearing horizons, basalt flows and a highly variable lithology. MIALL'S (1996) terminology was applied to establish lithostratigraphic units. A primary aim was to describe the lithological content, bed thicknesses, sedimentary structures, the nature of bed boundaries and the development of lateral variations of beds in detail. Furthermore, paleocurrent indicators (trough cross-bedding, imbrications) were measured and gravel lithologies determined.

Grain size analyses were carried out in order to interpret transport mechanisms. This involved wet sieving with ASTM sieves (the following sieve set was used: 4.0, 2.8, 2.0, 1.4, 1.0, 0.710, 0.500, 0.355, 0.250, 0.180, 0.125, 0.090, 0.063, 0.032 mm) and analysing <32 μm grain fractions with a sedigraph (Micromeritics Sedigraph 5100). These data were interpreted using cumulative frequency curves according to SINDOWSKI (1957) and VISHER (1969). The bulk mineralogy of the samples was determined with X-ray powder diffraction (Philips PW 3710 generator and PW 1820 goniometer with CuKa radiation at 45 KV and 35 mA) and step scan (step size 0.02°, 1s per step). The procedure after SCHULTZ (1964) for the semi-quantitative determination of mineralogical contents was applied. The rock colour was defined with the "Rock color chart" (GODDARD et al. 1951). Heavy mineral spectra of grain fractions between 63μ and 125μ were analysed by microscope and are presented without opaque phases. Paleocurrent data, gravel lithologies and MPS (maximum particle size) were interpreted in context with mapping results.

Along the sections paleontological samples were taken from different positions. These are:

* fossil horizons with visible fossil content,

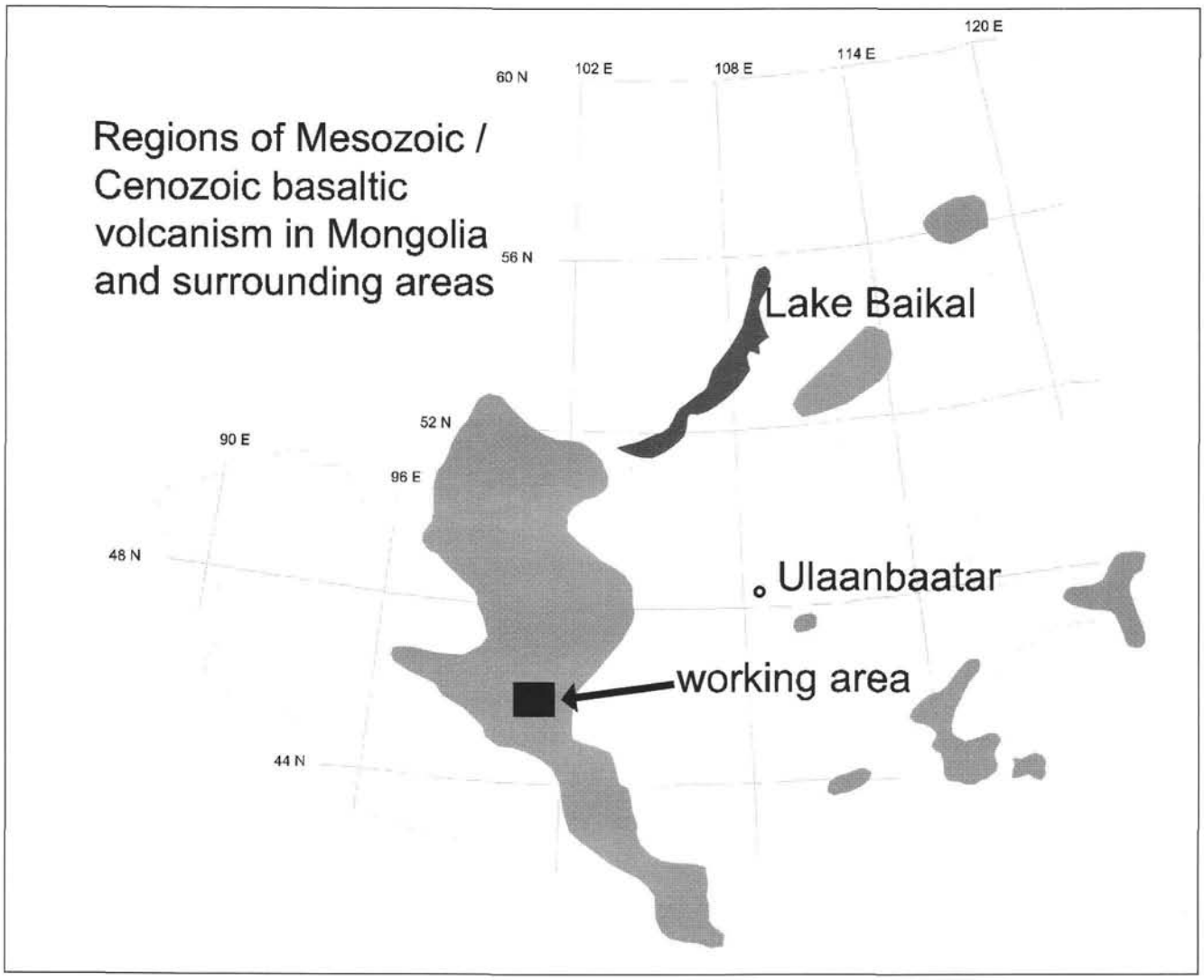

Fig. 1
Geographical outline of Mongolia including Lake Baikal with the distribution of Mesozoic and Cenozoic volcanics in Mongolia and surroundings.

- fine-grained sediment layers (silt and clay) without visible fossil content, but situated between coarse-grained sediment sequences,
- any fine- and middle-grained sediments contacting the basalts.

The test samples were of 20 - 50 kg each. Fifty percent of the test samples were rich in fossils. From these fossil horizons large sediment samples of five hundred to several thousand kg were taken. In total more than 50 tons of sediments were wet screened, yielding more than 80 vertebrate faunas. Fossils collected from the surface were studied separately because of their unclear stratigraphic position.

Wet screening was carried out in the field camp at the Taatsiin Gol. Sieves with mesh sizes of 0.5, 2.5 and 5.0 mm were used. A generator (Lombardini IM 359) operated the waterpumps (Asira 304) and the microscope-illumination. REM-photos were taken by a scanning electron microscope (Philips XL 20) at the Biozentrum/University of Vienna.

2.2 Petrological and Geochemical Methods

The basalts are partly heavily weathered even in the interior parts of the lava flows. Sampling was therefore difficult and required special care. Normal-sized hand specimens seemed large enough since the basalts are mainly aphyric or contain only microphenocrysts.

Mineral analyses were carried out on polished thinsections with an electron microprobe JEOL 8600 including a LINK control system. Measuring conditions were 15 KV acceleration voltage and 15 nA beam current. For quantitative analyses oxid and synthetic/natural minerals were used as standards. The correction procedure included background, dead time and ZAF calculation built into the LINK system. Major elements were also measured with the microprobe on fused glass tablets with a sample/flux (Lanthaniumtetraborate) ratio of 2:3. To achieve better homogenisation of the glass tablets the melting and quenching processes were repeated. USGS standards such as AGV or BHVO were used. The glass pellets were measured at 15 kV and 50 nA. The correction procedure is the same as with the minerals. Loss on ignition was determined gravimetrically.

Trace elements were measured by Philips PW 1410 XRF and REE by neutron-activation analysis. Trace elements were determined on powder pellets at 60 kV and 45 mA and corrected according to the program TRACES v.11/93 written by PETRAKAKIS and NAGL at the Institute of Petrology, University of Vienna. For INAA the samples were irradiated for (8 h at a neutron flux density of 10^{12}n $cm^{-2}s^{-1}$ at the research reac-

Table 1

Abbreviations – Full Mongolian Transcription

TGL	Taatsiin Gol left
TGR	Taatsiin Gol right
TGW	Taatsiin Gol west
SHG	Hsanda Gol
DEL	Del
TAT	Tatal Gol
IKH	Ikh Argalatyn Nuruu
ABO	Abzag Ovoo / Khutagt Khairkhan
RHN	Tavan Ovoony Deng
LOH	Loh
LOG	Luugar Khudag
UNCH	Unkheltseg
ODO	Olon Ovoony Khurem
BUK	Builstyn Khudag
UTO	Ulaan Tolgoi
MKT	Menkhen Teeg
KOOL	Kholbooldschi
BOR	Bor Ovoo
ELE	Elgen
KUN	Khunug
TAR	Tarimalyn Khurem
USK	Mt.Ushgoeg
HL	Khongil

Glossary of Mongolian words used in this paper

Baga	small
Baruun	west, right
Bayan	rich
Bogd	elevation, great
Bor	brown
Del	horse mane
Dzun	east, left
Gol	river
Hsir	goat foot
Ikh	great
Khudag	well
Khurem	basaltic plateau
Loh	dragon
Noor	lake
Nuruu	mountain ridge
Sair	dry stream/wadi
Tsagaan	white
Ulaan	red
Uul	mountain range

tor of the "Atominstitut der österreichischen Universitäten" in Vienna. Gammaspectrometric measurements were carried out with a HPGe-detector at the Institute of Biophysics (University of Salzburg). The spectra were calibrated for energy and efficiency with the program GammaVision v.2.00 (EG&G Ortec). The required correction procedures on the calculated peak areas were carried out using a program by LETTNER (1988). The USGS geostandards MAG-1 and AGV-1 were used to calculate the concentrations of the elements.

2.3 Geochronological Methods

The freshest basalt chips were crushed, ground in a disk mill, sieved to separate the grain size between 0.2 and 0.4 mm, and subsequently cleaned in an ultrasonic cleaner.

Table 2

General Profile Data

Name	GPS	Altitude (m)
ABO-A	N 45°40´16´´ E 101°02´20´´	1640
BUK-A	N 45°23´03´´ E 101°30´44´´	1522
BUK-B	N 45°24´09´´ E 101°31´34´´	1590
BUK-C	N 45°24´09´´ E 101°31´34´´	1590
BUK-D	N 45°24´37´´ E 101°30´35´´	1620
DEL-B	N 45°27´08´´ E 101°22´24´´	1520
HL-A	N 45°27´37´´ E 101°09´14´´	1530
LOG-A	N 45°32´18´´ E 101°00´48´´	1583
LOG-B	N 45°30´48´´ E 101°58´22´´	1530
LOH-A	N 45°17´22´´ E 101°47´04´´	1481
LOH-B	N 45°17´20´´ E 101°47´39´´	1481
LOH-C	N 45°15´44´´ E 101°43´03´´	1490
ODO-A	N 45°32´24´´ E 101°08´17´´	1670
ODO-B	N 45°32´58´´ E 101°08´16´´	1685
RHN-A	N 45°29´37´´ E 101°12´17´´	1490
SHG-A	N 45°16´01´´ E 101°45´45´´	1445
SHG-B	N 45°16´14´´ E 101°45´50´´	1470
SHG-AB	N 45°16´00´´ E 101°46´37´´	1460
SHG-C	N 45°15´47´´ E 101°43´03´´	1410
TAR-A	N 45°31´06´´ E 101°18´23´´	1650
TAT-C	N 45°18´21´´ E 101°38´01´´	1389
TAT-D	N 45°17´37´´ E 101°37´32´´	1390
TGL-A	N 45°26´57´´ E 101°16´18´´	1460
TGR-A	N 45°25´08´´ E 101°15´44´´	1372
TGR-B	N 45°24´53´´ E 101°15´44´´	1440
TGR-AB/21	N 45°24´42´´ E 101°15´22´´	1570
TGR-AB/22	N 45°24´47´´ E 101°15´21´´	1570
TGR-C	N 45°23´09´´ E 101°14´36´´	1435
TGR-ZO	N 45°24´03´´ E 101°16´00´´	1430
TGR-1564	N 45°27´30´´ E 101°12´44´´	1540
TGW-A	N 45°22´19´´ E 101°06´01´´	1410
UNCH-A	N 45°27´41´´ E 101°12´05´´	1550
UTO-A	N 45°20´49´´ E 101°50´16´´	1519

The samples were enclosed in high purity quartz vials and irradiated at the 9MW ASTRA reactor at the Austrian Research Center Seibersdorf. Ten samples including one monitor were stored in a single level of a rotating sample holder; up to 5 levels were irradiated simultaneously. The usual radiation duration for these samples was 2 h. After a cooling period of at least four weeks the samples were filled in small, annealed (low blank) cylindrical tantalum capsules where the whole rock grains are stored safely, but the released gas can escape through the small slit approximately 1mm^2 between bottom and cover.

For Ar extraction the radiofrequency (RF) heating method was used. The extraction furnace is made from quartz glassware in a pyrex envelope glass. The hot portion of the extraction furnace is double walled and this volume is continuously pumped to avoid diffusion from ambient air during the high-temperature steps. After finishing the experiment, the sample can be dropped out, so only one sample is in the heating position. The geometry of the cylindrical tantalum capsules, which always have a horizontal position within the RF-induction spiral, guarantees a uniform temperature distribution in the sample. Temperatures were monitored by a calibrated pyrometer. The heating period was 10 min for the low-temperature steps and was continuously lowered to 3 min at the high-temperature steps. Between the heating procedures the RF was switched off and no gas is released.

Cleaning of the released gas was done by a combination of liquid nitrogen cold trap and SAE-getters. Two-thirds of the gas were introduced into the mass spectrometer, a VG-5400 model from MICROMASS ISOTOPES (Winsford, GB); the rest of the gas was pumped out from the extraction line.

Isotopic ratios were determined from a 10 min measuring period, regressed to the time of sample inlet. Age calculation was done after corrections for mass discrimination and radioactive decay, especially of the ^{37}Ar, using the formulas given in DALRYMPLE et al. 1981. The specific production ratios of the interfering Ar isotopes at the ASTRA reactor of Seibersdorf are: $^{36}Ar/^{37}Ar(Ca)=0.00034$, $^{39}Ar/^{37}Ar(Ca)=0.0004$, $^{40}Ar/^{39}Ar(K)=0.0254$. The K/Ca ratio was determined from the $^{39}Ar/^{37}Ar$ ratio (calculated for the end of irradiation) using a conversion factor of 0.247. This factor was determined from a plagioclase with uniform and well-known composition.

The ^{40}Ar line-blank at 1000°C was approx. $1x10^{-15}$ moles; the $^{40}Ar/^{36}Ar$ ratio of the line blank was similar to air composition. The long-term (2 h) leakage rate of the line was $2x10^{-15}$mbar l/s. Interference of ^{36}Ar, ^{37}Ar, and partly ^{39}Ar with a low background of hydrocarbon radicals in the masspectrometer can be a limiting factor for reliable measurements of very low intensities. Carefully checked peak positions, background determinations and corrections are routinely performed to overcome such difficulties. J-values are determined with internal laboratory standards, calibrated by international standards including muscovite Bern 4M (BURGHELE 1987), amphibole Mm1Hb (SAMSON and ALEXANDER 1987), and Fish Canyon sanidine. The errors given on the calculated age of an individual step include only the 1σ error of the analytical data. The error of the plateau ages or total gas ages includes an additional error of $\pm 0.4\%$ on the J-value. Within these latter errors the age results are reproducible with the same analytical equipment. Interlaboratory reproducibility can be expected to be within 1-1.5%.

3. Geological Framework

Large parts of Mongolia formed in the time intervall from the Late Proterozoic to the Late Permian (ZORIN et al. 1993). Reactivated Proterozoic metamorphics, Paleozoic sediments of various provenances, magmatites and metamorphics are sandwiched between the Angara Craton in the north and the North China Craton in the south. Several models were developed in the last few years to explain the Late Proterozoic to Paleozoic succession of orogenic events (e.g. ŞENGÖR et al. 1993, ŞENGÖR and NATAL'IN 1996, TOMURTOGOO 1997). It is beyond the scope of this paper to discuss the merits of these models in detail. We shall discuss here only shortly the geological frame of the "Valley of Lakes", i.e. the Khangai and Gobi Altai mountains, respectively.

Neither the Angara Craton nor the North China Craton are present in Mongolia. Nevertheless, the Tuva-Mongolian microcontinent, derived from the Angara Craton, is composed of *Proterozoic rocks as old as 2.65 Ga* (TOMURTOGOO 1997). It forms a tight arc structure ranging from the N (NE) of Mongolia over the W to the central part of Mongolia. On both sides it is bordered by various accretionary complexes, ophiolites, island arc volcanics and turbidites, all intruded by granitoid rocks from Late Proterozoic (Riphean?) to Late Paleozoic (Permian).

The northern boundary of Mesozoic to Cenozoic sediments in the Valley of Lakes is built up by a sequence of fault-bounded zones ranging from the Proterozoic to the Carboniferous and even Permian (Fig. 2). The southernmost Baidrag zone is the direct equivalent of the Proterozoic rocks from the Tuva-Mongolian microcontinent and contains, among others, high grade gneisses, charnockites and amphibolites (ZORIN et al. 1993, TERAOKA et al.1996). The rocks of the Baidrag zone are the direct, mainly fault-and thrust-bounded, basement of the Cenozoic sediments in the Taatsiin Gol area and are represented in the geological map (suppl. 1) by the signature: "Crystalline Basement".

The Burdgol zone (TERAOKA et al. 1996) is not separated in Fig. 2 from the Baidrag zone. It is simply the northern part and consists predominantly of metapelites and metapsammites including metacherts with olistoliths composed of basic rocks, all in greenschist to lowgrade amphibolite facies metamorphism. Muscovite K-Ar dating from metapelites gave an age of 699 ± 35 Ma (TERAOKA et al. 1996).

The next zone towards the north, the Bayan Khongor zone (Fig. 2), is made up mainly of metamorphosed basic rocks and contains an ophiolite sequence. Subordinate pelitic schists occur. K-Ar ages yielded approximately 450 Ma (Late Ordovician) for the metamorphism (KURIMOTO et al. 1998). The metamorphism varies from the very low-grade (pumpellyite) to medium-grade (epidote-amphibolite) facies.

The Dzag zone (Fig. 2) in turn is again built up of metapelites and metapsammites in greenschist facies. K-Ar ages of micas (395 ± 20 and 440 ± 22) indicate a Silurian to Early Devonian age of metamorphism (TERAOKA et al. 1996). The Khangai zone consists of unmetamorphosed, but folded sandstones, mudstones and intercalated olistoliths. Fossil findings such as brachiopods, corals and plants indicate a Devonian to Carboniferous age.

All zones are intruded by granitoids ranging from the Riphean to the Late Paleozoic and even to the Early Cretaceous in the Khangai zone. In Fig. 2 the granite is shown only for the Baidrag (including the Burdgol) zone and the Bayan Khongor zone. The Late Proterozoic granitoids are dominated by ilmenite series, the Late Paleozoic by magnetite series. The early Paleozoic granitoids show both series. There is no systematic distribution of the granitoids with age (TAKAHASHI et al. 1998), except that the Riphean granites are restricted to the Baidrag and Burdgol zone and that the Khangai granites are exclusively of Late Paleozoic age and younger.

At the southeastern end of the Ushgoeg Mountains a small zone of Permian rocks occurs (geological map in suppl. 1 and 2). They consist of silts and sandstones with some conglomerates composed of quartz pebbles and basic, intermediate to acidic volcanics. The Permian tuffs contain fragments of the Late Paleozoic granites and are in turn intruded by the youngest Late Paleozoic granitoids (TAKAHASHI et al. 1998). The Permian rocks are only slightly metamorphosed and contain at their eastern boundary fossil leaves and woods of Late Paleozoic age.

Towards the south of the Valley of Lakes the geological knowledge is even poorer. The Baga Bogd and Ikh Bogd are

Fig. 2 →
Tectonic sketch map of the Valley of Lakes in the vicinity of the Taatsiin Gol area. Legend: oblique hachures to the right: Khangai Zone; horizontal hachures: Dzag Zone; oblique hachures to the left: Bayan Khongor Zone, vertical hachures: Baidrag and Burdgol Zone; +: granites (undifferentiated); x: basement rocks (undifferentiated); black lines: faults, small lines: indication of dip; black line with teeth: thrusts. *Abbreviations:* BB: Baga Bogd, BBU: Barun Bayan Ulaan som , BKH-F: Bayan Khongor Fault, BO: Bor Ovoo, BS: Bogd som, IB: Ikh Bogd, ON: Orog Noor; TAG: Taatsiin Gol; TUG: Tuyn Gol, TTN: Taatsiin Tsagaan Noor, UG: Mt. Ushgoeg.

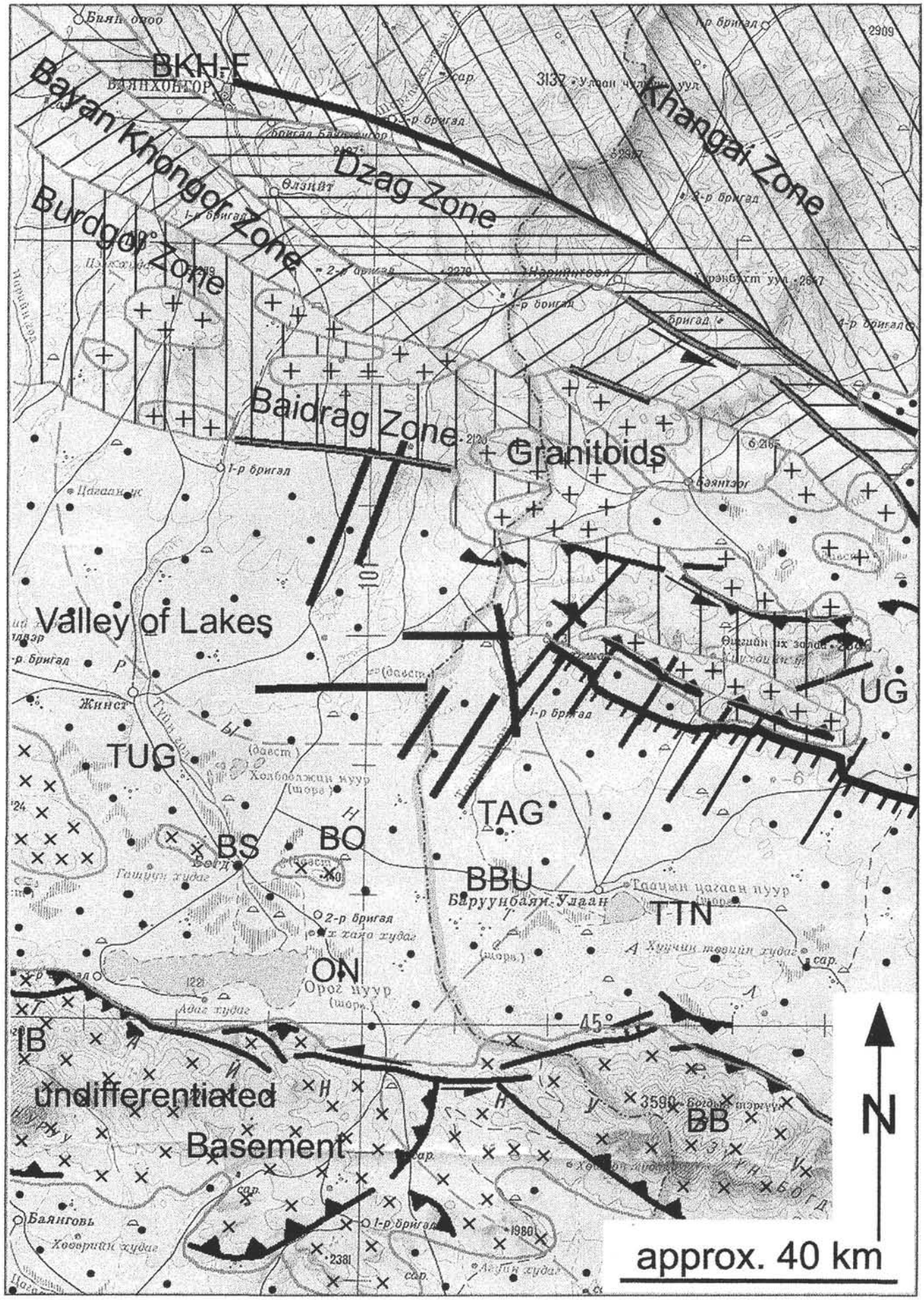

similar to the Bayan Khongor zone in that they are made up of lower Paleozoic (Cambrian?) metasediments and metavolcanics intruded by granites of variable composition and age (ZORIN et al. 1993). At least near Bogd som (Fig. 2) along the Tuyn Gol, quartzite-bearing conglomerates are distributed, identical with the probably Permian conglomerates S of Mt. Ushgoeg. The Bor Ovoo east of Bogd som (Fig. 2) consists beneath the Cenozoic sediments and basalts of aphyric and/or plagioclase phyric, slightly metamorphosed volcanics which strongly resemble the Late Proterozoic to Early Cambrian (island arc) volcanics in the Han Tashiri Range S of the town of Altai.

4. Lithological Units: Lithostratigraphy and Sedimentology

4.1 Lithostratigraphy

The first lithostratigraphic nomenclature in the working area was developed by BERKEY and GRANGER (1923), BERKEY and MORRIS (1927) and BERKEY et al. (1929). Apart from the Early Cretaceous Ondai Sair formation they established among others the Cenozoic Hsanda Gol and the Loh formations. Later on these formations, also discussed in this paper, have been modified. According to the Russian transcription the Hsanda Gol Formation was termed Shand Gol formation (DEVYATKIN et al. 1973). DEVYATKIN 1981 also introduced the Ergilin Dzo formation (YANOVSKAYA et al. 1977) for clastic sediments below the Shand Gol formation and the Tuyn Gol formation (DEVYATKIN et al. 1973) for the clastic sediments on top of the Loh formation.

Our field evidence showed clearly that the definition of the hitherto used formation names had serious shortcomings such as:

* inappropriate definition of formations and their boundaries
* usage of lithostratigraphic terms for chronostratigraphy
* insufficient interpretation of depositional processes

As a consequence we formally redefined these formations and established one new formal formation name according to the International Stratigraphic Guide (SALVADOR, 1994; STEININGER & PILLER, 1999) in order to have a basis for adequate geological mapping. The following five formations will be used: Ondai Sair formation, Tsagaan Ovoo Formation, Hsanda Gol Formation, Loh Formation and Tuyn Gol formation. Two of them, the Ondai Sair (BERKEY and MORRIS, 1927) and the Tuyn Gol (DEVYATKIN et al. 1973, LISKUN and BADAMGARAV 1997) fms. are used in the original informal sense, because they were not the direct subject of our research. The remaining three formations are newly formalized and classified.

4.1.1 Tsagaan Ovoo Formation

Name: The sediments of the Tsagaan Ovoo Fm. were originally assigned to the Hsanda Gol fm. by BERKEY and MORRIS (1927) and later on by MELLET (1968). Subsequently, DEVYATKIN 1981, DEVYATKIN and BADAMGARAV (1993) and DEVYATKIN (1993b and c) correlated these sediments with Yanovskaya's Ergilin Dzo formation, defined approximately 450 km SSE of Ulaan Baatar. Because of the lack of important outcrops between the type area of Ergilin Dzo formation and the Taatsiin Gol area over a distance of at least 700 km and a questionable lithological similarity (YANOVSKAYA et al. 1977, LISKUN and BADAMGARAV 1977, DEVYATKIN 1981), we decided to introduce this new formation name.

Derivatio nominis: The name is taken from Tsagaan Ovoo, a small but significant hill inmidst the Taatsiin valley approximately 35 km NNW of Taatsiin Tsagaan Noor.

Type area (see suppl. 1 & 2): The type area is situated in the central part of the Valley of Lakes. It includes the region from west of the Taatsiin Gol to the east of the Hsanda Gol and south of Mt. Ushgoeg. In terms of geographic coordinates this area ranges from 100° 00´ to 102° 00´ E and from 45° 10´ to 45° 40´N.

Type and reference profiles (see suppl. 1-4 and table 2): The type profile of the Tsagaan Ovoo Fm. is TGR-B (Taatsiin Gol right). For the exact location, geographical coordinates and altitude of the basis of the profile see table 2. The profiles BUK-D, BUK-C and BUK-B (Builstyn Khudag) serve as reference profiles, where BUK-D represents the lowermost part and BUK-B the uppermost part of the reference profiles. Their coordinates and their respective altitude are also given in table 2. Unfortunately the stratigraphic footwall of the Tsagaan Ovoo Fm. is not exposed anywhere in the area. The footwall boundary in the BUK-profiles is tectonic. The hangingwall boundary against the overlying Hsanda Gol Fm. is exposed in the type profile TGR-B at an elevation of 1460 m. The upper boundary towards the Hsanda Gol Fm. in TGR-B is marked by a significant decrease in grain size from gravel and sand to clay and silt together with a change in colour from white to brick-red.

Short description and geochronological position (see also Fig. 22): Further outcrops of the Tsagaan Ovoo Fm. are shown in the geological map and were studied in columnar sections RHN-A, TGR-A and BUK-B, C, D (suppl. 1-3 and table 2). The maximum outcropping thickness of the Tsagaan Ovoo Fm. is about 150 m found in Builstyn Khudag (combined thickness of the reference profiles BUK-D, BUK-C, BUK-B). No fossil horizons and no basalt flows appear in the Tsagaan Ovoo Fm. The detailed lithological content and sedimentological interpretation is found in chapter 4.2.2. Presently, only indirect evidence for the geochronological position exists, as the Tsagaan Ovoo Fm. underlies the Hsanda Gol Fm., which can be dated by basalt I (see chapter 5 & 6) at least as Lower Oligocene. For further discussions see chapter 9.

4.1.2 Hsanda Gol Formation

Name: The formation name was first introduced by BERKEY and MORRIS (1927 p. 234 ff). Apart from the brick-red clays and silts they included coarser-grained clastics, well-rounded, fine-grained gravels and sands, but also a series of clays to the Hsanda Gol fm., sediments which now must be added to Mesozoic successions. Later, DEVYATKIN (1981), DEVYATKIN and BADAMGARAV (1993) and DEVYATKIN (1993b and c) restricted the Hsanda Gol fm. to fossiliferous red beds, and partially to the coarse clastics above basalt I, and termed this succession Shand Gol fm. (Russian transcription). We will, not following the Russian transcription, use the original name but restrict the lithology as described below and in more detail in chapter 4.2.3.

Derivatio nominis: BERKEY and MORRIS (1927) derived the name from the Hsanda Gol, a stream bed in the easternmost part of the geologic map area (see suppl. 1 & 2).

Type area (see suppl. 1 & 2): The type area is situated in the central part of the Valley of Lakes. It includes the region from west of the Taatsiin Gol to the east of the Hsanda Gol and south of Mt. Ushgoeg. In terms of geographic coordinates this area ranges from 100° 00´ to 102° 00´ E and from 45° 10´ to 45° 40´N.

Type and reference profiles (see suppl. 1-4 and table 2): The type profile of the Hsanda Gol Fm. is TGR-B (**T**aatsiin **G**ol **r**ight). For the exact location, geographical coordinates and altitude of the basis of the profile see table 2. The reference profiles are SHG-C, SHG-A and SHG-B (Hsanda Gol) from footwall to hangingwall. Their coordinates and their respective altitude are also given in table 2. The lower boundary towards the Tsagaan Ovoo Fm. in TGR-B in 1460 m is marked by a significant decrease in grain size from gravel and sand to clay and silt together with a change in colour from white to brick-red. The upper boundary to the Loh Fm. (altitude of 1500 m) is in turn characterized by an increase in grain size and a predominance of lighter colours.

Short description: Sediments of the Hsanda Gol Fm. were additionally studied in the following sections: DEL-B, LOH-B, LOH-C, TAT-C, TGL-A, TGR-A, TGR-C, UNCH-A (see suppl. 1-3 and table 2). The Hsanda Gol Fm. consists of fine clastic red beds just below and above basalt I (see chapter 5), which becomes part of this formation. The total thickness of the Hsanda Gol Fm. varies from zero (e.g. Tavan Ovoony Deng area) to about 70 m (see reference sections SHG-A, SHG-B, SHG-C in suppl. 3). Generally the thickness increases towards the center of the Valley of Lakes. The detailed lithological content and sedimentological interpretation is found in chapter 4.2.3.

Geochronologic position and biostratigraphy (see also Fig. 22): The geochronologic situation is determined by the position of the brick-red clays and silts immediately above and below basalt I, which has been dated as 31.5 Ma (compare chapter 6). The total geochronologic range includes the Late Oligocene as thoroughly discussed in chapter 9. The biostratigraphy is characterized by rodent assemblages as discussed in chapter 8.2. The biozones A and B are typical for the lower parts, C and C1 for the highest parts of the Hsanda Gol Fm. (see Fig. 22).

Remarks: BRYANT and MCKENNA (1995) suggested to divide the Hsanda Gol Fm. in the vicinity of the Tatal Gol into two members, the Tatal and the Shand Member. According to our regional mapping and sedimentological studies we assign their Tatal Member and Mellet Lava (= basalt I in the Tatal Gol area) as well as the lower part of their Shand Member to the Hsanda Gol Fm., their upper part of the Shand Member to our Loh Fm. As shown in the geological map in suppl. 1 basalt I is not continuously present within the Hsanda Gol Fm. Thus, it can be used only locally, but never regionally as a marker to separate potential members.

4.1.3 Loh Formation

Name: The term Loh formation was also first described by BERKEY and MORRIS (1927) and is left unchanged but the lithological content is broadened. BERKEY and MORRIS (1927) restricted the Loh fm. to Miocene olive green clays. DEVYATKIN (1981) and DEVYATKIN and BADAMGARAV (1993) used this formation name for Miocene light-grey sands interbedded with green clays plus pebble material. LISKUN and BADAMGARAV (1977) added to this description white sands and brownish clays in a profile whose position is almost identical to profiles LOH-A and LOH-B (see below).

Derivatio nominis: The name of this formation refers to a locality near Hsanda Gol which BERKEY and MORRIS (1927, p. 365) describes as follows: "The name of this place is Loh, which, the Mongols told us, means dragon, and refers to the presence of the "dragon bones" in the clays. Accordingly, the clays were called the Loh formation."

Type area (see suppl. 1 & 2): The type area is situated in the central part of the Valley of Lakes. It includes the region from west of the Taatsiin Gol to the east of the Hsanda Gol and south of Mt. Ushgoeg. In terms of geographic coordinates this area ranges from 100° 00´ to 102° 00´ E and from 45° 10´ to 45° 40´N.

Type and reference profiles (see suppl. 1-4 and table 2): The type profile for the Loh Fm. is TGR-B (**T**aatsiin **G**ol **r**ight). For the exact location, geographic coordinates and altitude of the basis of the profile see table 2. The reference profiles are TAR-A (Tarimalyn Khurem), LOH-A, LOH-B (Loh) and BUK-A (Builstyn Khudag). Their coordinates and their respective altitude are also given in table 2. Profile TAR-A was selected as an important reference profile because it exposes the thickest sequence in the area with a great lithological variability and contains the stratigraphically important basalts II and III (see chapter 5). The reason for including BUK-A into the reference profiles is the exposure of the occasionally fine-grained facies within the Loh Fm. The lower boundary is exposed in the type profile TGR-B at 1500 m and is marked by a change in grain size from silt and clay to sand and gravel together with a change in colour from brick-red to a variety of lighter colours (yellow, green, white, pink, orange, brown). The upper boundary is only exposed in the type profile TGR-B at an altitude of 1520 m, where the Loh Fm. is overlain by the Tuyn Gol fm. (suppl. 3). The lowermost sediments of the Tuyn Gol fm. are characterized by cobbles stained with Fe_2O_3.

Short description: Loh sediments were additionally studied in the following sections: ABO-A, LOG-A, LOG-B, LOH-B, LOH-C, ODO-A, ODO-B, RHN-A, SHG-B, TGL-A, TGR-C, TGW-A, UNCH-A, UTO-A (see suppl. 3). The maximum outcropping thickness of the Loh Fm. is up to 150 m in the north of the mapping area, more precisely in the north of the Tarimalyn Khurem region (see suppl. 1 & 2). DAXNER-HÖCK et al. (1997) already proposed to extend the lithological variety of the Loh Fm. considerably to create a mappable lithological unit. The separation between Hsanda Gol Fm. and Loh Fm. is often difficult to achieve. As a rule, we assigned in the field all sediments above the clayey – silty Hsanda Gol Formation to the Loh Formation, as the sandy character of the sediments becames visible. The detailed lithological description is given in chapter 4.2.4.

Geochronologic position and biostratigraphy (see also Fig. 22): The geochronologic situation is determined by the position of basalts II and III in the reference profile TAR-A. They have been dated as 27 - 28 Ma and 13 Ma, respectively (compare chapter 6). This indicates an age from Late Oligocene to Late Miocene, as thoroughly discussed in chapter 9. The biostratigraphy is characterized by rodent assemblages C to E as discussed in chapter 8.2.

4.2 Sedimentology of Mesozoic and Cenozoic formations

In this chapter the formations are presented from bottom to top as Ondai Sair fm., Tsagaan Ovoo Fm., Hsanda Gol Fm., Loh Fm. and Tuyn Gol fm. All described lithostratigraphic units, except the Ondai Sair formation, can be found in the columnar sections presented in suppl. 3. In this figure, sedimentary structures are omitted because of presentation reasons. MIALL'S (1996) terminology for fluvial environments is used for facies classification. In the geological map (suppl. 1) the Ondai Sair fm. is not presented separately from the Mesozoic successions. The Ondai Sair and the Tuyn Gol formation were not within the scope of our primary investigations, but

are briefly described because they represent the footwall and hanging wall successions of the investigated formations. The working area with the best outcrops is located at the northern margin of the Valley of Lakes, as are the described sections. This means that the measured and given maximum thickness for each formation is not necessarily representative of the central, covered part of the basin.

4.2.1 Ondai Sair formation

The Ondai Sair formation was defined by BERKEY and MORRIS (1927) on the east side of "Mount Uskuk block" and classified as Cretaceous. The "Mount Uskuk block" is equivalent to the mountain range named "Mt. Ushgoeg" north of the "Valley of Lakes" in suppl. 2. According to their description it includes gray sandstones and dark paper shales, with a few beds of red sandy clay, which are disturbed by faulting and tilting. Our geological mapping focused on the Cenozoic sediments of the Valley of Lakes and did not differentiate Jurassic and/or Cretaceous formations. Nevertheless, we mapped Ondai Sair sediments in the vicinity of Dzun Hsir in the easternmost part of the working area, and in the Builstyn Khudag area and Del area, where they are overlain by the Tsagaan Ovoo Formation.

The Ondai Sair fm. contains loose yellowish brown, poorly sorted, matrix-supported gravels. These layers are interbedded with dark brownish clay layers, which bear rare root traces. Distinct cobble horizons with MPS (maximum particle size) up to 10 cm also occur. Sedimentary structures like trough cross-bedding and imbrications are sometimes observable. Sandy gravel layers contain fine-grained rip up clasts with diameters up to 80 cm. The lithological spectrum of well-rounded gravel components is as follows: granite, gneis, quartz, sandstone, siltstone, pegmatite, radiolarite.

In fine sand layers of the Ondai Sair formation in the Builstyn Khudag area we found plant fossils (Conifera) and bones of an ornithopod *(Psittacosaurus)*.

4.2.2 Tsagaan Ovoo Formation

Important occurrences of the Tsagaan Ovoo Fm. (see suppl. 1 & 2) include the Builstyn Khudag, Del, Tavan Ovoony Deng region and the foot of the plateau west of Taatsiin Gol. In addition the sediments appear in some localities in the west of the working area and in the east near Barun Hsir and Dzun Hsir. In the field this formation is noticeable by its gravelly and sandy, rarely silty and clayey facies interfingering with each other. Generally bright, white-coloured, massive, but also cross-bedded layers crop out. As for example displayed in Fig. 6a showing a part of the plateau west of Taatsiin Gol, the Tsagaan Ovoo Fm. is represented by the white sediments just below the brick red Hsanda Gol Fm. According to the "Rock Color Chart" (GODDARD et al. 1951) the colours of the coarse clastic Tsagaan Ovoo Fm. also include further grayish yellow green (5 GY 7/2) and light brown (5 YR 6/4); the fine clastics have colours like dark reddish brown (10 R 3/4).

Sediments of the Tsagaan Ovoo Fm. consist predominantely of quartz with variable amounts of sheet silicates. If present, smectite is the most important constituent followed by micas. Kaolinite, vermiculite and chlorite are only present in very small amounts. Additional constituents are plagioclase (up to 10%), very little K-feldspar and some carbonate minerals such as ankerite and calcite.

In Table 3 all lithofacies types, their facies code, sedimentary structures, interpretation and their frequency of occurrence are listed according to MIALL (1996, p.79, Table 4.1). The facies codes used throughout the following section and given mostly in brackets refer to those by MIALL (1996) in Tab. 3.

The stratigraphically lower parts of the Tsagaan Ovoo Formation crop out in the Builstyn Khudag region. There they are deposited on the Mesozoic Ondai Sair fm and tilted by the Del fault. They are dominated by massive gravel beds (MPS: 2.2 cm – 12.8 cm), mostly without any visible structures (Gmm, Gmg). The sediments are poorly sorted and polymict. Bed thicknesses up to 5 m can be observed. A confinement of channels is not observable. The use of bounding surfaces between depositional units as proposed by MIALL (1996, p. 82, table 4.2) could not be applied because of the outcrop situation in the working area. In Fig. 5a the cumulative-frequency curve (VISHER 1969) of a poorly sorted, clay-rich (about 15%) sand (BUK-C1) is presented (Sm). It was taken from the hanging part of a massive graded bed within the stratigraphically lower layers of the Tsagaan Ovoo Fm. This diagram does not concern particles larger than 1 mm = 0Φ (defined according to KRUMBEIN 1934, as $\Phi = -\log_2 S$; where S is the grain size in mm). The curve shows four segments, which represent two transport mechanisms. The truncation point at 1.75Φ separates grain fractions transported by saltation from grains transported by suspension. To the left of this truncation point, lower Φ-values indicate the saltation population, to the right, higher Φ-values the suspension population. The saltation and the suspension population consist of two weakly developed subpopulations. The sediment was transported exclusively in saltation and suspension. In sample BUK-C1 less than 5% of the grains are larger than 0Φ and more than 25% are smaller than 7Φ (0.0078 mm), a composition which is consistent with high viscosity debris flow (MAIZELS 1989). Sometimes beds with a similarly composed matrix, bearing clasts of MPS up to 12.8 cm, occur in these stratigraphically lower layers of the Tsagaan Ovoo Fm. According to WALKER (1980) and MIALL (1996) the beds reflect debris flow deposits.

The hanging parts of the Tsagaan Ovoo Fm. are generally finer clastic and show trough and planar cross-bedding (Gt, Gp, St, Sp) with set thicknesses up to 1m maximum, lamination (Sm) and ripples (Sr). Minor channel fills (Gt), transverse bedforms (Gp, Sp), 3-D dunes (St), sediment-gravity flow deposits (Sm) and ripples (Sr), in descending importance, characterize these sediments. Furthermore sediments from overbanks, fillings of abandoned channels or deposits of waning floods (Fl, Fm) occur in minor quantities. In general, bed thicknesses are smaller than in the footwall parts of the Tsagaan Ovoo Fm. Normal graded, but also inverse graded beds with rip up clasts in dm size occur. Normal graded sandy beds pass up into fine-grained ones, which show laminations and root-traces indicating possible paleosols (Fr).

Frequency-cumulative curves of two poorly sorted sands (TRG-B1 and BUK-B8) are presented in Fig. 5a. The curve shape of sample TGR-B1 is comparable with sample BUK-C1, showing the same position of the truncation point at 1.75Φ separating the saltation from the suspension population, except that this sand is coarser-grained and the saltation population is not subdivided. It represents facies Sm. Sample BUK-B8, reflecting facies St, was deposited by three mechanisms. The traction population is represented by the segment to the left of the truncation point at 1Φ. Two subpopulations between the truncation point at 1Φ and truncation point at 4.25Φ represent the saltation population. Finally the segment to the right of the truncation point at 4.25Φ reflects the grains transported by suspension.

In general, the Tsagaan Ovoo sediments are loose. Some beds are cemented with calcite, a feature interpreted to in-

Table 3

Facies classification modified after Miall (1996, p.79, table 4.1.)
Occurences of facies within each fm. are indicated with following symbols: ***=dominant; **=frequently; *=rare; ~=missing.

Facies code	Facies	Sedimentary structures	Interpretation	Occurrence of facies		
				Tsagaan Ovoo Fm. (strat. lower parts)	Tsagaan Ovoo Fm. (strat. higher parts)	Loh Fm.
Gmm	Matrix-supported, massive gravel	Weak grading	Plastic debris flow (high-strength, viscous)	***	~	**
Gmg	Matrix-supported gravel	Inverse to normal grading	Pseudoplastic debris flow (low strength, viscous)	***	~	**
Gcm	Clast-supported massive gravel	~	Pseudoplastic debris flow (inertial bed load, turbulent flow)	~	~	*
Gh	Clast-supported crudely bedded gravel	Horizontal bedding, imbrication	Longitudinal bedforms, lag deposits, sieve deposits	~	~	*
Gt	Gravel stratified	Trough cross-beds	Minor channel fills	~	**	***
Gp	Gravel, stratified	Planar cross-beds	Transverse bedforms, deltaic growth from older bar remnants	~	**	**
St	Sand, fine to very coarse, may be pebbly	Solitary or grouped trough cross-beds	Sinuous-crested and linguoid (3-D) dunes	~	**	***
Sp	Sand, fine to very coarse, may be pebbly	Solitary or grouped planar cross-beds	Transverse and linguoid bedforms (2-D dunes)	~	**	**
Sr	Sand, very fine to very coarse	Ripple cross-lamination	Ripples (lower flow regime)	~	**	**
Sh	Sand, very fine to coarse, may be pebbly	Horizontal lamination parting or streaming lineation (not observable in vertical sections)	Plane-bed flow (critical flow)	~	~	~
Sl	Sand, very fine to coarse, may be pebbly	Low angle (<15%) cross-beds	Scour fills, humpback or washed-out dunes, antidunes	not observed	not observed	*
Ss	Sand, fine to very coarse, may be pebbly	Broad, shallow scours	Scour fill	~	~	**
Sm	Sand, fine to coarse	Massive, or faint lamination	Sediment-gravity flow deposit	~	**	~
Fl	Sand, silt, mud	Fine lamination, very small ripples	Overbank, abandoned channel or waning flood deposits,	~	*	**
Fsm	Mud, silt	Massive	Backswamp or abandoned channel deposits	~	~	*
Fm	Mud, silt	Massive, dessication cracks	Overbank, abandoned channel, or drape deposits	~	*	~
Fr	Mud, silt	Massive, roots, bioturbation	Root bed, incipient soil	~	*	*

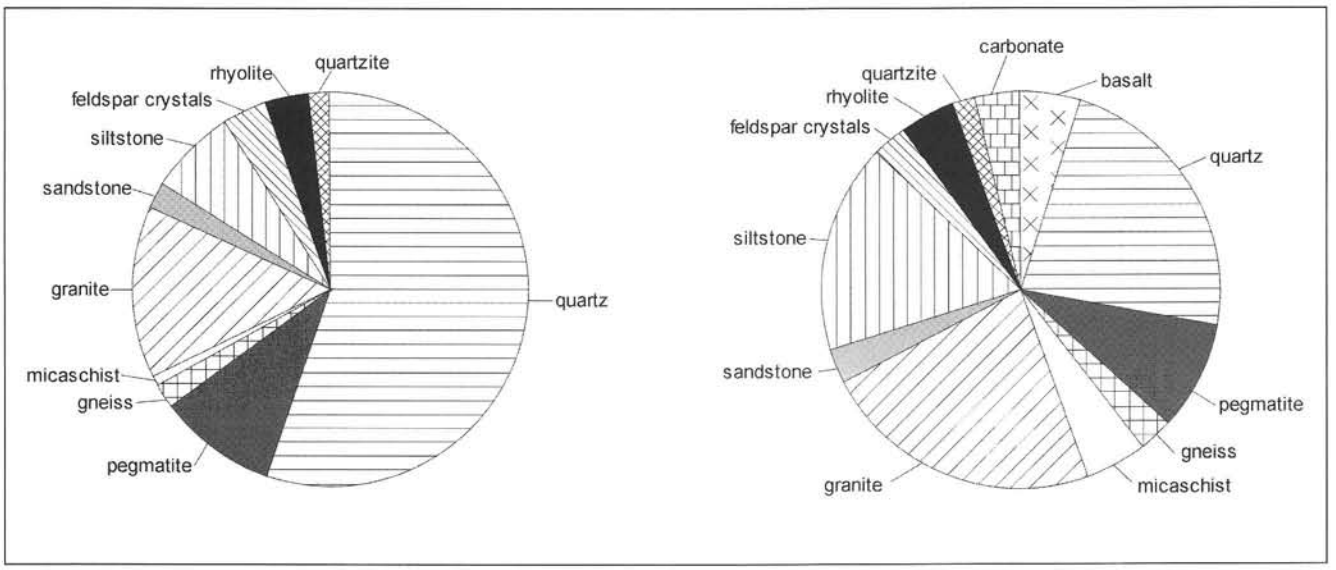

Fig. 3
Gravel lithologies of the Tsagaan Ovoo Formation (left) and the Loh Formation (right). The Tsagaan Ovoo samples (n=6) are dominated by quartz, granite and pegmatite components. Loh samples (n=9) are dominated by granite, pegmatite, siltstone clasts and have in addition basalt, carbonate and carbonate tuff components.

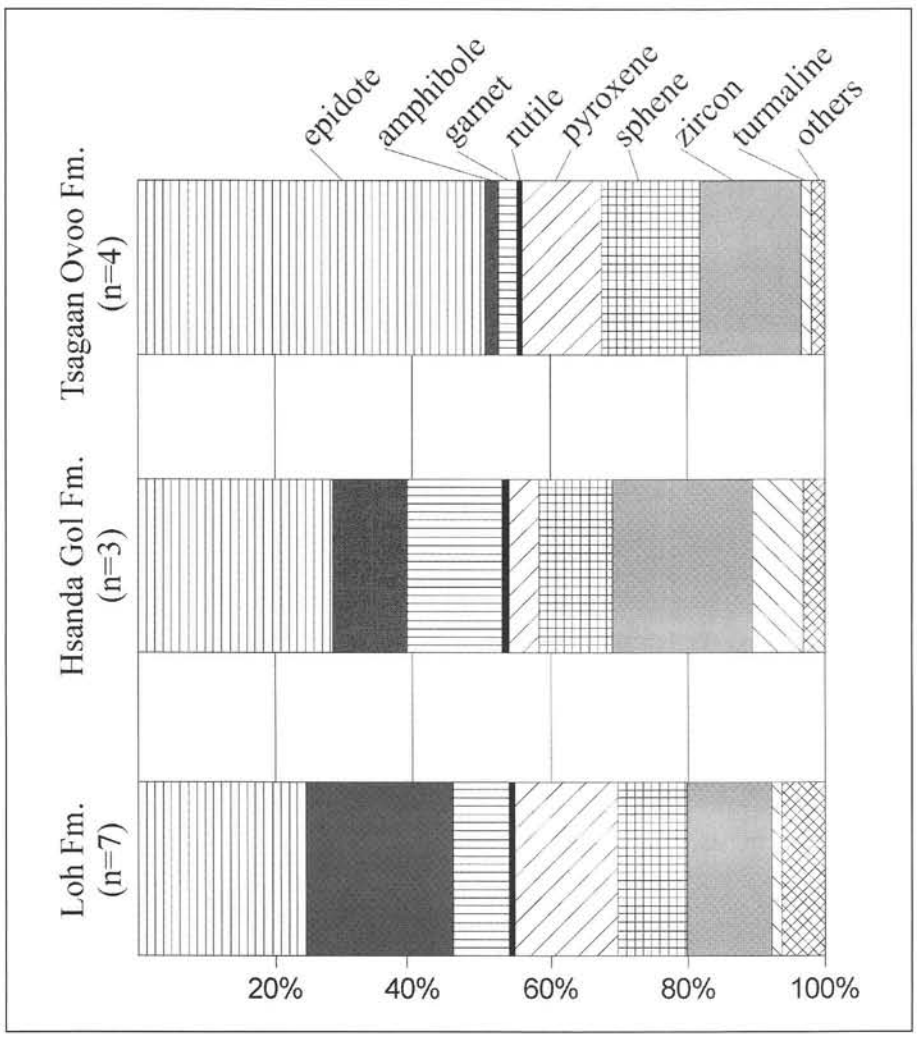

Fig. 4
Heavy mineral spectra of the Tsagaan Ovoo, the Hsanda Gol and the Loh Formations. "Others" (=maximal 2% for each mineral phase) in the Tsagaan Ovoo Formation are: staurolite, andalusite, sillimanite and brookite; in the Hsanda Gol Formation: andalusite, kyanite, apatite; in the Loh Formation: staurolite, sillimanite, kyanite, brookite, apatite and monazite.

volve cementation through groundwaters (pedogenic crusts). The measurement of paleocurrent indicators in the Tsagaan Ovoo Fm. was a problem. Nevertheless, pebble/cobble beds of the stratigraphically higher parts show imbrications with average paleocurrent directions from N to S. The same results can also be inferred from the trough and planar cross-bedded gravelly/sandy facies. These facts lead to the interpretation that also at this time, when the Tsagaan Ovoo sediments were deposited, a mountainous region in the position of the recent Khangai Mtns. formed the hinterland for the Valley of Lakes.

Six gravel samples, each containing between 200 and 600 components, were examined in the field. The gravel spectrum consists, in descending order, of quartz, pegmatite, granite, siltstone, feldspar crystals, rhyolite, sandstone, gneis, quarzite and micaschist (Fig. 3). The distribution pattern of the heavy mineral spectra (Fig. 4) shows a dominance of epidote (with zoisite included > 50%), zircon and sphene. Epidote is nearly exclusively restricted to low-to medium-grade metamorphic rocks, whereas zircon and sphene are common in magmatic rocks and even in reworked sediments. Turmaline can also be derived from older sediments. Frequently appearing minerals such as amphibole (mostly green hornblende), garnet and rutile point also to a medium-grade metamorphic

hinterland. Pyroxene (mostly augite) is found in intermediate to basic magmatic rocks, but also in amphibolite facies metamorphosed rocks of basic composition. The field "others" sums up mineral phases occurring in minor percentages: staurolite (0.3%), andalusite (0.2%), sillimanite (1.2%) and brookite (0.3%). They are minerals of magmatic and metamorphic rocks.

A problem arises in the comparison of the gravel spectrum and the heavy mineral spectrum. Judging from the distribution of the gravels one would expect a predominance of zircon, apatite, possibly garnet, sillimanite and andalusite, – typical minerals associated with granites, gneisses and micaschists. Surprisingly the spectra are dominated by epidote, sphene, pyroxene and amphiboles commonly found in basic to intermediate magmatic and metamorphic rocks. Note here that heavy mineral samples are derived exclusively from sandy to fine gravelly beds and most probably represent deposits of greater transport widths and therefore multiply reworked material. The question about the hinterland can only be answered very vaguely and will be discussed briefly together with the similar situation in the Loh Formation (chapter 4.2.4). Especially the mineral assemblage epidote (with zoisite), andalusite, sillimanite and staurolite points to a metamorphosed hinterland in greenschist and amphibolite facies.

With the interpretation of the fluvial style we followed MIALL'S (1996, p. 93, table 4.3) terminology of the architectural element analysis. The stratigraphically lower parts of the Tsagaan Ovoo Fm. are domiated by debris flows (Gmm, Gmg) which correspond to sediment gravity flows (SG) as the architectural element. This element interfingers with finer clastic sedimentary gravity flows of lithofacies Sm. Unconfined channels and the broad absence of overbank fines (element FF) indicate that the lower parts of the Tsagaan Ovoo Fm. are a product of flash-flood depositional processes. This fluvial style would be best characterized by MIALL'S (1996, p. 199, table 8.3) "gravel-bed braided river with sedimentary-gravity-flow deposits".

As a whole the Tsagaan Ovoo Formation is a fining and thinning upward sequence. Two facies assemblages characterize the upper Tsagaan Ovoo Fm.: lithofacies Gt and Gp represent gravel bars and bedforms (GB) and lithofacies St and Sp reflect sandy bedforms (SB). Thus, gravel blankets and lenses interfinger with sandy sheets and wedges. Infrequently, minor channel fills (CH) passing up into overbank fines (FF) crop out. A transition between two fluvial styles after MIALL'S (1996, p. 199, table 8.3) terminology probably characterizes the described environments. On one hand typical characteristics of a "distal, sheetflood, sand-bed river" occur in this fluvial style. On the other hand similar facies assemblages and resulting architectural elements can be observed in his fluvial model of a "flashy, ephemeral, sheetflood, sand-bed river". The latter is distinguished from the previous model by lithofacies Sh and lithofacies Sl. Unfortunately, lithofacies Sh can only be observed on bed surfaces; thus, it is impossible to define it in our vertical profiles. Also lithofacies Sl could not be identified with certainty (Tab. 3).

The systematic sedimentological study of the Tsagaan Ovoo Fm. suggests that it forms an alluvial fan. We use here the term alluvial fan according to the definitions of BATES and JACKSON (1987, p. 17) and MIALL (1990, p. 345). Such fans, according to READING (1996), develop along tectonically active basin margins. In semi-arid environments the relief is commonly governed by a faulted mountain front and denudation is promoted by sparse vegetation and occasional intense rainfall (WALKER 1980). In the mapping area we were unable to identify a tectonic zone which could be related in such a way to the Tsagaan Ovoo Fm. A possible candidate might be faults connected with the Bayan Khongor fault zone, but this question requires further investigation. The alluvial fan developed prograding from N to S in its initial stage and retrograded back to the N later on. According to STEEL et al. (1977), however, a fining upward can be expected if the sedimentary response to tectonic uplift has time to return to equilibrium. Another explanation could be shifting of depositional centres on alluvial fans (autocyclic mechanisms) or tectonic processes (allocyclic mechanism).

According to the STANISTREET and MCCARTHY (1993) classification, the very initial, proximal stage of the Tsagaan Ovoo fan can be described as a transitional form between "debris flow dominated fan", typically less than10 km in radial length and a slope between 0.1 and 0.01 (modern examples: Death Valley fans, USA) and a "braided fluvial fan" with a slope between 0.001 and 0.0003 (modern example: Kosi Fan, India). Perhaps as a response to the topographic equilibrium the alluvial fan evolved a more distal facies, reflected by the upper parts of the Formation. At this time the alluvial fan had a geomorphology best described by the model of a "braided fluvial fan". The braided fluvial fan could act as source rock for the Hsanda Gol dust deposits.

4.2.3 Hsanda Gol Formation

The Hsanda Gol Fm. (see suppl. 1 & 2) crops out – apart from the vicinity of Hsanda Gol – in the east, is abundant in the central region of the working area (Tatal Gol and Del) and occurs also in the west at both sides of the Taatsiin Gol (Taatsiin Gol left and right as well as in the Khunug area). The sediments are poorly sorted clays. Generally, massive horizontally bedded layers with non erosive boundaries are common. These clayey sediments, which are "brick red", show a tendency to fracture along vertical joints. Within these sediments, duricrusts (OLLIER and PAIN 1996), namely caliche (also called calcrete) horizons, exist; they are characteristic for arid and semiarid regions (FRIEDMAN and SANDERS 1978). These observations and the high fossil content make the Hsanda Gol Fm. the most prominent lithological unit in the working area (Figs. 6a, 6b, 7). A detailed description of the fossil content is given in chapter 8. The basalt and its age are discussed in chapter 5 and 6.

The major minerals are sheet silicates with a variable amount of micas, kaolinite, chlorite and sometimes smectite. Quartz and feldspar range approximately from 25% to 40% of the total minerals. Calcite is also a major constituent in some samples, forming up to 25%. Minor constituents include hematite and goethite, responsible for the colour. The colours range from dominating moderate reddish brown (10 R 4/6), to moderate reddish orange (10 R 6/6), pale reddish brown (10 R 5/4) and dark reddish brown (10 R 3/4).

Field investigations indicate dust deposits. Furthermore, some authors (DEVYATKIN and BADAMGARAV 1993, BADAMGARAV 1993) considered at least a partially lacustrine origin. To distinguish between both origins a comparison of transport mechanisms, based on cumulative-frequency curves, of Hsanda Gol sediments with modern dust and loess deposits, respectively, seemed advisable. In Fig. 5b typical Hsanda Gol sediments (samples TGR-B14 and TGR-B23) are compared with a modern dust fall from Kansas (FRIEDMAN and SANDERS 1978) and a loess sample, Sanborn Loess 1, Kansas (SWINEFORD AND FREY 1945).

The Hsanda Gol samples consist of three populations. The truncation point between traction and saltation population lies between 3Φ and 4Φ, the truncation point between saltation and suspension around 5Φ. At least 50% and more of the

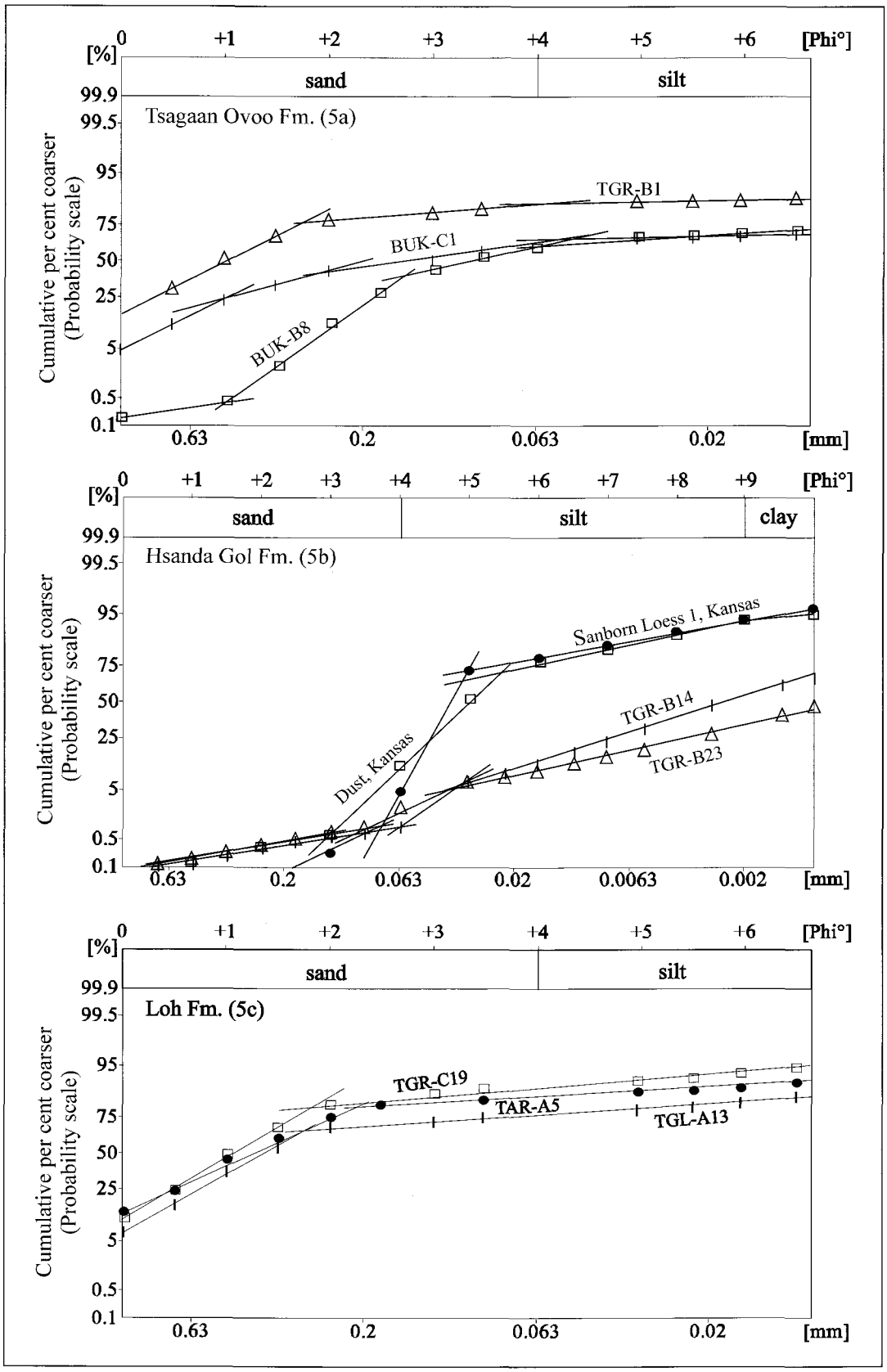

Fig. 5
Cumulative-frequency curves of samples of the Tsagaan Ovoo Formation (5a), the Hsanda Gol Formation (5b) and the Loh Formation (5c). 5a: Channel fills of the Tsagaan Ovoo Formation: TGR-B1 and BUK-C1 represent lithofacies Sm, BUK-B8 lithofacies St. 5b: Aeolian sediments of the Hsanda Gol Formation (TGR-B14 and TGR-B23) are compared with a modern dust fall deposited in a third-floor room, 7 m above the ground in the Lakeway Hotel, Meade, Kansas (FRIEDMAN and SANDERS 1978) and Sunborn Loess 1 according to SWINEFORD and FRYE (1945). All curves are equally developed and show three transport mechanisms (traction, saltation and suspension). TGR-B14 and TGR-B23 are finer grained, the saltation population is poorly developed. 5c: Channel fills of the Loh Formation: TGR-C19 and TAR -A5 represent lithofacies St and TGL-A13 lithofacies Sr.

samples are composed of the clay fraction. The sand fraction is <1%. All three populations are poorly sorted. The other two samples show also three populations, whereby the Sanborn Loess 1, Kansas, shows a better-sorted traction population. The truncation points between the traction and saltation populations are situated between 3Φ and 4Φ, those for the saltation and suspension populations again around 5Φ. FRIEDMAN and SANDERS (1978) state that cumulative-frequency curves of dust and thus loess deposits are characterized by three well-defined populations (traction, saltation, suspension). This is found in all samples. The difference between Hsanda Gol samples and the others is mainly the better sorting of the saltation populations and the higher amount of silt in the latter. The higher clay portion in the Hsanda Gol Fm. could be due to either weathering effects and multiple reworking or to increasing distance of deposits from their source (TSOAR and PYE 1987). In addition, the large clay portion of the Tsagaan Ovoo Fm. could have contributed substantially to the amount of clay in the Hsanda Gol Fm. The comparison of the Hsanda Gol curves with the typical loess curves (e.g. SINDOWSKI 1957, FRIEDMAN and SANDERS 1978, PYE 1987) indicates an aeolian origin of the Hsanda Gol sediments. On the other hand obviously differences in the grain size distribution and sorting currently not allow a clear assignment of the Hsanda Gol sediments to loess deposits. This would need further investigation.

Caliche horizons consist of sheets of secondary calcium carbonate cementing soil material or other sediments and can move by means of downward leaching, upward diffusion and most probably lateral transfer (OLLIER and PAIN 1996). The following observations have been made. Varying calcite contents in different features (dm-sized nodules, but also distinct marl layers) are evident. Marl layers thicken and thin irregularly and can be traced laterally up to several meters. In beds bearing less carbonate root traces may occur and sometimes burrows are visible. Rarely, sand and granule lenses are found, attributed to fluvial and or lacustrine reworking processes. XRD analyses prove, that evaporitic minerals such as anhydrite and rarely halite also appear in Hsanda Gol sediments. These minerals are abundant in caliche horizons. Such features point to a genesis of these layers as caliche horizons, which are described by PYE (1987) as paleosols (pedocomplexes) formed during slow or intermittent dust deposition.

In general the heavy mineral spectrum is comparable to that of the Tsagaan Ovoo Fm. (Fig. 4). Again, epidote, garnet, sphene and amphibole (green hornblende) dominate the spectrum. In contrast to the Tsagaan Ovoo spectrum the pyroxene amount decreases and the turmaline content is higher. In Fig. 4 the following minerals are summed up under the field "others": andalusite (0.3%), sillimanite (0.3%), kyanite (1.0%), apatite (2.1%). Note that the concentrations of heavy minerals in the Hsanda Gol samples are very low and the grains are poorly preserved. This supports the interpretation of their aeolian origin. The similar heavy mineral spectra of Tsagaan Ovoo and Hsanda Gol sediments are interpreted such that Hsanda Gol sediments are primarily derived from the braided fluvial fan, which generated the later Tsagaan Ovoo sediments.

A braided fluvial fan, together with a high clay proportion (about 25%) of the Tsagaan Ovoo sediments (Fig. 5a), favour the potential to act as net source for Hsanda Gol sediments. PYE (1987) stated that the grain size distribution of local dust deposits is strongly controlled by that of the source material. As already described by other authors (NICKLING 1994, NORTON 1984) our field observations also revealed that dust deposits like Hsanda Gol sediments are trapped by surface roughness elements (e.g. topographic lows, vegetation). The original topography was buried. Hsanda Gol sediments form a wedge-shaped body of rock in cross section with increasing thickness in the direction to the basin center. This could be explained by the assumption, that the "Tsagaan Ovoo braided fluvial fan" had already prograded quite far towards the basin center when the Hsanda Gol sedimentation set in. As indicated by the similarity of the heavy mineral spectrum with that of the Tsagaan Ovoo Fm., at least large portions of the Hsanda Gol dusts were derived from Tsagaan Ovoo sediments. Local syndepositional reworking (e.g. surface wash) of the primarily aeolian deposits must have taken place. Rarely occurring sandy and gravelly lenses within the beds, the existence of salt minerals, and erosion features on caliche horizons contribute to the interpretation of fluvial, lacustrine reworking of Hsanda Gol sediments. Caliche layers are impermeable and serve to perch an ephemeral water table (HUNT 1972), which contributed to the development of water holes. Large, shallow playas, as indicated by salt minerals, within a low relief landscape may have occupied the central parts of the basin.

Examinating the Tsagaan Ovoo Fm. and the Hsanda Gol Fm. together, we find alluvial fans, ephemeral streams, aeolian plains and playas, which may occupy structural depressions or shallow basins of interior drainage. These are the main components of arid systems according to FRASER (1989). This may reflect a simplified scenario valid in the Valley of Lakes during this period.

4.2.4 Loh Formation

The Loh sediments are the most widespread ones in the investigated area (see suppl. 1 & 2). In the field this formation is characterized by cross-bedded sands and gravels intercalating with silts and clays of fluvial and aeolian origin. Bright white, brown, but also red colours can be observed. In Fig. 6b (section TGR-C) the contact of the white and brownish sediments of the Loh Fm. on top of the Hsanda Gol Fm. is visible. Among others the following colours dominate the gravelly and sandy facies of the Loh Fm.: light greenish gray (5 GY 8/1), dusky yellow green (5 GY 5/2). The silty-clayey and sometimes also the sandy facies show colours such as light brown (5 YR 6/4) and dark reddish brown (10 R 3/4), light olive brown (5 Y 5/6), moderate reddish orange (10 R 6/6). The sediments consist mainly of quartz with highly variable amounts of sheet silicates. Plagioclase (up to 20%), carbonate minerals like calcite (up to 20%), dolomite and ankerite, together with anhydrite and pyrite can occur. Sheet silicates play an important role especially in the mineralogy of aeolian sediments. Mica, chlorite, smectite and kaolinite dominate the sheet silicate portion, which can reach up to 70% in some samples. Hematite in minor quantities is responsible for the frequently occurring red Loh deposits. The red colouration of Loh deposits is most probably due to the erosion of Hsanda Gol sediments.

The lithofacies types, their code and their frequency can be taken from Table 3. One important lithofacies, quite similar to the Hsanda Gol sediments, must be added to complete the lithofacies variety in the Loh Formation: in the whole working area poorly sorted, broadly structureless sandy clays with variable rodent assemblages crop out in addition to the dominating fluvial sediments. We interpret them as dust deposits.

The sediments of the Loh Fm. are dominantely trough cross-bedded, poorly sorted (Fig. 5c), polymict, matrix-supported gravels and sands (Gt, St). MPS between 2 cm and 11 cm are observed within gravel beds. Minor channel fills (Gt) and sinuous-crested and linguoid (3-D) dunes (St) dominate the Loh Fm; transverse bedforms (Gp, Sp) sometimes

occur. Channel fillings, 3-5 m in thickness with width/depth ratios of about 2, show fining upward sequences. A sequence starts with facies Gt or St, frequently containing rip up clasts composed of material of overbank fines, passing up to ripples (Sr), and ends with fine clastic overbank fines (Fl, Fsm, Fr). Facies Fl and Fsm can be interpreted as abandoned channel or waning flood deposits. The frequently occurring facies Fr represents incipient soils. Root-traces have been observed. Stacked channel complexes are occasionally visible. Channel filling sequences and sheet floods interfinger with debris flow deposits of gravel facies Gmm, Gmg and infrequently Gcm. Sometimes scour fills (Ss, Sl) occur; these are difficult to separate from channel fillings. A mighty pebble horizon of facies Gh (bed thickness=3.5 m; MPS=11 cm) below basalt II (lower left corner in Fig. 10b) occurs in columnar section TAR-A (suppl. 3). Such channel fillings are exceptionally rare events.

Cumulative-frequency curves in Fig. 5c show three sand samples of channel fills: TGR-C19 (St), TAR-A5 (St) and TGL-A13 (Sr). They show only two transport mechanisms represented by the saltation and the suspension population. The truncation point separating them lies between 1.75Φ and 2.15Φ. Sample TGL-A13 is taken from a rippled bed and thus slightly finer grained (lower flow regime). Samples TGR-C19 and TAR-A5 are generated by 3-D dunes. The traction population is totally missing, which could be explained by hyperconcentrated grainflows (MAIZELS 1989) that transport their load by saltation and suspension. The high clay content (about 15%) increases the viscosity and yield strength of the flow and thus supports this interpretation.

Within the Loh Fm. several layers are of aeolian origin and are associated with caliche horizons, which show the same features as those in the Hsanda Gol sediments. Especially these aeolian deposits are rich in fossils, whereas the fluvial facies is poor in small mammals but contains large mammals. In profiles ABO-A, LOG-A, LOG-B, LOH-A, ODO-A, ODO-B, RHN-A, TGW-A, TAR-A and UTO-A the aeolian lithofacies can be examined (suppl. 3). They were primarily deposited as dusts but show clear features of reworking processes. First investigations of cumulative-frequency curves showed distinct differences in the transportation mechanisms compared to Hsanda Gol sediments as, they have almost no saltation population. In the field the aeolian Loh sediments can be differentiated from Hsanda Gol sediments by their coarser grain size and their more brownish-red colour. The distinction in the field is sometimes problematic.

Paleocurrent indicators like trough and planar cross-bedded sands and imbricated gravel beds reflect the same average paleodrainage pattern from N to S as documented in the Tsagaan Ovoo Fm. Flow structures of both basalt events (II and III) also indicate a paleorelief dipping to the S.

Nine gravel samples each containing between 500 and 2200 grains, have been examined in the field. The gravel spectrum consists in descending amounts of quartz, granite, siltstone, pegmatite, micaschist, basalt, rhyolite, carbonate-tuff, feldspar crystals, sandstone, gneiss, quarzite and carbonate (Fig. 3). Some gravel samples bear carbonate and carbonate-tuff components, which are certainly derived from the underlying Hsanda Gol sediments. The gravel spectra of the Tsagaan Ovoo and Loh Fm. show qualitatively the same lithologies, except that Loh gravels have basalt, carbonate and carbonate-tuff components, due to erosion of Hsanda Gol sediments and basalts (I, II and III), too. These differences make the two gravel-bearing formations distinguishable in the field. The dominance of quartz along with granite and pegmatite components, compared with the much more balanced distribution of lithologies in Loh gravels, is interpreted to reflect differences in geomorphology and thus fluvial style on the alluvial fans, which characterized the deposition of the Tsagaan Ovoo and the Loh sediments.

The heavy mineral spectrum of the Loh Fm. is in general comparable with that of the Tsagaan Ovoo and Hsanda Gol Formations (Fig. 4). It is dominated by epidote, amphibole (green hornblende), pyroxene, zircon and sphene. Additional minerals under the heading "others" include: staurolite (0.5%), sillimanite (1.4%), kyanite (1.0%), brookite (1.0%), apatite (1.6%) and monazite (1.2%). Tsagaan Ovoo and Loh sediments are of fluvial origin and thus better comparable. Once again a greenschist and amphibolite metamorphosed hinterland was eroded. The increasing amount of pyroxene (augite) can be explained by the erosion of basalts I, II and III. The obvious increase of amphibole and the decrease of epidote is caused by one sample dominated almost exclusively by amphibole and does not necessarily indicate a change in the hinterland. Note again that the heavy mineral spectra are derived from sandy samples and thus reflect multiple reworking processes and at least a greater transportation distance. As for the gravels, the basalts, carbonate and carbonate tuff components are at least partly derived from Hsanda Gol and Loh sediments.

The occurrence of granitic rocks, metamorphics and sediments in the gravel spectrum, as well as the corresponding heavy mineral spectra, are both consistent with the geological frame of the Valley of Lakes as described in chapter 3 (see also Fig. 2). The Baidrag zone is a likely candidate for the origin of high-grade gneisses and micaschists and heavy minerals such as garnet, kyanite or sillimanite. The large amount of epidote, amphibole, sphene (partly) and pyroxene (possibly) may be derived from the Bayan Khongor zone with its metamorphic volcanics and ophiolites. The low-grade metamorphic pebbles and the accordingly heavy minerals may stam from the Burdgol and the Dzag zones, the sediments from the Paleozoic Khangai zone. The numerous granites (Fig. 2) are responsible for the granitic pebbles and heavy minerals such as zircon or apatite. In general, the hinterland of the Tsagaan Ovoo and the Loh Formations has not changed very much since the Eocene(?) and is well comparable to that seen today in the Khangai and Ushgoeg Mtns.

An interpretation of a possible facies model of the Loh Formation is given below. The Loh Fm. is characterized by lithofacies Gt and, of minor importance, Gp, which represents – on the architectural element level – gravel bars and bedforms (GB). Examples for sandy bedforms (SB) are samples TGR-C19 (St), TAR-A5 (St) and TGL-A13 (Sr). Sometimes overbank fines (FF) and rare sedimentary gravity flows (SG) are visible. In the facies model "shallow, gravel-bed river", element GB predominates; furthermore, element SB with minor thicknesses and rare debris flows of element SG can occur. The main architectural components in the fluvial type "shallow, perennial, sand-bed braided river" are element SB and FF. Both facies models represent perennial flowing river types. The samples presented in Fig. 5c are typical channel fillings (St and Sr) of different flow regimes, which broadly dominate the depositional processes. In addition debris flows, typical for ephemeral streams, interfinger with these lithofacies (St, Sr). This observation limits the interpretation of a perennial flowing river system. The Loh Fm. probably reflects a fluvial system between a "shallow, gravel-bed river" and a "shallow, perennial, sand-bed braided river", but with restrictions to a more ephemeral character. After STANISTREET and MCCARTHY (1993) the type of the respective alluvial fan would be a transitional form of a "braided fluvial fan" and a "low

Fig. 6a
View of the plateau W of the Taatsiin Gol seen from across the Taatsiin Gol valley towards southwest. The bright white sediment layer above the Quaternary sediments represents the Tsagaan Ovoo Formation, which is overlain by the brick red Hsanda Gol Formation. The black basalt layer I has a thickness of 15 to 20 m here. The thin Hsanda Gol silts and clays above the basalt I cannot be seen from the view point; the white and red sediments on top of the basalt are part of the Loh Formation and are in turn covered by the brownish gravels and sands of the Tuyn Gol Formation.

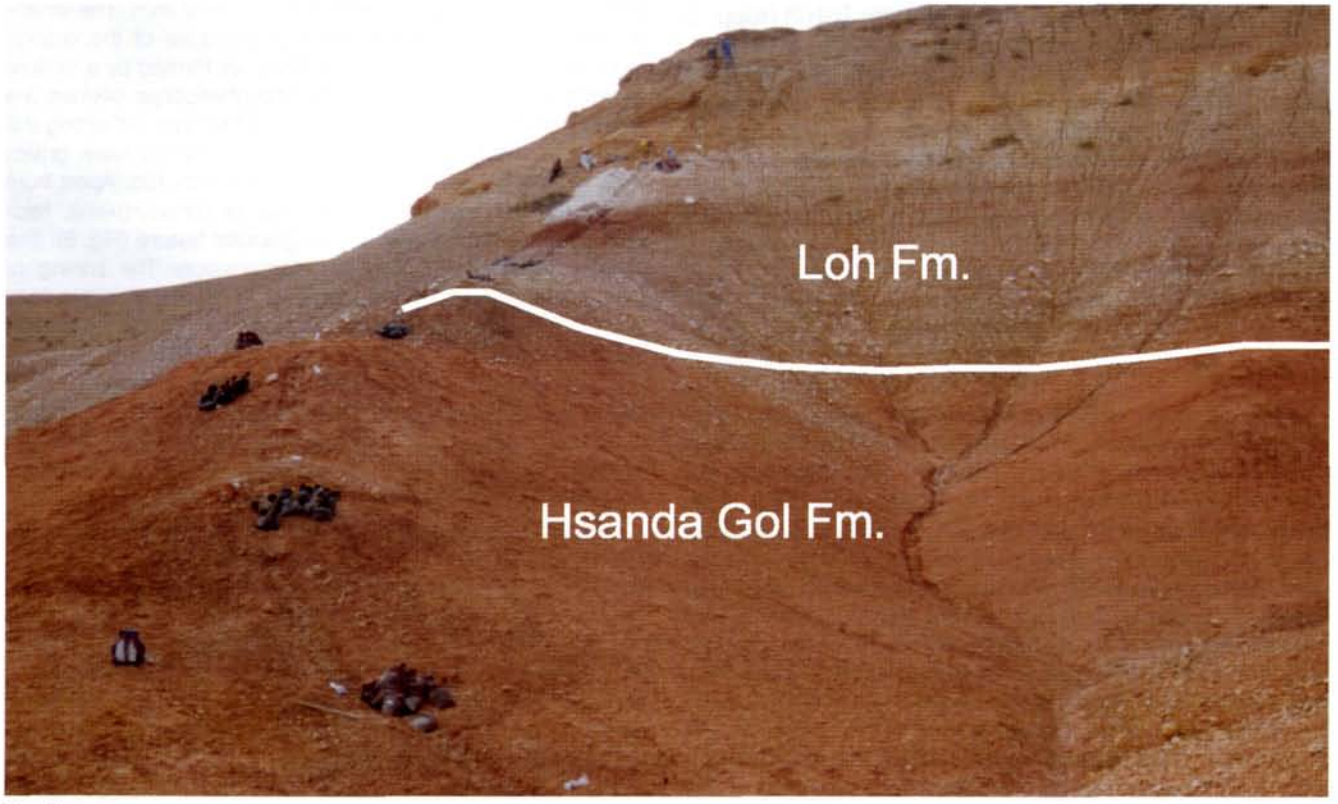

Fig. 6b
Close-up view of the Hsanda Gol and Loh Formation at the profile TGR-C. The boundary between both formations is visible at the bottom of the white sediments in the upper quarter of the photo. The sediments of the Loh Formation on top contrast with their brownish-red colour to the brick red sediments of the Hsanda Gol Formation at the bottom. The white pebbles and horizons in the higher parts of the Hsanda Gol Formation (center of the photo) come from caliche horizons. The dark holes along the profile stem from paleontological sampling.

sinuosity/meandering fluvial fan". The latter type is represented by the Okavango Fan, which is a very large example (150 km in axial length) for subaerial fans – a dimension hardly imaginable for the "Loh braided fluvial fan". Several progradations and regressions of the "Loh braided fluvial fan" are indicated by the interfingering of aeolian and fluvial sediments. The aeolian sediments must have had a source in their immediate vicinity. The sedimentological analysis reveals differences in the deposition of the Tsagaan Ovoo and Loh braided fluvial fans. This is expressed in their geomorphology and fluvial style. It is also supported by the different distribution of gravel lithologies of both formations. They contain the same rocks, but the distribution is more balanced in the Loh Fm. Apparently, during the sedimentation of Loh deposits a more humid climate prevailed. Field observations and cumulative-frequency curves showed intensive reworking of the Loh dusts. In comparison, Hsanda Gol dusts did not undergo such intensive weathering processes. Features such as well-defined stacked channel complexes support this view. Furthermore, frequently occurring overbank fines with paleosol developments point to a river type dominantly flowing within its confinements. The more humid climate and the river type gave the vegetation the possibility to develop a denser cover, which in turn increases the potential to preserve overbank fines.

4.2.5 Tuyn Gol formation

DEVYATKIN (1994) described the Tuyn Gol fm. as sediments younger than 2 Ma directly underneath Quaternary deposits. In the working area this formation crops out rarely and is restricted to the plateaus west and east of the Taatsiin Gol (suppl. 1). It will be characterized very briefly.

The Tuyn Gol formation crops out in profile TGR-B (suppl. 3 & 4). The sediments are poorly sorted, matrix-supported, grey-brown gravels. In general a clayey matrix can be found. Quartz components with Fe2O3 coatings along with basalt, siltstone, granite, quarzite, gneiss, rhyolite, micaschist, sandstone and pegmatite dominate the gravel spectrum. Two gravel samples were analysed, showing an MPS of about 9 cm. No basalt flows or fossil-bearing horizons were found in this formation.

5. Basalts

Cenozoic, partly also Mesozoic basaltic volcanism is concentrated in a relatively small, approximately NW-SE to NNW-SSE striking corridor in Central Mongolia (Fig. 1) between 98° and 104°E (KEPEZHINSKAS 1979, WHITFORD-STARK 1987). It extends from China at the southern border of Mongolia (YARMOLUK et al. 1995) up to Siberia just west of Lake Baikal in the north. Other occurrences are found in eastern Mongolia near the Chinese border and east of Lake Baikal in Siberia. The Taatsiin Gol area is positioned in the center of this corridor (Fig. 1) and is well known for its basalt layers in Paleogene and Neogene sediments (e. g. BERKEY and MORRIS 1927, DEVYATKIN 1981, 1993b, DEVYATKIN et al. 1973, GENSHAFT and SALTYKOVSKY 1990, GENSHAFT et al. 1990, KEPEZHINSKAS 1979). Only little is known on the mineralogy and petrology. A few geochemical analyses of major elements of the basalts were published in recent years (GENSHAFT and SALTYKOVSKY 1990, GENSHAFT et al. 1990, KEPEZHINSKAS 1979). BARRY and KENT (1998) published a comprehensive study on the Cenozoic magmatism in Mongolia.

5.1. Occurrence and Petrography

The geological map (suppl. 1) shows that basalts are found in the Hsanda Gol and Loh Formations. In the Taatsiin Gol area we distinguished in total three coherent basaltic and/or trachybasaltic to trachyandesitic layers. For the sake of simplicity we named them from the oldest to the youngest: basalt I, II (including IIa) and III. Basalt I is found in the Hsanda Gol Fm, whereas basalt II, IIa and III occur in the Loh Fm.

The basalt I occurrences are concentrated in the southern and central part of the mapped area (suppl. 1). The most prominent outcrops are found in the plateau W of the Taatsiin Gol (TGR and TGW; Fig. 6a,b), the plateau east of the Taatsiin Gol (TGL), in a small strip along the Del fault, in the Tatal Gol, and in the lava flows east of Tatal Gol (see also suppl. 1 & 2). Minor occurrences are found in the Hsanda Gol. The Del fault terminates the basalts towards the north. The thickness of basalt I varies from a minimum of 5 m up to a maximum of 15-25 m. Occasionally it is entirely missing. The basaltic sequence starts with a few centimeters to decimeters thick, dark red tuff horizon (Fig. 7) which is locally the only volcanic layer (e. g. profile DEL-B in suppl. 3). Among the basalt flows at least two individual layers can be recognized: a deeper, thicker bed and an upper, thinner layer separated by a cooling horizon and in some places by thin Hsanda Gol type sediments. Two centers of eruption were identified from which the basalt I flows originated. They form approximately 100 m high volcanic cones just north of the Del fault and are named Barun Hsir (Fig. 8) and Dsun Hsir (for the location see suppl. 2). Rare tuffs are associated with the cones.

The basalts form flows that show a highly vesicular surface in parts. Macroscopically small olivines form phenocrysts in a mostly well-crystalline matrix with an intergranular texture. The size of the phenocrysts varies from 0.5 to 2 mm. The olivine phenocrysts are often conspicuous because of the orange red weathering rims (iddingsite). They are formed by a mixture of iron(hydr)oxide and smectite. The phenocryst olivines are zoned from Fo_{83} in the core to Fo_{40} at the rims, reflecting the cooling of the lavas. The groundmass olivines have grains varying from 0.1 to 0.5 mm and are iron rich, too. Apart from the olivine the groundmass consists of clinopyroxene, feldspar and ilmenite forming an intergranular texture (Fig. 9). The clinopyroxene has a diopsidic composition. The zoning of plagioclase (~An 60 in the core and An 30 at the rim) is seen in the backscattered electron image (BEI) in Fig. 9. Regarding the feldspars a wide variety of compositions were identified, covering all compositions from labradorite, andesine, oligoclase to a ternary feldspar and alkalifeldspars. The corresponding characteristic compositions would be for example $An_{58}Ab_{40}Or_{02}$ (labradorite), $An_{14}Ab_{72}Or_{14}$ (ternary feldspar), or $An_{04}Ab_{50}Or_{46}$ (alkali feldspar).

Basalt II is found in the very north of the mapped area near the Tarimalyn Khurem (TAR) region (suppl. 2), where it is deposited within the Loh Formation (Fig. 10a). More prominent outcrops occur in the northwest, where basalt II is partly directly overlain by basalt III, partly separated from the latter by a small horizon of Loh sediments. Basalt II is restricted to the Loh Formation; it never occurs, despite a stratigraphic overlap (comp. chapter 9), in the Hsanda Gol Formation.

The thickness of this basaltic layer in the TAR area is 5-7 m; in the northwest it can exceed 25 m. In some places up to eight individual lava flows were distinguished. For paleoenvironmental considerations it is worthwhile to note that, in TAR pillow structures formed locally where the basalt obviously flowed into a shallow water pond with clay and silt sediments (Fig. 10b). The typical basalt II samples are mineralogically

Fig. 7
Footwall contact of basalt I with the underlying Hsanda Gol Formation. A 20 cm to max. 40 cm thick horizon of pinkish tuff separates the red Hsanda Gol silts and clays from basalt I.

Fig. 8
View of the volcanic eruption center Barun Hsir (for location see suppl. 2) from the north. The rocks in the foreground are Permian sediments and volcaniclastics. The lower part of the eruption center is built up by Mesozoic sediments (Ondai Sair Formation) and Tsagaan Ovoo sediments. In the background towards the south the crystalline massif of the Baga Bogd is visible.

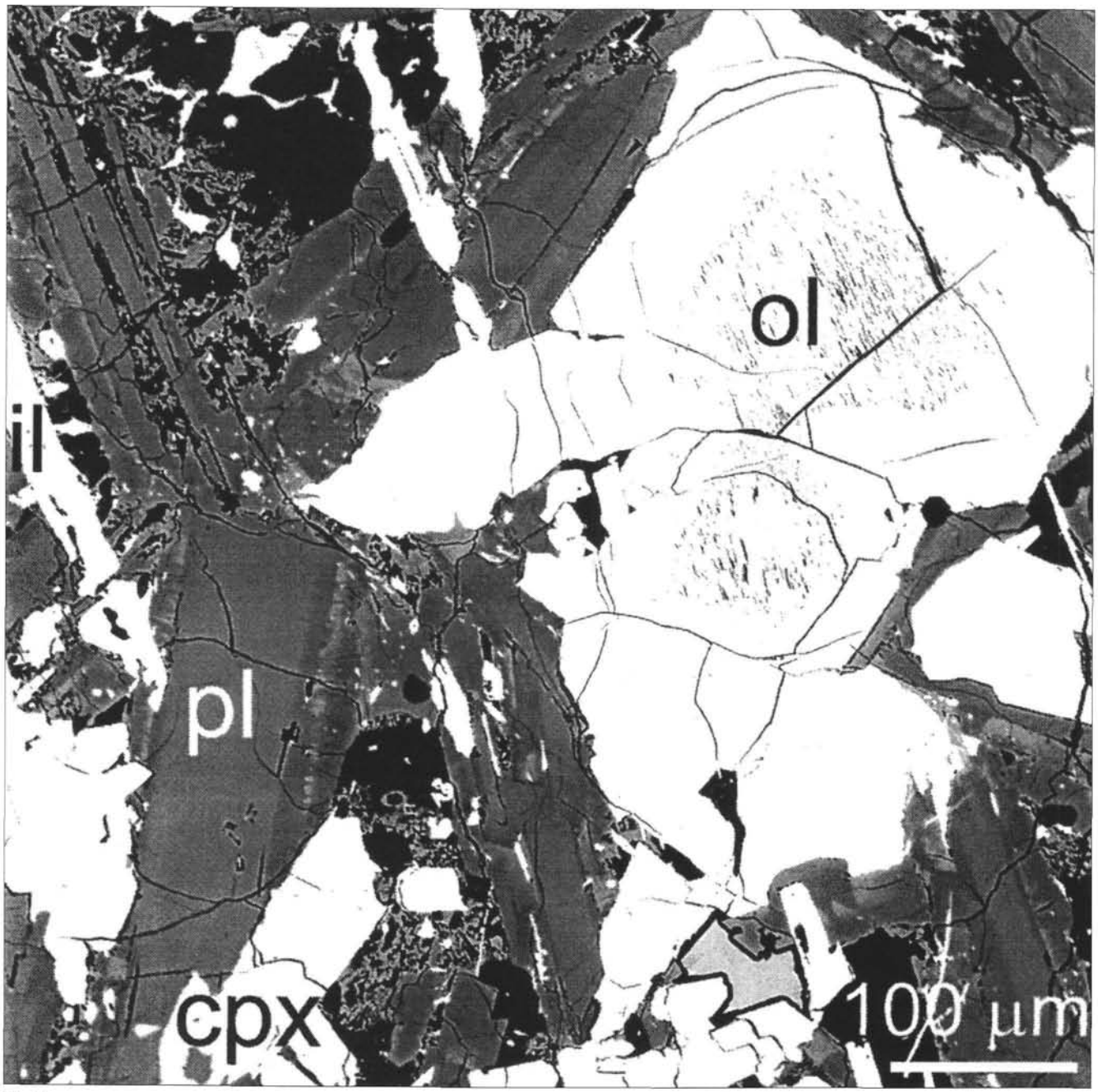

Fig. 9
Backscattered electron image (BEI) of a thinsection from basalt I. The section displays a compositionally zoned olivine (ol) in a crystalline matrix of clinopyroxene (cpx), plagioclase (pl), olivine and ilmenite. Due to the brightness, cpx and ilmenite are completely white, the zoning of plagioclase (pl) is shown here with light grey (An_{55-60}) in the core and dark grey at the rims (An_{35-40}).

and texturally identical with basalt I. $^{40}Ar/^{39}Ar$ dating on basalts from the Barun Hsir and Dzun Hsir indicated 27-28 Ma for some of the basalts, which have an appearance like basalt II but show an intermediate geochemistry between basalt I and III. Therefore, these basalts were labeled IIa. Both eruption centers acted during the 27-28 Ma volcanic event.

Basalt III, finally, is found as top of the plateau east of the Taatsiin Gol (TGL) and in the same area as basalt II, i.e. north and northwest of the mapped area (Fig. 10a and suppl. 1 & 2). In fact, the volcanics of basalt III can be classified as basaltic trachyandesites and trachyandesites, but for the sake of simplicity will still be referred to here and in the following sections as "basalt III". It forms flows which are 10-20 m thick in the north but thin out to less than 1 m at their southern end. In many areas the basalts are highly vesicular and form blocky surfaces. Several flows were distinguished. Basalt III forms in most of the plateaus the uppermost layers (Fig. 10a) and was found only rarely to be overlain by the Tuyn Gol formation, e.g. in the plateau east of the Taatsiin Gol (suppl. 1). Basalt III is significantly different in its mineralogy and geochemistry from the former basalts. Olivine phenocrysts occur, but their size (0.1 to 0.5 mm) and their amount is smaller compared to basalts I and II. The groundmass consists of clinopyroxene and a wide variety of feldspars ranging from alkalifeldspars ($An_{06}Ab_{47}Or_{47}$) and ternary feldspars ($An_{15}Ab_{70}Or_{15}$) to plagioclase with a andesine composition ($An_{40}Ab_{56}Or_{04}$). Here, alkalifeldspar and ternary feldspars dominate. Brown glass is occasionally preserved; in the very north, remnants of glasses with olivine microphenocrysts were found. The BEI image in Fig.11 shows a typical section with the intergranular texture,

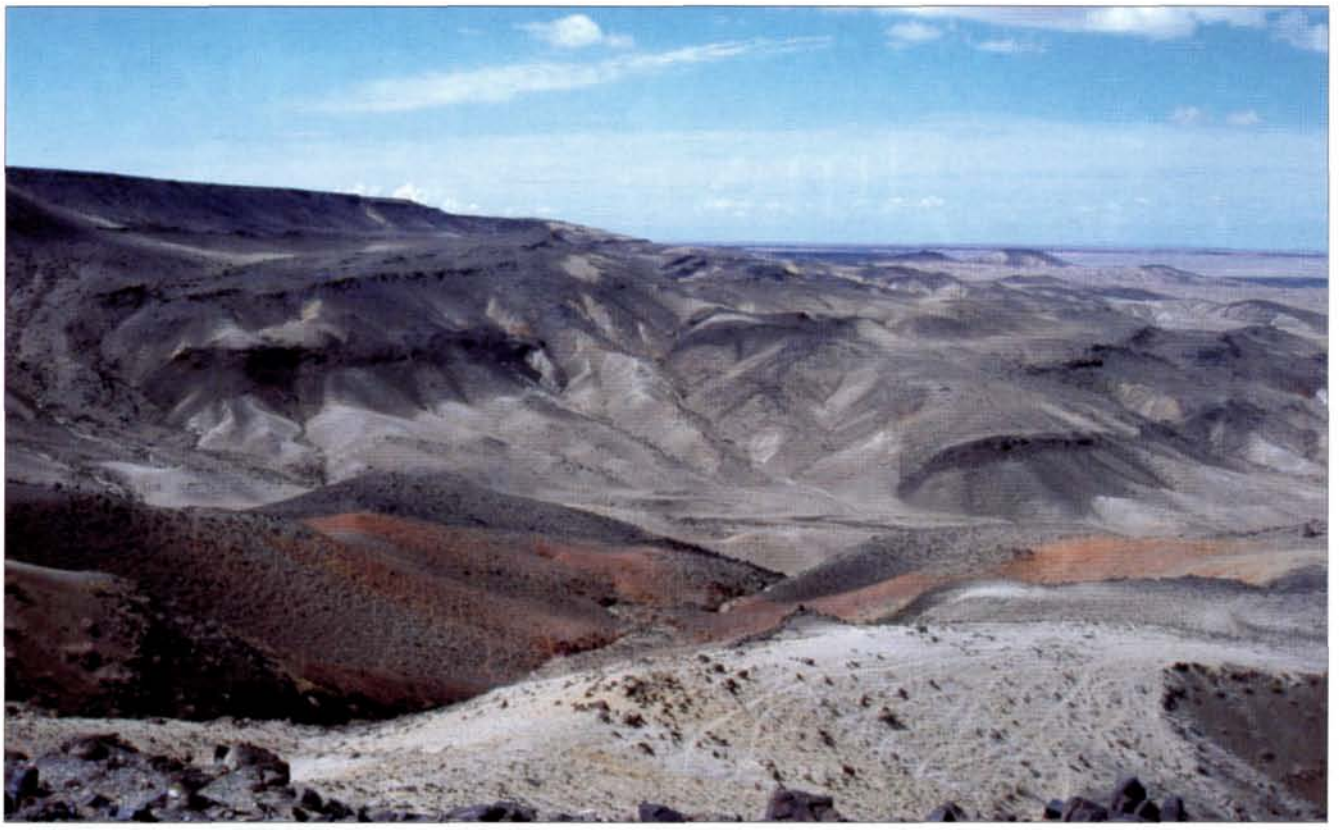

Fig. 10a
View from the north to the basalt plateau near Tarimalyn Khurem (left side). The plateau is topped by basalt III and the second basalt layer can seen embedded in sediments below basalt III at the extreme left-hand side. This is the trace of basalt II. The basalt layers below the upper two basalts are not separate flows but are downfaulted (towards the northwest along northeast-southwest striking faults) by small mass movements. The sediments belong entirely to the Loh Formation.

Fig. 10b
Basis of basalt II at Tarimalyn Khurem. The basalts form pillows indicating an ephemeral lake or pond into which the basalt poured. The very fine-grained silty to clayey sediments are lake sediments. They cover gravels typical in this area for the Loh Formation.

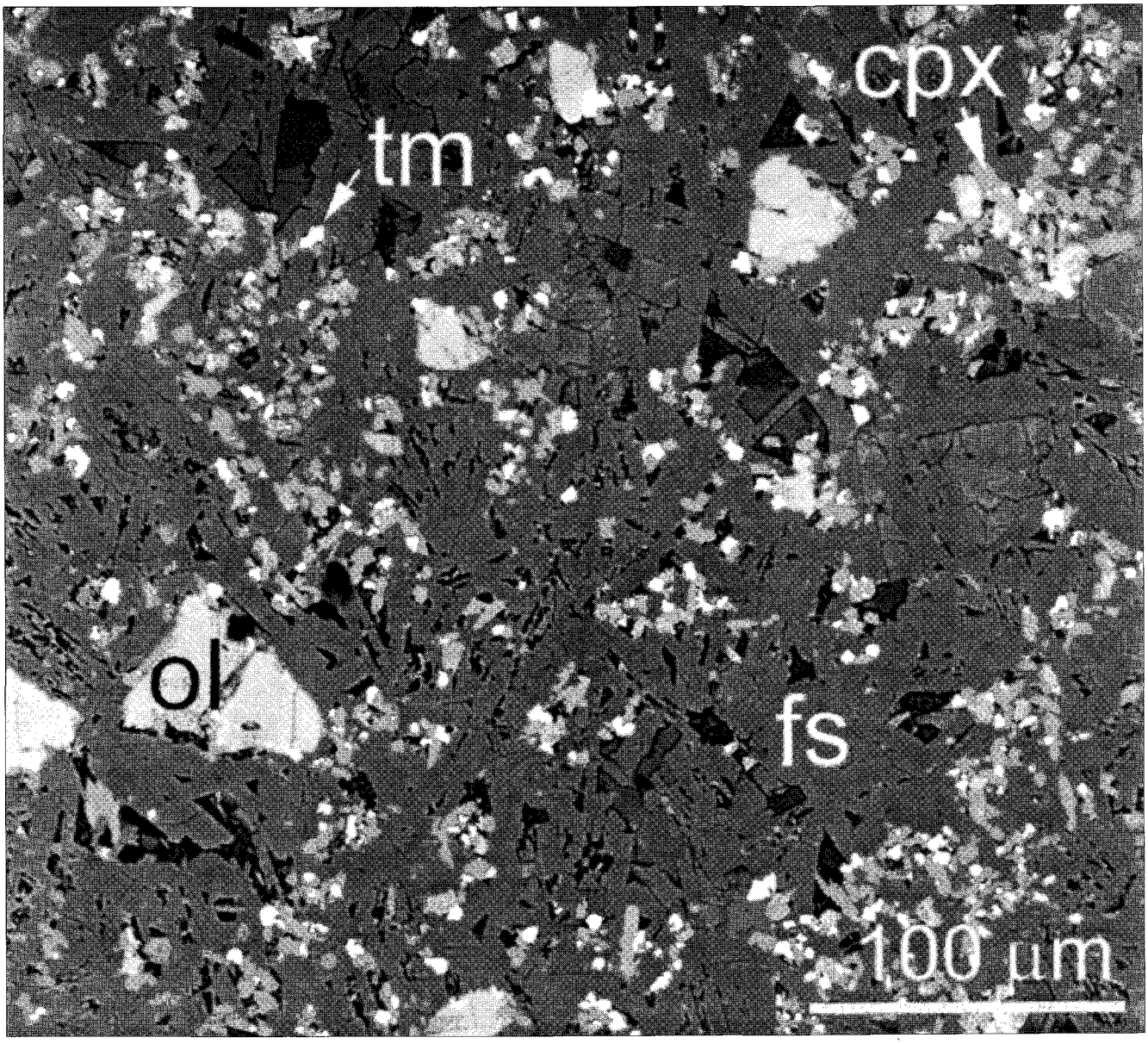

Fig. 11
Backscattered electron image (BEI) of a thinsection from basalt III. The section displays in a crystalline matrix of feldspar (fs=dark grey with a composition ranging from alkalifeldspar over ternary feldspars to relatively albite-rich plagiclase), clinopyroxene (cpx with a diopsidic composition), olivine (ol) and Fe-Ti oxides (tm=titanomagnetite). Embedded in the matrix are Fe-rich olivine microphenocrysts (< 100i in diameter).

some olivine phenocrysts and the groundmass composed of feldspars, olivine, clinopyroxene and ore-minerals.

5.2. Geochemistry

A representative selection of geochemical analyses for all three basalt groups is given in Table 4. Their SiO_2 content ranges from 45% to 57% normalized on a waterfree basis. The total alkalies vary from 4 to 10%. Thus, according to LE MAITRE (1989), all the volcanics can be classified in the TAS diagram (Fig. 12) as basalts, trachybasalts, basaltic trachyandesites and trachyandesites. Most of basalts I and basalts II are basalts to trachybasalts, and the basalt III group ranges mainly from basaltic trachyandesites to trachyandesites. A small subgroup of basalt II (see below) has also been classified as basaltic trachyandesites. This geochemical classification is consistent with the mineralogy. In many of the major elements (Tab. 4 and Figs.12, 13a-c), basalt I and basalt II are indistinguishable. Basalt group III has more Si, Al, Na and K, but less Ti, Mg and Ca.

Associated with the eruption centers Barun Hsir and Dzun Hsir are relatively coarse-grained doleritic lavas. They occur in the centers of the volcanic cones and are most likely the youngest magmatic products, cooling relatively slowly in the volcanic feeder channels. Preliminary age dating (see below) assigned these lavas to basalt group II with an age between 27 and 28 Ma. While these basalts are mineralogically and texturally very similar to basalt group II, they are – geochemically at least –, partly different and were classified as basaltic trachyandesites (Fig. 12). Their geochemistry in respect to many elements is intermediate between basalt II and basalt III, but they are separated from these groups by low MgO, high Al_2O_3, and the highest Ti content between 2.65 and 2.95% TiO_2.

There is a very well-developed covariation between major elements such as CaO vs SiO_2, Al_2O_3 vs SiO_2, K_2O vs MgO,

Sample	Mon04/96	Mon09/96	Mon10/96	Mon18/96	Mon21/96	Mon23/96	Mon37/96	Mon56/96	MonDV/95	Mon09/97	Mon10/97
SIO2	47.98	49.81	46.83	53.60	47.84	52.78	47.69	48.84	54.43	50.79	50.54
TIO2	2.42	2.43	2.58	1.96	2.52	1.92	2.52	2.62	1.84	2.88	2.77
AL2O3	14.34	14.55	14.07	15.38	13.77	15.23	13.82	13.93	15.86	15.34	15.52
FEO	10.01	9.48	10.28	8.98	9.32	9.09	9.84	10.04	9.07	8.98	9.28
MNO	0.15	0.19	0.26	0.12	0.22	0.11	0.17	0.19	0.10	0.11	0.14
MGO	6.85	6.78	6.00	4.57	7.81	4.69	8.85	7.75	3.89	4.28	4.02
CAO	9.34	8.78	10.08	5.45	10.42	6.14	9.57	9.31	4.95	7.54	7.43
NA2O	3.48	3.63	3.21	4.36	2.81	4.44	3.06	2.87	4.55	4.40	4.16
K2O	2.48	2.33	2.97	3.98	2.15	3.70	2.10	2.13	3.91	3.07	3.11
P2O5	0.87	0.76	0.92	0.83	0.78	0.82	0.80	0.62	0.94	0.91	1.03
LOI	1.44	1.40	2.75	0.66	2.29	1.58	1.85	1.26	0.99	1.89	2.63
SUMME	99.37	100.14	99.96	99.88	99.94	100.49	100.26	99.54	100.53	100.18	100.62
NB	56	49	69	47	60	43	58	59	48	58	62
ZR	218	211	256	228	207	211	206	206	237	251	259
Y	24	23	27	18	22	18	21	22	19	23	23
SR	1008	932	1438	1183	973	1127	953	965	1217	1154	1128
RB	47	45	60	42	34	39	38	36	43	47	39
NI	129	100	130	90	127	82	136	132	100	36	40
CR	166	163	170	104	230	101	254	234	99	75	n.a.
U	1.93	1.18	1.37	1.77	1.19	1.98	1.22	1.47	1.63	n.a.	n.a.
TH	4.45	3.53	1.15	3.25	3.47	2.30	3.94	3.43	3.29	n.a.	n.a.
GA	23	23	23	27	22	27	22	22	28	26	25
BA	877	740	1057	629	738	584	672	727	668	794	787
ZN	114	107	123	127	107	119	106	106	134	83	94
V	166	155	165	102	173	102	180	177	97	126	121
SC	13	14	14	7	16	6	16	15	6	10	10
CO	40	36	36	23	43	29	45	40	24	n.a.	n.a.
CU	43	31	46	24	39	25	40	38	28	35	45
TA	3.24	2.90	2.88	2.84	3.61	2.77	3.53	3.74	2.99	n.a.	n.a.
HF	5.08	4.74	4.71	5.28	4.70	4.93	4.81	4.91	5.22	n.a.	n.a.
LA	42.00	30.00	50.00	37.00	30.00	34.00	35.00	35.00	40.00	38.40	36.70
CE	70.27	72.01	71.51	79.17	46.42	0.00	62.53	64.63	11.35	85.90	69.40
ND	40.00	26.00	38.00	37.00	21.00	32.00	32.00	44.00	43.00	n.a.	n.a.
EU	2.79	2.59	2.57	2.74	2.51	2.66	2.44	2.50	2.86	n.a.	n.a.
GD	2.67	2.21	7.30	6.90	7.44	6.57	9.07	8.64	8.23	n.a.	n.a.
TB	1.29	0.89	0.88	0.87	1.07	1.07	0.99	1.09	0.82	n.a.	n.a.
YB	1.67	1.62	1.54	0.99	1.67	1.01	1.55	1.67	0.69	n.a.	n.a.
LU	0.25	0.18	0.22	0.16	0.18	0.18	0.25	0.27	0.15	n.a.	n.a.

Tab. 4

Representative geochemical anlyses for all basalt groups. Group I: Mon 04/96, Mon 09/96, Mon 10/96; Group II: Mon 21/96, Mon 37/96, Mon 56/96; Group IIa: Mon 09/97, Mon 10/97; Group III: Mon 18/96, Mon 23/96, Mon DV/95.

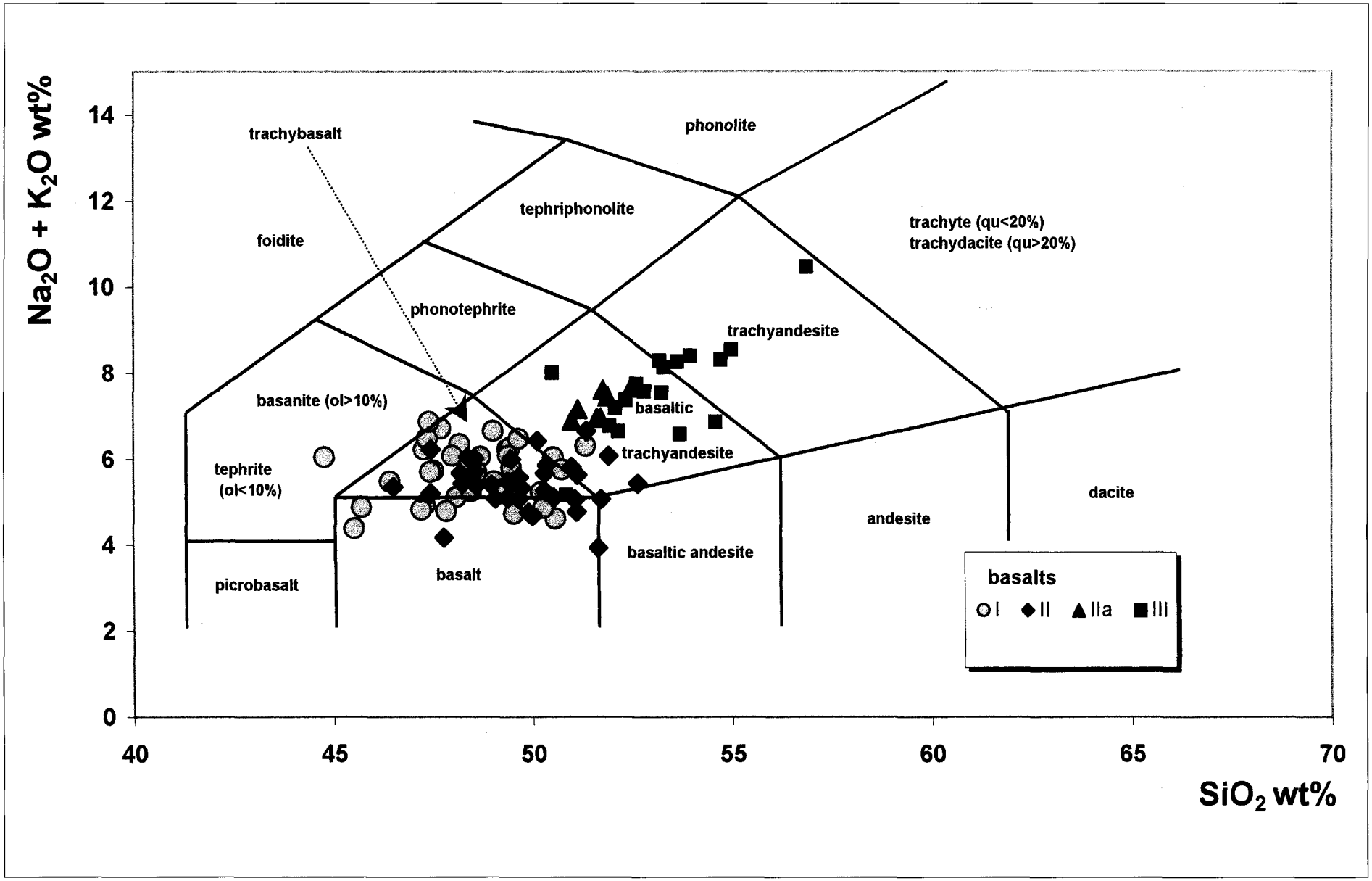

Fig. 12
TAS diagram for the classification of volcanic rocks according to LE MAITRE (1989). The legend for the basalts is given in the insert. All analyses are shown on a anhydrous basis. The majority of basalts I and II plot in the field of trachybasalt, some plot near the boundary in the basalt field, few in the basanite field. While only four analyses from basalt I and II can be found in the basaltic trachyandesite field, all analyses of basalt IIa and most of basalt III plot in this field. Few basalt III analyses extend towards the trachyandesite field.

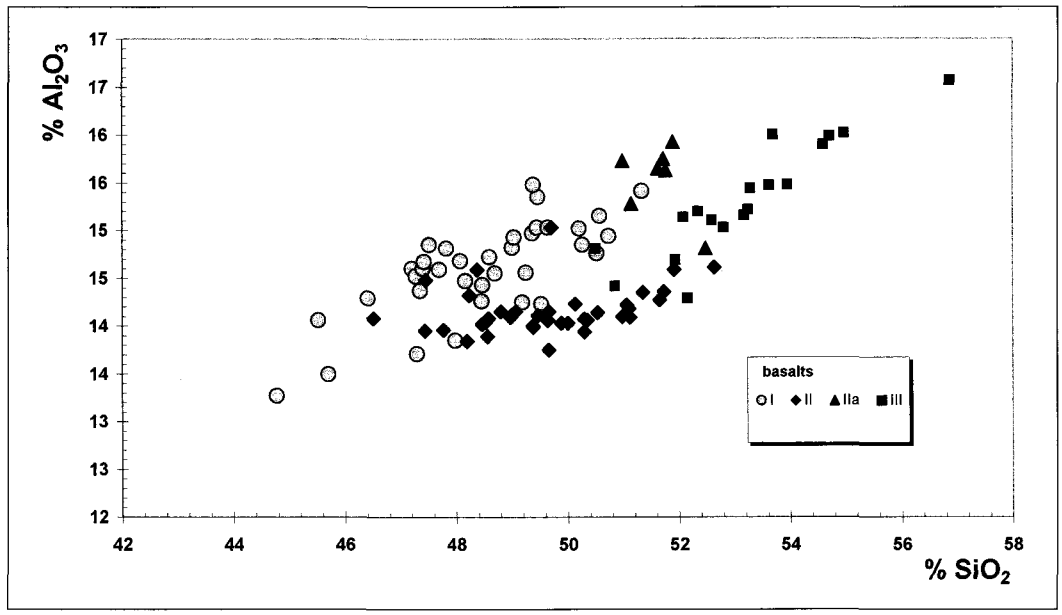

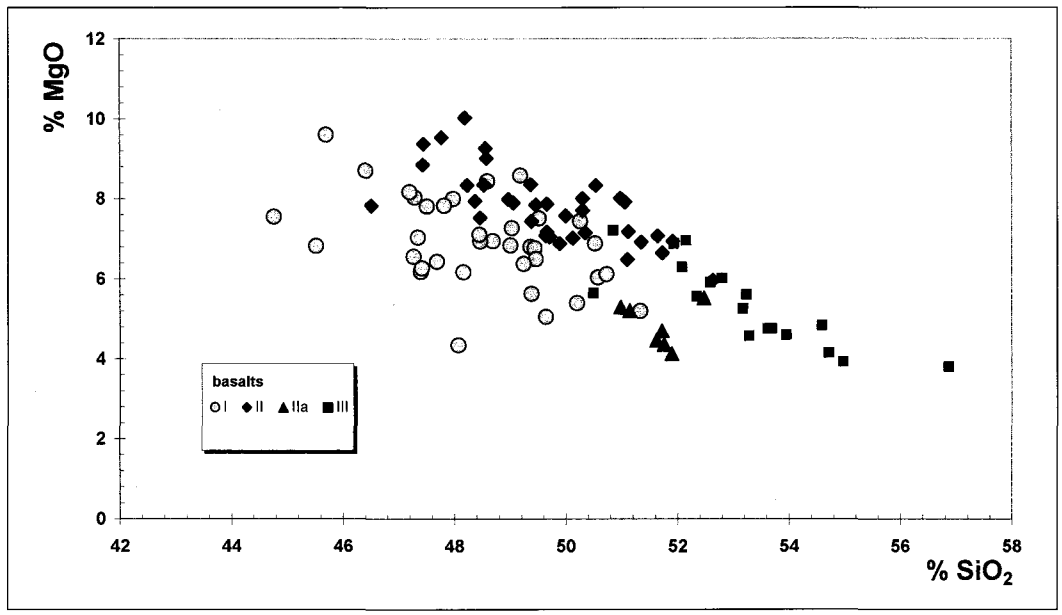

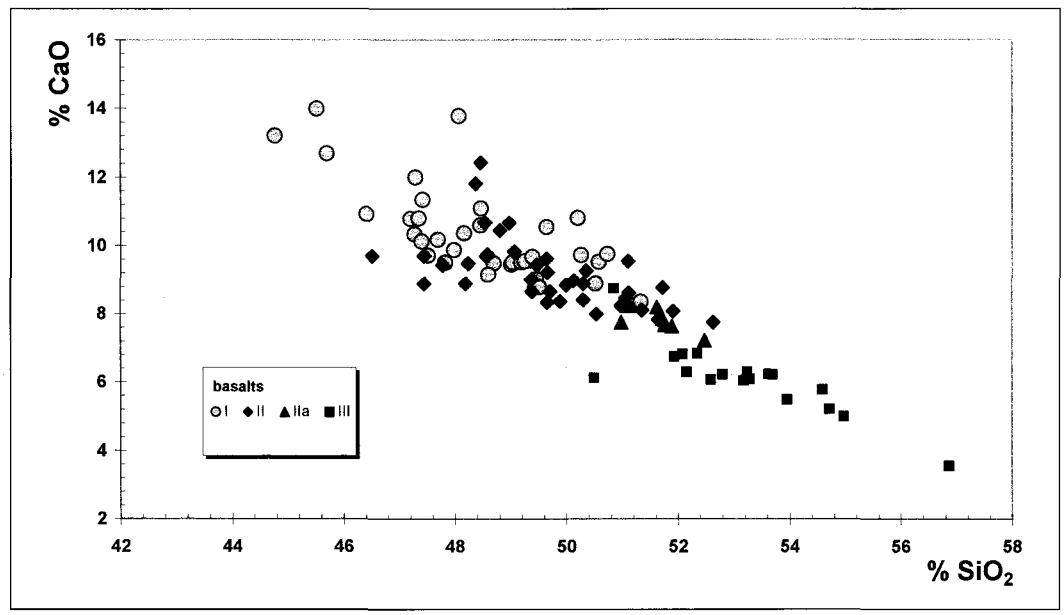

Fig. 13
Harker diagrams with Al_2O_3, MgO and CaO for basalts I, II, IIa, and III. The legend for the basalts is given in the insert. There is a general positive covariation with Al_2O_3 (Fig. 13a) and a negative covariation with MgO (Fig. 13b) and CaO (Fig. 13c). Basalts I and IIa have a higher Al and a lower Mg content at a given SiO_2 compared with basalt II. A small compositional overlap can be observed between basalt II and basalt III in the range between 51 and 52.5% SiO_2.

and CaO vs MgO among all three groups. As an example the Harker diagrams of Al_2O_3, MgO and CaO are given in Fig. 13a-c. From these covariation diagrams several conclusions can be drawn.

- The covariation of each group is compatible with some fractionation of anorthite and forsteritic olivine. As can be seen from the thin sections, only the forsteritic olivine (Fo 83-85 in the core) appears as phenocryst, but no anorthite. Plagioclase is found only in the groundmass with a composition of andesine and labradorite. The originally crystallized anorthite must have been removed from the system.
- Some diagrams such as CaO vs SiO_2, CaO vs MgO or Al_2O_3 vs SiO_2 clearly show, that the three groups cannot be derived from each other by fractional crystallization because of their parallel to subparallel evolution trend with different oxide concentration at a given SiO_2 level. Groups I and II for example have the same range of SiO_2 concentrations, but the Al_2O_3 content in group I is generally higher and the MgO content lower compared to group II.
- It is also clear that group IIa has to be separated from group III despite a certain similarity, because of significantly higher Ca or Al at a given SiO_2 level compared with group III lavas.

The separation of the groups is also highlighted by the trace element behavior, where basalt groups I and II form – for example in the Zr/Y vs Zr diagram (Fig. 14) – according to PEARCE and NORRY (1979) a distinct array with a relatively high variation in the Zr/Y ratio between 8.5 and 12.5 and a Zr variation from 170 to 300. The array of basalt III has a similar variation in the Zr/Y ratio but even a smaller variation in Zr combined with a higher Zr/Y ratio at a given Zr content. This again indicates a different petrogenetic process and/or source for the formation of basalts I and II compared with basalt III. A similar behavior can also be seen in the Zr/Nb ratio from all basalt groups.

Another petrogenetically important ratio is that of Nb and U. According to HOFMANN (1997), an Nb/U ratio of 46±10 is typical for astenospheric basalts, while lower contents will indicate some strong influence from the continental crust. Again, basalts I and II exhibit an Nb/U ratio of 48, ranging from 41 to 50, which falls exactly into the range of astenospheric basalts (Fig. 15). On the other hand basalt III shows a variation from 34 to 21 with a mean of 25. This would indicate some influence of continental crust during the uprise of the trachyandesitic lavas.

The REE concentration normalized against a C1 chondrite (SUN and MCDONOUGH 1989) shows a pattern typical for intraplate basalts with an enrichment of the LREE around 100 - 200 times chondrite and a systematic decrease of the normalized values towards the HREE (Fig. 16a,b) with a concentration of 5-12 times chondrite. There again is no difference in the REE pattern between group I and II (Fig. 16a). The difference to basalt III is restricted to the concentration of HREE, which is significantely lower for basalt III (Fig. 16b).

A multi-element diagram normalizing the sample against primitive mantle composition expresses nicely the relative difference in the concentration of a number of elements between a sample and some standard compositions such as average MORB or OIB. Such a diagram is shown in Fig.17. The normalizing values are taken from SUN and MCDONOUGH (1989). There are only few differences between basalt I and II on the one hand and basalt III on the other: as expected, the U content is higher in basalt III and so is the K content. Nb, Y and Lu are lower and in addition there is a tendency toward lower Th and Ti. When compared with an ocean island basalt (SUN and MCDONOUGH 1989) there is a fair agreement with both basalts. As a consequence of the major and trace element features, we assume here that all three basalts are derived from a probably asthenospheric source, whereby the source for basalts III was significantly different from that for basalt I and II. In addition, basalt III is most likely contaminated by incorporation of continental crust during uprise of the magmas. A more detailed discussion on the origin of the basalts is in preparation (HÖCK et al. in prep.).

6. Age Dating of Basalts

The necessity of dating the basalts has been recognized long ago because of their importance for the chronology of the sedimentary beds. A wealth of age data have been published, mainly based on K-Ar determination from all over the Mesozoic to Cenozoic basic volcanics from Central Mongolia (EVERNDEN et al. 1964, Devyatkin 1981, 1993b,c, DEVYATKIN et al. 1973, DEVYATKIN unpubl. data, DEVYATKIN and DUDICH unpubl. data, GENSHAFT and SALTYKOVSKY 1990 with citations, GENSHAFT et al. 1990, YARMOLUK et al. 1995). They show a younging of the basalt eruptions from south (Mongolian – Chinese border) to the north (Khangai – Huvs Gol area). The ages range from the Late Cretaceous in the south to the Pleistocene in the north.

In the Taatsiin Gol area, published ages were reported between 32 Ma to 16 Ma, including many ages in between. The unpublished data include ages as old as 42 Ma and as young as 12 Ma. One of the problems in interpreting these ages is that the samples were collected randomly and not clearly related to their actual position in the stratigraphic column. Reported ages, presumably of basalt I (sofar it could be verified from the literature and personal communications), range from 42 to 20 Ma (e.g. DEVYATKIN 1981 and unpublished data by DEVYATKIN and DEVYATKIN and DUDICH), not a plausible time span for a maximal 25 m basalt layer. Similiarly, ages for basalt III range from 19 to 12 Ma. The wide variety of age data even for one single basaltic layer is at least partially caused by the mineralogy and texture of the basalts themselves, as discussed below.

Basaltic rocks are usually fine-grained and may sometimes contain a glassy matrix which can be more or less altered or devitrified distinctly after crystallisation. Mineral separation is often not possible due to the very small grain size. Minerals like zircons are generally absent and phenocrysts of sanidine, ideal for $^{40}Ar/^{39}Ar$ laser dating of fine-grained volcanic rocks, hardly occur in such rocks. K/Ar- or $^{40}Ar/^{39}Ar$-dating of whole rock samples is therefore the state of the art method to date fine-grained basaltic rocks. The stepwise heating method of the $^{40}Ar/^{39}Ar$ dating technique has an important advantage compared to the total gas ages obtained either by the total fusion $^{40}Ar/^{39}Ar$ technique or the K/Ar procedure. Contrary to these single ages, one obtains information on whether the different mineralogical components or grain size fragments show a homogeneous or – for various reasons – inhomogeneous age distribution. This information does not necessarily solve the question of whether the age obtained is geologically meaningful, but among other information it is an important prerequisite to decide this question. Therefore, incremental heating $^{40}Ar/^{39}Ar$-dating should be applied whenever possible and has greatly improved the precision of ages of plateau basalt events or continental basalts dated earlier by the classical K/Ar method, which otherwise has the advantage that it is not affected by the ^{39}Ar recoil effect (see below).

Depending on the original grain size, mineralogy and lithology of the sample, the diffusion experiment with the small

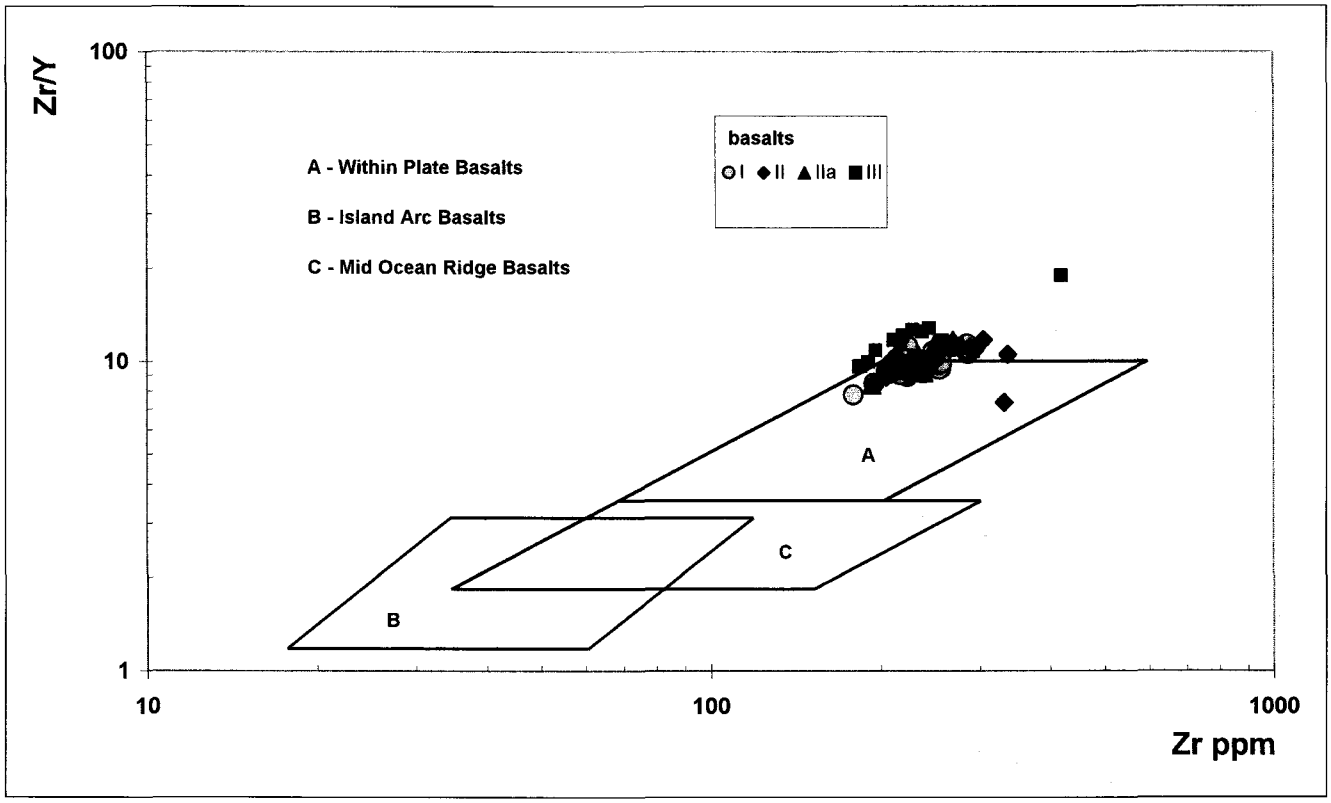

Fig. 14
Zr/Y vs Zr diagram according to PEARCE and NORRY (1979). The legend for the basalts is given in the insert. As expected, all analyses fall in the field of within-plate basalts. It is noteworthy here that (a) basalt I, basalt II and IIa cover virtually the same array (explaining why almost no basalts II are shown on the diagram, they are completely covered by basalt I) and (b) basalt III covers a separate±parallel array with higher Zr/Y ratio at a given Zr content. This excludes a crystal fractionation mechanism leading from basalt I or II to basalt III.

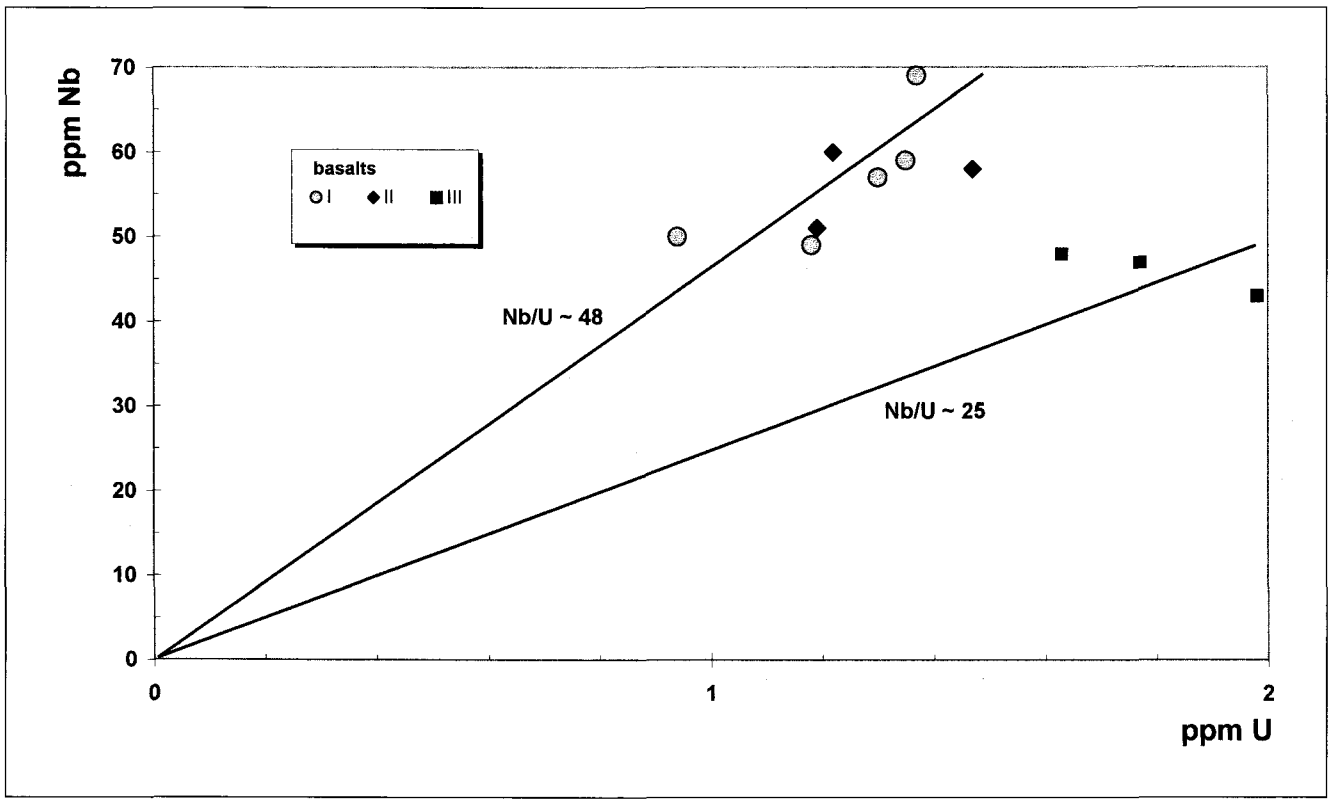

Fig. 15
U vs Nb diagram according to HOFMANN (1997). The legend for the basalts is given in the insert. Basalts I and II show a comparatively low U content (1 to 1.5ppm) combined with a high Nb content. This yields a Nb/U ratio of ~48 compared with 25 in basalt III. The lower value could indicate a considerable contamination of the basalts by the continental crust.

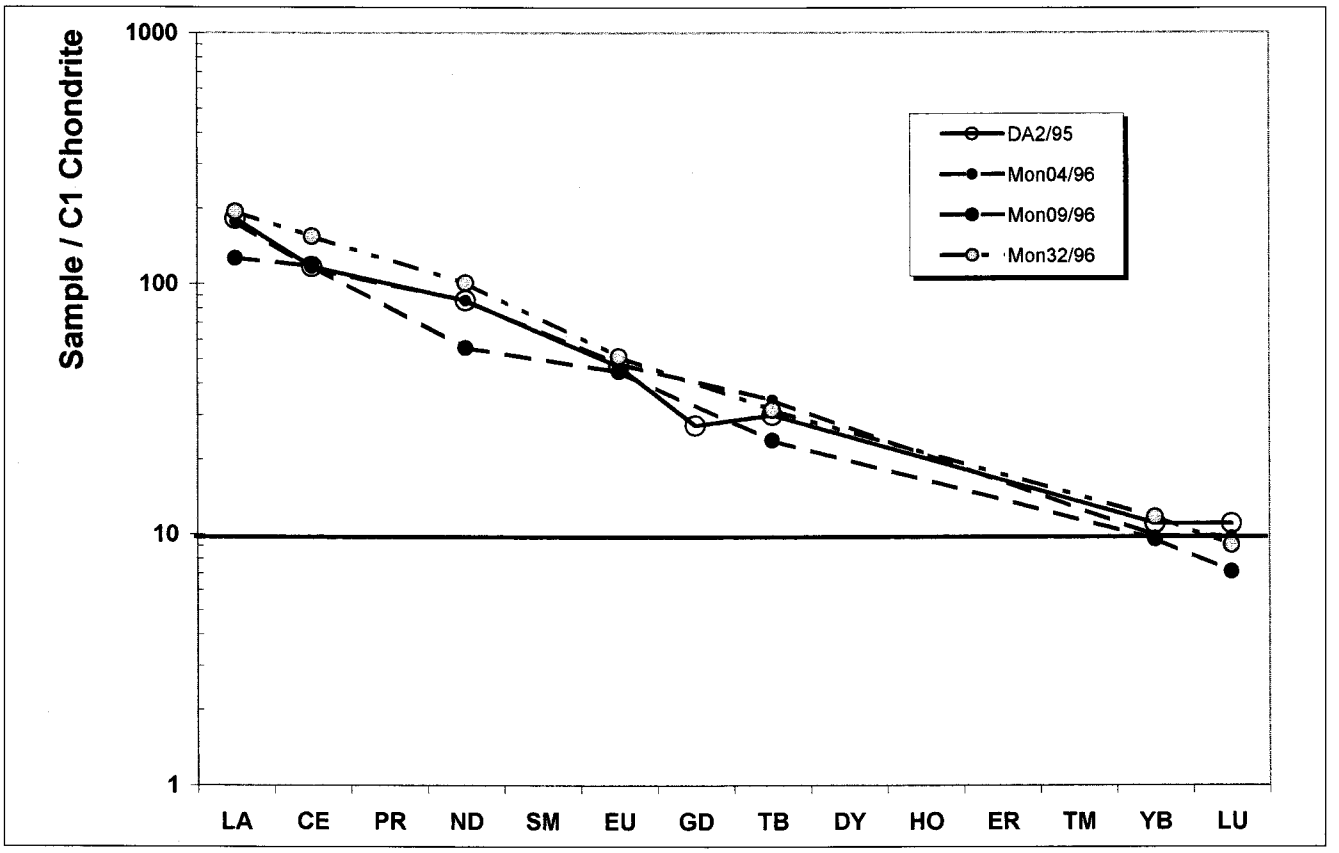

Fig. 16a

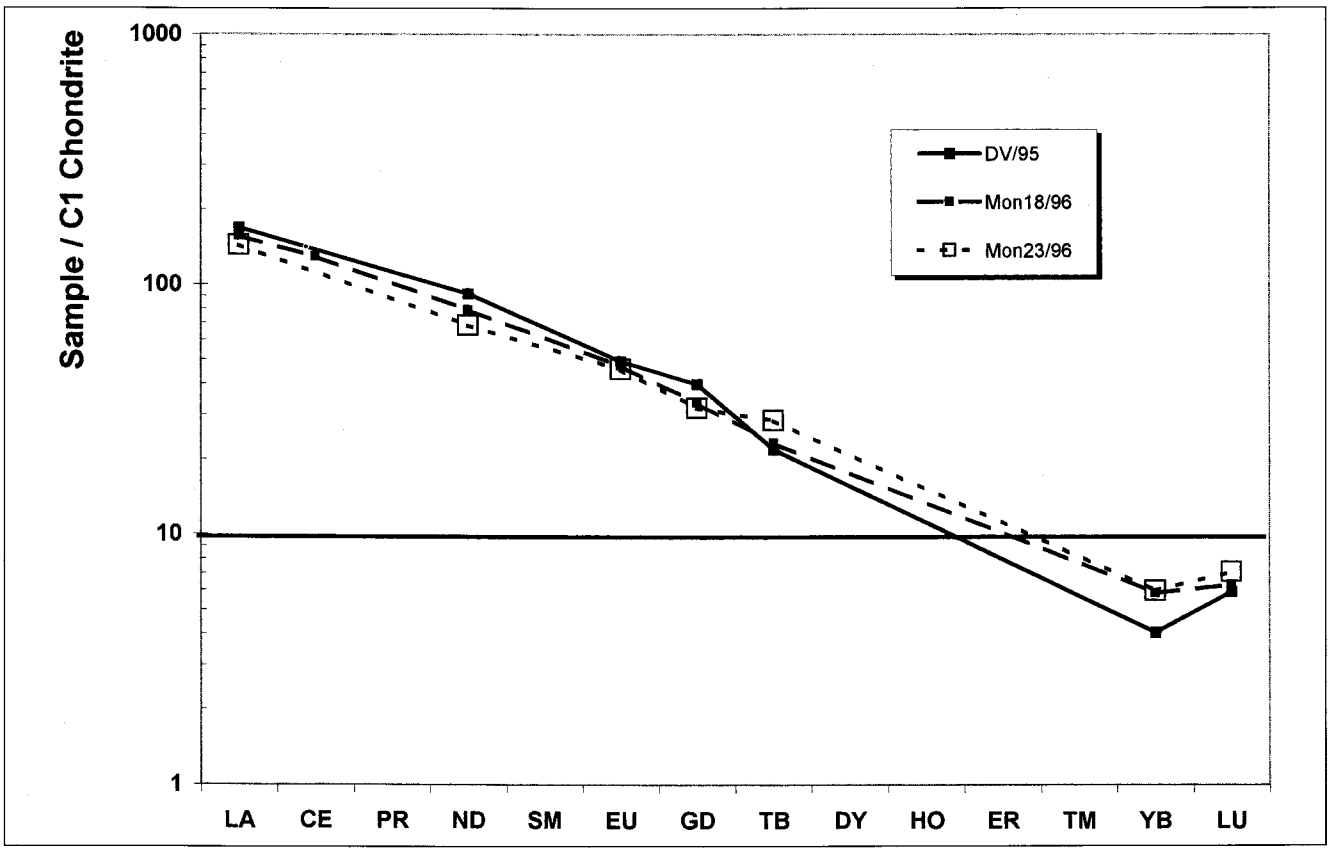

Fig. 16b
The REE concentration normalized against a C1 chondrite (SUN and MCDONOUGH 1989) shows a pattern with an enrichment of the LREE around 100-200 times chondrite and a systematic decrease of the normalized values towards the HREE with a concentration of 5-12 times chondrite. The sample numbers are given in the insert. Fig. 16a displays REE patterns for group I and II; there is no difference in the REE pattern. The difference to basalt III is restricted to the concentration of the HREE, which is significantly lower for basalt III as displayed in Fig. 16b.

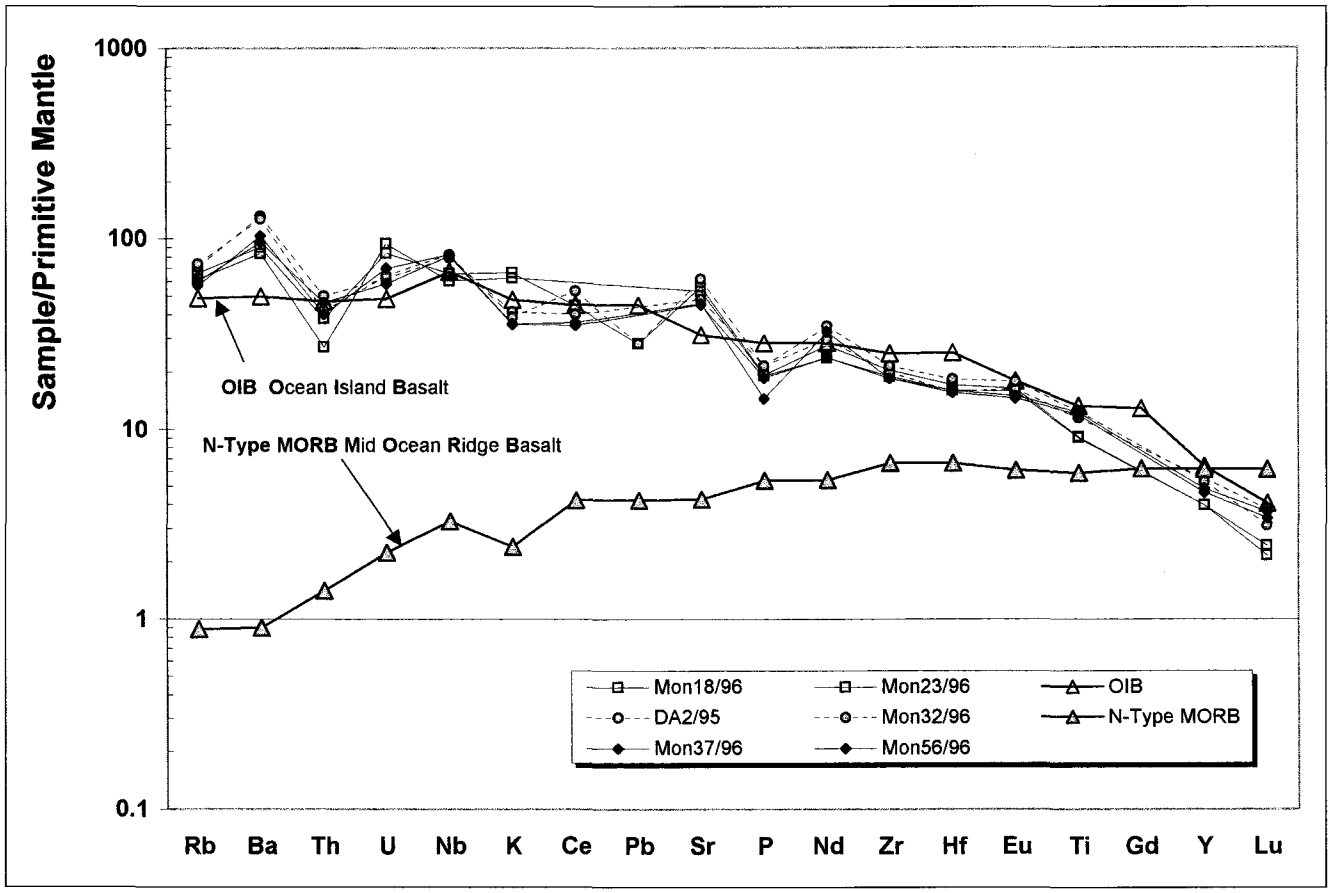

Fig. 17
Multi-element diagram normalizing the sample against primitive mantle composition. The normalizing values are taken from SUN and MCDONOUGH (1989). Standard compositions such as average MORB or OIB are given for comparison. The sample numbers are given in the insert. There are only few differences between basalt I (circles) and II (diamonds) on the one side and basalt III (squares) on the other: the U content is higher in basalt III, as is the K-content. Nb, Y and Lu are lower and in addition there is a tendency to lower Th and Ti.

grain size fraction can be more easily adjusted to yield steps of similar intensity than with larger grain sizes, which often release most of the gas in a narrow temperature range when a partial breakdown of the mineral lattices occurs. Dating of mixtures from different, mostly K-poor minerals with different diffusion characteristics and a different ability to incorporate Ar in their lattice is usually less precise than data from pure K-rich minerals. Very good UHV- and clean static vacuum conditions in the extraction line and the mass spectrometer are technical prerequisites for measuring steps with low and high intensities without systematic errors and a reasonable precision. Due to their higher interference with blanks of various sources, steps with low intensities were critically checked and evaluated.

If a set of carefully selected samples of an individual flow of (unaltered) basalt yields concordant ages of reasonably well-defined plateau type, one can be virtually certain that the lava is reliably dated.

The ^{39}Ar recoil effect is an often observed problem of fine-grained basaltic rocks; it represents a technical problem caused during irradiation in the nuclear reactor: ^{39}Ar is produced by fast thermal neutrons from ^{40}K. Due to the recoil energy of this nuclear transformation, some ^{39}Ar atoms close to the surface are lost from the mineral lattice. When Ar is released from the outer domains during the low temperature steps the unchanged amount of radiogenic ^{40}Ar is released but a fraction of ^{39}Ar (a measure of the K-content) is missing. The low temperature ages can therefore turn out too old. Sometimes the interior of grains can gain ^{39}Ar by the same effect and high temperature steps may be too young. These two counteracting effects are not necessarily combined, the first being more frequent than the second. This recoil effect is strongly related to small grain sizes of high surface/volume ratios and poorly defined chemical composition (e.g. fine-grained alteration products); it is missing or negligible when well-crystallized samples are investigated. From dating clay fractions it is known that poorly crystallized sizes $<2\mu$ are rather prone to show this effect and zhat 2-6μ sizes are only seldom and distinctly less affected. From the samples investigated in this study we interpret several release spectra (e. g. TGR-B 1) which show distinctly higher ages at low temperatures to be affected by the ^{39}Ar recoil effect.

Alteration due to hydrothermal effects or weathering can cause strong discordant release patterns of various shapes, and such samples often show distinctly higher contents of Ar with air composition compared to unaltered samples. Such spectra should not be considered in a meaningful data base.

Fluid and melt inclusions are primary features which can be a serious obstacle for dating. Unexpectedly large amounts of various gases can be incorporated therein, are released at a certain temperature, and can destroy the cleanliness of the analytic system for some time. Such samples should be discarded from further investigation. One such case occured during our investigation of the Mongolian basalts.

Incorporation of ^{40}Ar-excess can always be a problem when small volumes of basalts penetrate continental crust. Along the feeder fissures, radiogenic ^{40}Ar can be released from the crystalline wall rocks, especially when they are rich in ^{40}Ar due

to rather old age, as can be assumed for the basement of the Valley of Lakes. This effect may be responsible for some unexpected old ages up to 42 Ma reported from the area investigated here by DEVYATKIN and DUDICH (unpublished data). From our samples, at least one from basalt I in profile TGR-B is considered to be seriously affected by excess Ar giving an age of 49 Ma. The error is obvious when a single sample of a well-dated layer shows a completely different age. It may, however, be difficult to recognize when only a small amount of excess Ar is present. Although we can assume that the bulk of the minerals has been crystallized at surface or near-surface conditions with a good chance for thorough degassing, some minerals such as alkali feldspar are mainly responsible for incorporation of excess Ar. If it is distributed more or less homogeneously in all domains of the sample, as is usually the case, there is no chance to determine the true age; also, treatment of the analytical data in the isochron correlation plots cannot reveal the amount of ^{40}Ar excess incorporated. Only investigations (if possible) of closely spaced samples with variable mineralogy can be of some help. Excess Ar generally tends to be variable at short distances. To investigate a certain number of geochronological data from regionally representative samples from an individual outpouring event is the best strategy to sort out such erratic and misleading results.

From all three basalt layers (I-III), samples for age dating were carefully selected in terms of their geological postion (also within the layers) and their quality in respect to weathering. Exclusively the least weathered samples were used for dating. Careful screening of the data set taking in account the above described problems and difficulties yielded the following results given below and displayed graphically in Fig. 18. This diagram includes only samples which show no or only a small recoil effect and no 40 Ar excess: out of 51 measured samples only 31 were used in Fig. 18.

Basalt I erupted around 31.5 Ma ago, with ages ranging from 30.4 to 32.1. The individual standard deviation varies from 0.3 to 0.8. There is no significant age difference recognizable between the different volcanic flows of basalt I. These values agree well with some reported published or unpublished age dates (DEVYATKIN 1981 and unpublished data by DEVYATKIN AND DEVYATKIN and DUDICH) ranging from 34 to 30 Ma and centering around 31/32 Ma. On the other hand our data do not account for some lower ages (29-20 Ma) from localities we identified as basalt I. These data obviously suffered from the problems discussed above and should not be regarded further. The basalt dating indicates an Early Oligocene age of eruption.

Basalt II, interbedded in sediments of the Loh Formation, shows an age of around 28 Ma, ranging from 27 to 29 Ma. The individual standard deviation varies from 0.4 to 0.9. The relatively wide range of age data in basalt II could be due partly to recoil effects and partly to assimilation of small Ar portions from the continental crust. Basalt group IIa was separated from the main group because of its geochemical tendency towards basalt III. Age dating from this group is not very well defined because of a low intensity, but all measured ages point unanimously to an eruption age of 28 Ma. This regards basalts from Barun Hsir, Dsun Hsir and from the Mount Ushgoeg itself. These results put the lower part of the Loh Formation into the Late Oligocene. There are no ages reported which can be assigned based on their description to basalt II with the exception of one sample (basalt Nr. 9 in Tab. 21 in DEVYATKIN 1981), which might come from the area covered by basalts IIa.

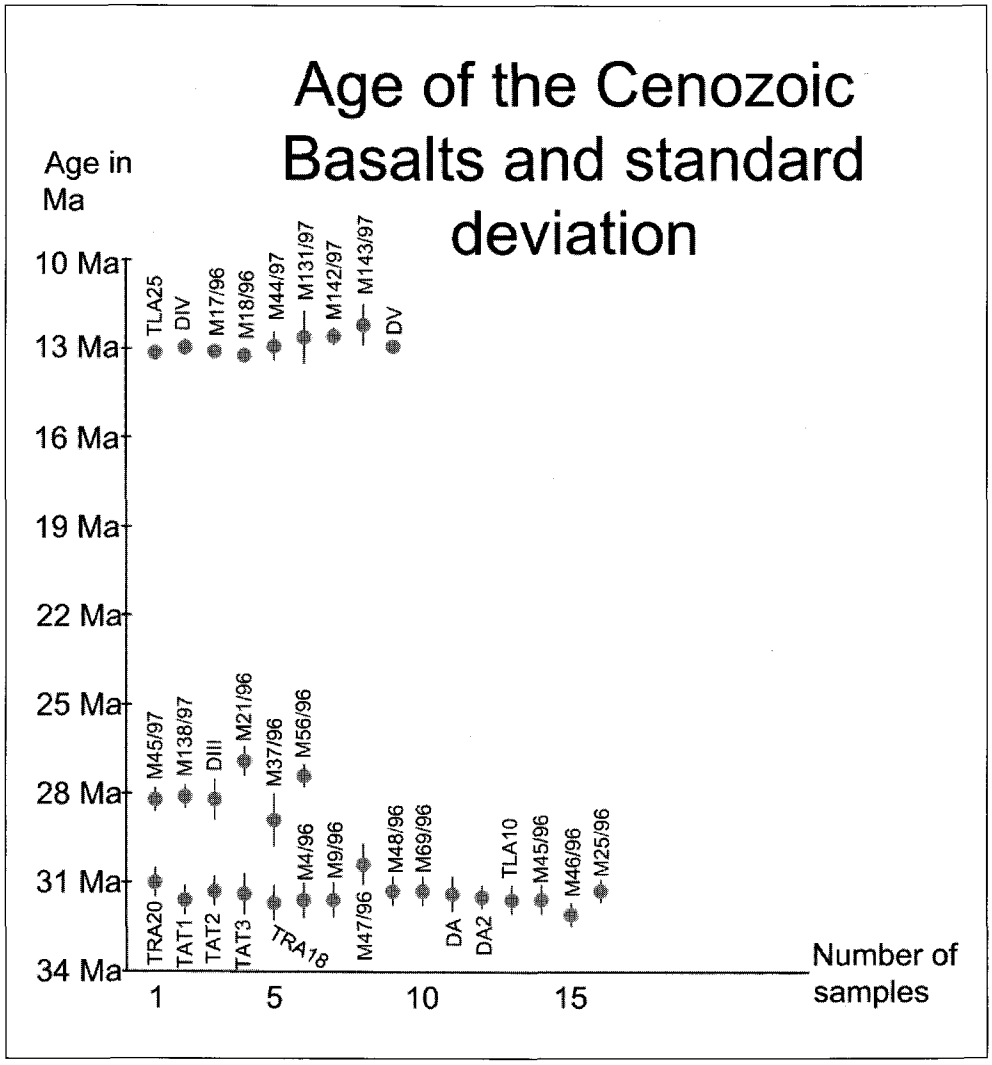

Fig. 18
The measured ages of 31 basalts. The bars give the 2ó errors. Basalt I erupted around 31.5 Ma ago, with ages ranging from 30.4 to 32.1. The individual errors vary from 0.3 to 0.8. Basalt II, interbedded in sediments of the Loh Formation, shows an age of around 28 Ma, ranging from 27 to 29 Ma. The individual errors vary from 0.4 to 0.9. The basaltic trachyandesite and trachyandesite III gives a well-defined age of 13 Ma ranging from 12.2 to 13.2 Ma. The individual errors vary from 0.2 to 0.7 Ma.

The basaltic trachyandesite and trachyandesite (basalt III), finally, topping the Loh Formation in many places, also gives a well-defined age of 13 Ma (Middle Miocene), ranging from 12.2 to 13.2 Ma. The individual standard deviation varies from 0.2 to 0.7 Ma. The only comparable data with 12.0 and 12.5 Ma for these volcanics are found in the unpublished data by DEVYATKIN and DEVYATKIN and DUDICH. Earlier data assigned to this layer show an age of 17 to 19 Ma.

7. Tectonics

As already outlined in chapter 4 on lithology, the development of the basin of the Valley of Lakes most probably already started in the Jurassic and continued during the Cretaceous with interruptions into the Cenozoic. We will outline here shortly the tectonic evolution of the basin, although this was not the main topic of our research. The frame of the Valley of Lakes and the most important tectonic lines are shown in Fig. 2.

The Mesozoic, very coarse conglomerates and other clastic sediments call for a high relief and thus for a formation of a relatively deep, most probably fault bounded basin. This can be seen mainly N of Builstyn Khudag and E of Mt. Usghoeg, where Jurassic/Cretaceous formations directly overlay the crystalline (including the Permian basement) along steep dipping contacts (see suppl. 1 & 2). Later Cretaceous sediments are obviously missing, indicating a time of erosion rather than sedimentation. A temporary basin inversion may be the tectonic cause of the lack of Late Cretaceous sediments. Sedimentation started again with the Paleocene (?) to Eocene Kolbooldschi formation, not described in detail here.

The sediments of the coarse-grained Eocene to Early Oligocene(?) Tsagaan Ovoo Formation require again a strong relief with high energy streams, but no tectonic features can be associated with the formation. The overlaying Hsanda Gol Formation does not call for a high relief but rather a flat landscape. The only indication of a smooth relief is the continuous decrease in thickness of the Hsanda Gol Formation towards the north until it reaches zero and the Loh Formation directly overlays the Tsagaan Ovoo Formation (suppl.1).

A major fault is found close to the northern end of the Hsanda Gol Formation, the Del fault (see suppl. 1). It strikes NW-SE to W-E and can be mapped from E of the Dzun Hsir in the east along the southern escarpment of the Ushgoeg range until the vicinity of Tarimalyn Khurem. Its continuation towards the northwest and west is questionable. The Del fault parallels approximately the Bayan Khongor fault system. Whether it is genetically related to it is unclear. The fault plane varies from moderately south dipping to vertical (Fig. 19a). As already described correctly by BERKEY and MORRIS (1927), the movement along the fault is a dip-slip towards the south (southwest) with an offset of at least 20 to 30 m.

As far as we were able to study the Del fault and its vicinity, it is clear that the Hsanda Gol sediments as well as the Tsagaan Ovoo were inclined near the Del fault, whereas the Loh sediments are±horizontally bedded and not deformed. A direct sedimentation of the Loh Formation across the Del fault could not be ovserved. The transition form the Hsanda Gol Formation to the Loh sediments took place in the intervall between the end of the Early Oligocene and the end of the Late Oligocene (see chapter 10 and Fig. 22). These two boundaries put a lower and upper limit on the formation of the Del fault.

A younger fault system strikes NE-SW. It is responsible for many morphological features such as the southern (southeastern) rim of the Taatsiin Gol West Plateau, the NE-SW striking valley south of the Taatsiin Gol E Plateau, or the boundaries of the TAR Plateau, and the spectacular offset of the Del fault near the DEL-A profile. This offset indicates a dextral strike slip component. The NE-SE fault system clearly offsets Loh sediments but was never observed in the Tuyn Gol sediments which seem to cover it. This puts the NE-SW fault system into the Early to Middle Miocene.

A third E-W striking fault system, with a southward directed dip-slip of several meters, is obviously restricted to the area W of the Taatsiin Gol. It affects the Loh sediments. Small E-W striking faults are also observed in the Tuyn Gol formation, indicating an activity of the system until the very Late Miocene or Pliocene.

The mapped faults in the very NW of the area are difficult to interpret. The almost E-W striking fault separating some older sediments from a crystalline basement areaclearly affects Oligocene Loh sediments but is in turn overlain by the younger (Miocene ?) Loh sediments and the Middle Miocene lava flow III. This supports the view of this fault as acontinuation of the Del fault. The NNE-SSW striking faults are younger than the basalt flows but most probably predate the Tuyn Gol formation for which they form a suitable relief.

The recent seismic activity is restricted to the south of the Valley of Lakes and takes place along the northern rim of the Gobi Altai along the Gobi Altai fault or Ikh-Bogd fault (Fig. 2). It has a sinistral sense of movement but also a dip-slip component towards the N. Because of the recent earthquakes occurring along the faults, such as in 1957 with a magnitude 8/9, it is well studied and was described in detail recently (BALJINYAM et al. 1993, KURUSHIN et al. 1997, SCHLUPP 1996). It demonstrates very well the longlasting and ongoing fault activity along with extensional processes in the Valley of Lakes, which started (apart from earlier extensional episodes) in the Late Oligocene and can be traced to recent times.

Apart from the widespread Cenozoic strike-slip and dip-slip faults, some regions are characterized by compressive structures. For example, north of the Del fault near the Taatsiin Gol and Del as well as Builstyn Khudag the contact between the Meso- and Cenozoic sediments is characterized by thrusting. Fig. 19b shows an excellent exposed outcrop on which retrogressive phyllites are overthrust on conglomerates of the Loh Formation over the distance of several meters towards the south. This overthrust of the Baidrag crystalline units onto the Meso- and Cenozoic sediments is a regional feature observed in many parts on the southern rim of the Ushgoeg mountains. According to SCHLUPP (1996) overthrusting features can also be observed at the northern boundary of the Ushgoeg mountains. The overthrusting features are not restricted to the Ushgoeg mountains, but can be found also e.g. south of the Gobi Altai mountains (BAYARSAYHAN et al. 1996) or south of the Han Tai Shiri range (own observations). The overthrust features in the south of Gobi Altai are genetically related to the rupturing along the Ikh-Bogd fault (BAYARSAYHAN et al. 1996). In a similar way, we suggest here that the thrusting south of the Ushgoeg mountains may be related to the strike-slip dominated faults in the Bayan Khongor zone. This hypothesis remains to be tested by future studies.

8. Paleontology and Biostratigraphy

8.1 General remarks and localisation of vertebrate faunas

In the present paper we concentrate exclusively on vertebrate faunas which were collected from fossil horizons along profiles and from some isolated but stratified fossil sites within

Fig. 19a
Steep inclined, almost vertical basalt I near Del (view to the east). This is not a dike, but an upright basalt flow displaced by the Del fault probably in the Late Oligocene. The sediments accompanying the basalts are also upright. The white Tsagaan Ovoo Formation, the lower part of the Hsanda Gol Formation and a small tuff horizon to the left and the upper part of the Hsanda Gol Formation to the right. The Loh Formation in the background lies horizontally. This is a type locality for "Del", which means "horse mane" in Mongolian.

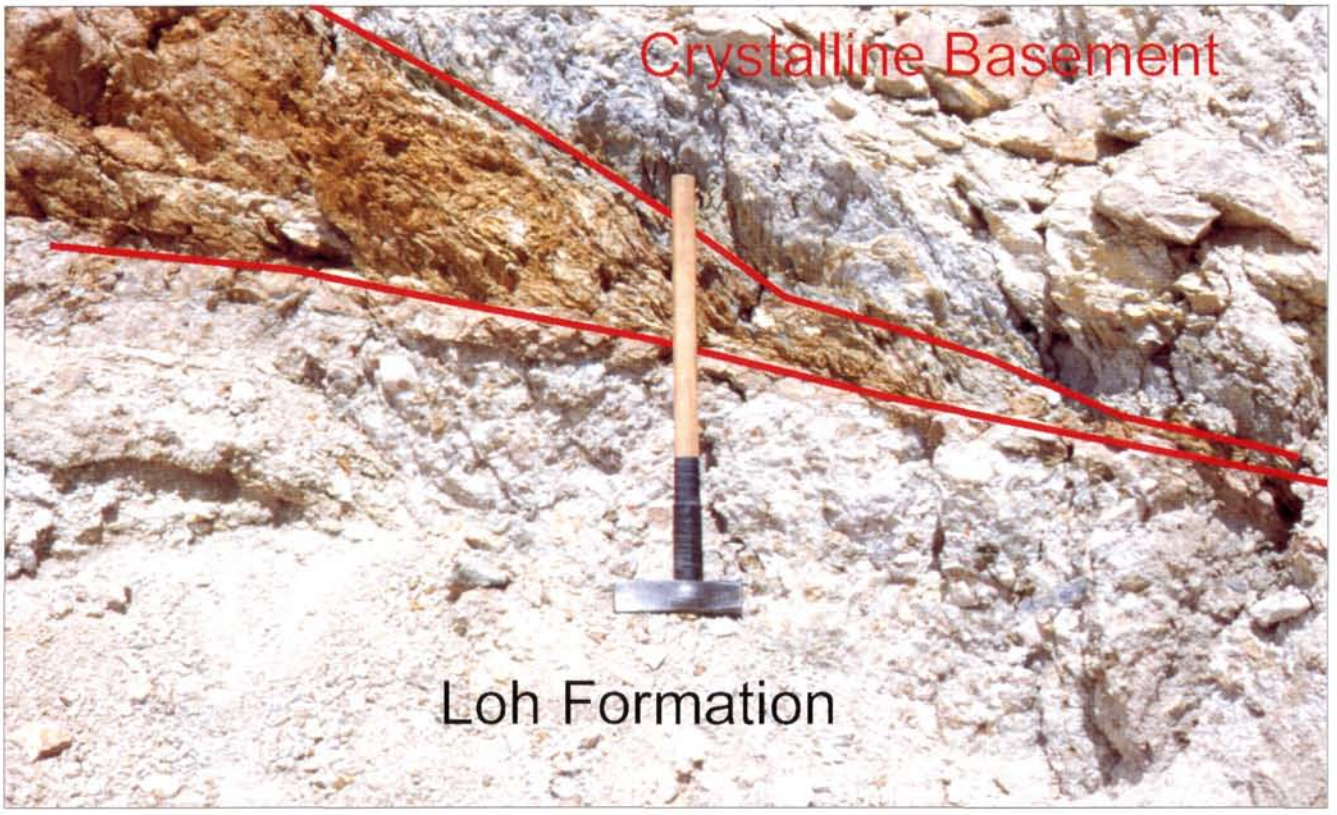

Fig. 19b
Overthrust of retrograde micaschists and paragneisses of the Baidrag zone onto gravels of the Loh Formation just north of Tavan Ovoony Deng. The outcrop is viewed to the west, the direction of thrusting is towards south.

the mapped area (suppl. 1 & 2). These profiles were subdivided into lithologically defined horizons, consequently numbered from bottom to top. The numbers of fossil horizons are visible on the right hand side of the respective profile in suppl. 3 and go together with the section label in the text. Acknowledging current investigations by the Museum of Natural History of New York in cooperation with the Paleontological Center of the Mongolian Academy of Sciences, we restricted our investigations in the Tatal Gol area to geological mapping and to test sampling (TAT-C and TAT-D).

Fossils were collected from sediment sequences of the Hsanda Gol and Loh Formations (for the lithology see chapter 4). No fossils were found in sediments of the Tsagaan Ovoo and Tuyn Gol Formations. In total, about 80 vertebrate faunas of varying fossil volume – 60 of them are included in this study – were collected from 30 profiles and fossil sites (suppl. 3). Besides mammal fossils, sporadically egg shells, gastropods, and jaws and bones from amphibians and lizards were found. There is no fossil record of plants (leaves, seeds, pollen), fish or ostracods. Based on wet screening, isolated teeth of rodents, insectivores and lagomorphs are very abundant, while jaws and more complete postcranial bones occur rarely. The evidence of large mammal fossils is very poor in screened samples. Sporadically, remnants of carnivores, creodonts, ruminants, rhinocerotids, proboscideans, and large-sized rodents and lagomorphs were collected from the surface.

In the red Hsanda Gol silts and clays the fossil content is rich. Fossils were collected below and above basalt I, and from sediment layers between two individual flows of basalt I (TGR-ZO/1, 2; TGR-1564). Above basalt I, fossil concentrations were observed basal and inside of marl layers within the Hsanda Gol sediments. The preservation of fossil teeth is excellent; above the basalt they are generally black, sometimes reddish, white or transparent. Below basalt I the colour of teeth is generally not black but varies from white, red, brown to gray. Preservation of bones is poor. Sometimes teeth can be found in their original position, whereas the corresponding jaw or maxilla is decomposed. Gastropod shells are preserved almost exclusively in fine-grained sediments below basalt I.

The coarser-grained Loh sediments are generally poor in fossil content. The colour of the teeth varies from white, pink, brown to gray; bones are poorly preserved. Gastropods are only found in fine-grained sediments beneath basalt III.

8.2 Biostratigraphy (suppl. 3, Fig. 22)

DAXNER-HÖCK et al. (1997; 172 p.) established a biostratigraphy for the Hsanda Gol and Loh Formations on the basis of 5 rodent assemblages (A,B,C,D,E). Since that time new paleontological data have become available from the Valley of Lakes, and the number of rodent assemblages, which serve as a basis for informal biozones, was extended from 5 to 7. Each biozone (A, B, C, C1, D, D1, and E) is characterized by its lithostratigraphic position and by a well-defined selection of rodent genera and species from all respective fossil horizons. In the following paragraph the description of biozones was given in the same scheme. It includes: 1) an integrated rodent list, 2) the characteristic species used for each biozone, 3) the first and last record, 4) the characterisation and/or most abundant rodents, 5) the localisation and lithostratigraphic position, and finally 6) remarks, if necessary. The correlation of fossil horizons among different profiles in suppl. 3 is given by connecting lines labelled by the respective biozones. A formalisation of biozones in terms of the "International Stratigraphic Guide" (SALVADOR 1994) will be postponed until the completion of current investigations on all mammals collected by our team from 1995 to 1997.

Biozone A: (Fig. 20/1-3)

1) Integrated rodent list:
Ardynomys sp.
Tsaganomys altaicus
Cyclomylus sp. = *(Tsaganomys cf. minor* in: DAXNER-HÖCK et al. 1997)
Anomoemys cf. *lohiculus*
Karakoromys decessus
Selenomys mimicus
Cricetops dormitor
Eucricetodon caducus = *(Eucricetodon* sp.1 in: DAXNER-HÖCK et al. 1997)
Eucricetodon asiaticus = *(Eucricetodon* sp. 2 in: DAXNER-HÖCK et al. 1997)
Cricetidae n.g.n.sp.
Parasminthus sp.1 = (Zapodidae indet. in: DAXNER-HÖCK et al. 1997)
Heosminthus sp.1
Heosminthus sp. 2
Eomyidae indet.
Haplomys sp.

2) Characteristic species: *Karakoromys decessus, Ardynomys* sp., *Cricetops dormitor, Eucricetodon asiaticus, Selenomys mimicus, Heosminthus* sp.1.

3) First/last record: First record: *Tsaganomys, Cyclomylus, Cricetops, Selenomys* and aplodontids. Last record: *Ardynomys* sp. and *Parasminthus* sp.1

4) Characterisation/most abundant rodents: Almost all rodents listed in **1)** are typical for Hsanda Gol sediments. Only one ctenodactylid, *Karakoromys decessus,* is known from biozone A. *Parasminthus* sp.1 is more primitive but thought to be the ancestor of *P. asiae-centralis*. The most abundant species is *Heosminthus* sp.1.

5) Localisation and lithostratigraphic position (suppl. 1-3): Lower part of the Hsanda Gol Formation; below basalt I or its tuff. Brick red silt and clay. The fossils were recovered in the following areas (sections/levels). Taatsiin Gol (TGL-A/1-2; TGR-A/13-14), Khongil (HL-A), Tatal Gol (TAT-C/1-3) and Hsanda Gol (SHG-C/1-2).

Biozone B: (Fig. 20/4-9)

1) Integrated rodent list:
Tsaganomys altaicus
Cyclomylus sp. = *(Tsaganomys* cf. *minor* in: DAXNER-HÖCK et al. 1997)
Anomoemys cf. *lohiculus*
Karakoromys decessus
Tataromys minor
Selenomys mimicus
Cricetops dormitor
Eucricetodon caducus = *(Eucricetodon* sp.1 in: DAXNER-HÖCK et al. 1997)
Eucricetodon asiaticus = *(Eucricetodon* sp. 2 in: DAXNER-HÖCK et al. 1997)
Eucricetodon sp.1
Cricetidae n.g.n.sp.
Parasminthus cf. *asiae-centralis* = (Zapodidae indet. in: DAXNER-HÖCK et al. 1997)
Parasminthus cf. *tangingoli* = (Shamosminthus sp.1 in: DAXNER-HÖCK et al. 1997)

Heosminthus sp. 1
Heosminthus sp. 2
Heosminthus sp. 3
Eomyidae indet.
Haplomys sp.
Promeniscomys sp.

2) **Characteristic species:** *Tsaganomys altaicus, Cyclomylus sp., Karakoromys decessus, Tataromys minor, Cricetops dormitor, Eucricetodon asiaticus, Selenomys mimicus,* Cricetidae n.g.n.sp., *Heosminthus* sp.1, 2.

3) **First/last record:** First record: *Promeniscomys* sp., *Tataromys minor, Parasminthus* cf. *asiae-centralis, P. tangingoli.* Last record: *Karakoromys decessus, Tataromys minor, Selenomys mimicus, Cricetops dormitor, Eucricetodon caducus, Eucricetodon asiaticus, Heosminthus* sp. 2, 3.

4) **Characterisation/most abundant rodents:** The biozones A and B share most rodents, except *Ardynomys,* which is restricted to A, and *Tataromys minor* and *Promeniscomys,* which appear first in B. The most abundant rodents are *Heosminthus* sp.1 and Tsaganomyidae.

5) **Localisation and lithostratigraphic position** (suppl. 1-3): Higher parts of the Hsanda Gol Formation, above and intra basalt I. Brick red silt and clay. The fossils were recovered in the following areas (sections/levels):

a) Hsanda Gol sediments above basalt I: Taatsiin Gol (TGL-A/11; TGR-AB/21-22; TGR-B/1), Del (DEL-B/7-8), Tatal Gol (TAT-C/6-7; TAT-D/1) and Hsanda Gol (SHG-A/1-20; SHG-AB/12, 17-20).

b) Hsanda Gol sediments between two basalt layers of basalt I exposed in the Taatsiin Gol area (TGR-ZO/1-2; TGR-1564).

Biozone C: (Fig. 20/10-14)

1) **Integrated rodent list:**
Tsaganomys altaicus
Cyclomylus sp. = *(Tsaganomys minutus* in: DAXNER-HÖCK et al. 1997)
Tataromys parvus = *(Karakoromys sp.* in: DAXNER-HÖCK et al. 1997)
Tataromys sigmodon
Yindirtemys sp. = *(Tataromys* cf. *deflexus* in: DAXNER-HÖCK et al. 1997)
Eucricetodon sp. 2 and sp. 3 = (Cricetidae indet sp. 1, sp. 2 in: DAXNER-HÖCK et al. 1997)
Cricetidae indet. sp. 1 and sp. 2 = (*Eumysodon* ? sp. 1, sp. 2 in: DAXNER-HÖCK et al. 1997)
Parasminthus cf. *asiae-centralis*
Parasminthus tangingoli = *(Shamosminthus* sp. 2 in: DAXNER-HÖCK et al. 1997)
Parasminthus parvulus
Heosminthus sp.1
Zapodidae n.g.n.sp.
Pseudotheridomys ? sp. = (Eomyidae indet. in: DAXNER-HÖCK et al. 1997)
Promeniscomys sp.
Tachyoryctoides obrutschewi = *(Tachyoryctoides* (small spec.) in: DAXNER-HÖCK et al. 1997)

2) **Characteristic species:** *Tachyoryctoides obrutschewi, Parasminthus parvulus, Tataromys parvus, Tataromys sigmodon, Eucricetodon* sp. 2 and sp. 3, Cricetidae indet.

3) **First/last record:** The first occurrences of species are identical with those listed in **2)**. Last record: *Tataromys parvus, Tataromys sigmodon, Yindirtemys* sp., *Eucricetodon* sp. 2, *E.* sp. 3, Cricetidae indet. and *Tachyoryctoides obrutschewi.*

4) **Characterisation/most abundant rodents:** There is a significant change in rodent taxa from biozone B to C. The most abundant rodents are: *Parasminthus parvulus, Tataromys parvus, Tataromys sigmodon, Eucricetodon* sp. 2 and sp. 3 and Cricetidae indet.

5) **Localisation and lithostratigraphic position** (suppl. 1-3): Highest part of Hsanda Gol Formation and lower part of Loh Formation /below and above basalt II.
a) High part of Hsanda Gol Formation: Taatsiin Gol (TGR-C/1-6).
b) Loh Formation below basalt II: Abzag Ovoo (ABO-A/3).
c) Loh Formation above basalt II: Tarimalyn Khurem (TAR-A/2).
d) Loh Formation: Khunug valley (TGW-A/1-2).

6) **Remarks:** Rodents of biozone C were observed in Hsanda Gol as well as in Loh sediments. This means that some parts of the Hsanda Gol and the Loh Formation were deposited at the same time (Late Oligocene). This age is evidenced by basalt II.

Biozone C 1:

1) **Integrated rodent list:**
Yindirtemys deflexus
Yindirtemys gobiensis
Parasminthus parvulus
Heosminthus sp.1

Fig. 20
Rodent fossils from the Hsanda Gol and Loh Formations representing the biozones A, B and C. The localities are situated within the Valley of Lakes / Central Mongolia. The magnification is approximately 20 times. Coll. Naturhistorisches Museum Wien, Geolog.-Paläontol. Abt.

20/1 *Selenomys mimicus;* M 2 l; TGL-A/2; locality Taatsiin Gol left; biozone A; Early Oligocene.
20/2 *Heosminthus* sp. 2; M 1-3 l, m 1-2 l, m 3 l; TAT-D/1; locality Tatal Gol; biozone A; Early Oligocene.
20/3 *Anomoemys lohiculus;* M sup. l; TGR-A/13; locality Taatsiin Gol right; biozone A; Early Oligocene.
20/4 *Karakoromys decessus;* M 2 l, m 3 l ; SHG-A; locality Hsanda Gol; biozone B; Early Oligocene.
20/5 *Eucricetodon asiaticus;* M 1 l, m 1 l; TGR-B/1; locality Taatsiin Gol right; biozone B; Early Oligocene.
20/6 *Heosminthus* sp. 1; M 1-3 l, m 1 l, m 2 l, m 3 l; TGR-B/1; locality Taatsiin Gol right; biozone B; Early Oligocene.
20/7 *Tataromys minor;* M sup. r; TGR-B/1; locality Taatsiin Gol right; biozone B; Early Oligocene.
20/8 Eomyidae indet.; M 1/2 r; TGR-B/1; locality Taatsiin Gol right; biozone B; Early Oligocene.
20/9 *Eucricetodon caducus;* M 1 r; TGR-B/1; locality Taatsiin Gol right; biozone B; Early Oligocene.
20/10 *Tataromys parvus;* M sup. l, m inf. r; DEL-B/12; locality Del; biozone C; Late Oligocene.
20/11 *Parasminthus parvulus;* M 1 l, m 1-2 l; TGR-C/1; locality Taatsiin Gol right; biozone C; Late Oligocene.
20/12 Eomyidae indet.; M 1/2 r; DEL-B/12; locality Del; biozone C; Late Oligocene.
20/13 *Eucricetodon* sp. 2; M 1 l; TGR-C/1; locality Taatsiin Gol right; biozone C; Late Oligocene.
20/13/1 *Eucricetodon* sp. 2; m 1 l; TGR-C/1; locality Taatsiin Gol right; biozone C; Late Oligocene
20/14 Cricetidae indet.; M 1 l, m 1 l; TGR-C/1; locality Taatsiin Gol right; biozone C; Late Oligocene. →

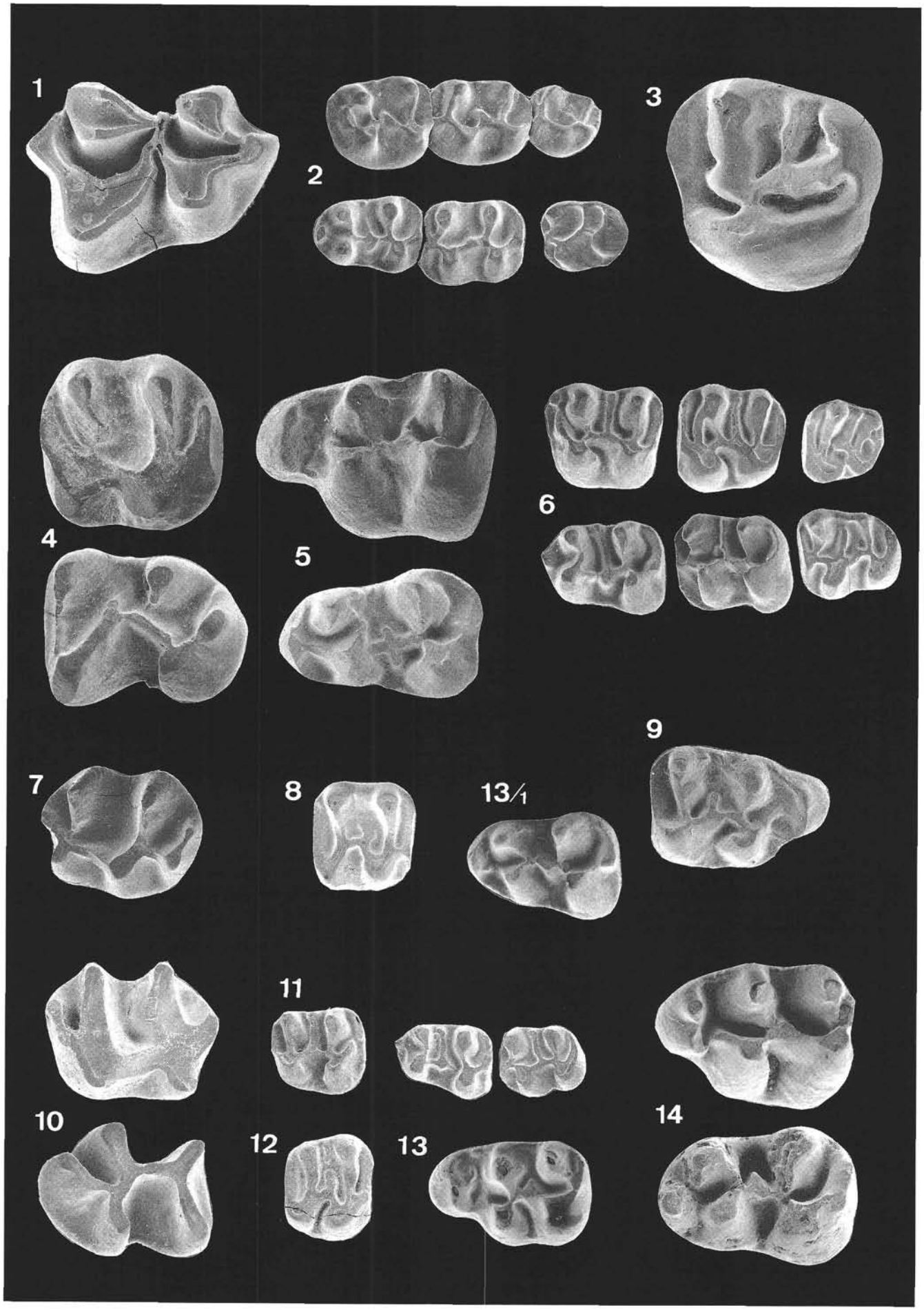

Zapodidae n.g.n.sp.
Plesiosminthus sp. 1 and sp. 2
Aplodontidae indet.

2) **Characteristic species:** *Yindirtemys deflexus, Plesiosminthus* sp. 1 and *P.* sp. 2.

3) **First/last record:** First record: *Yindirtemys deflexus, Yindirtemys gobiensis, Plesiosminthus*. Last record: *Yindirtemys deflexus, Yindirtemys gobiensis, Parasminthus parvulus.*

4) **Characterisation/most abundant rodents:** Biozone C1 is characterized by a reduced number of species. The most abundant rodents are *Yindirtemys deflexus, Yindirtemys gobiensis, Parasminthus parvulus.*

5) **Localisation and lithostratigraphic position** (suppl. 1-3): There is no age control by basalts. In section TGW-A rodents of C1 are positioned immediately above biozone C, in RHN-A immediately below biozone D.
   a) Silt and sand of the Loh Formation: Tavan Ovoony Deng (RHN-A/7-9), Khunug (TGW-A/5).
   b) Highest part of red silt of the Hsanda Gol Formation: Loh (LOH-C/1, LOH-B/3, DEL-B/12).

6) **Remarks:** Rodents of biozone C1 were observed in Loh sediments as well as in Hsanda Gol sediments.

Biozone D: (Fig. 21/1-4)

1) **Integrated rodent list:**
Tsaganomys sp.
Cyclomylus sp.
Prodistylomys sp. = (Ctenodactylidae indet. in: DAXNER-HÖCK et al. 1997)
Distylomys sp.
Democricetodon sp. = (Cricetidae indet. in: DAXNER-HÖCK et al. 1997)
Parasminthus asiae-centralis
Plesiosminthus sp. 3 = (*Plesiosminthus* ? sp. in: DAXNER-HÖCK et al. 1997)
Zapodidae n.g.n.sp.
Heterosminthus sp. 1 = (*Shamosminthus* sp. 3 in: DAXNER-HÖCK et al. 1997)
Eomyidae indet.
Aplodontidae indet.
Tachyoryctoides kokonorensis = *(Tachyoryctoides pachygnathus* in: DAXNER-HÖCK et al. 1997)
Tachyoryctoides indet.1
Petauristidae indet.
Sciuridae indet.

2) **Characteristic species:** *Tachyoryctoides kokonorensis, Plesiosminthus* sp. 3, *Heterosminthus* sp. 1, *Distylomys,* Zapodidae n.g.n.sp., *Democricetodon.*

3) **First/last record:** First record: *Prodistylomys, Distylomys, Heterosminthus, Democricetodon,* Petauristidae, Sciuridae, *Tachyoryctoides kokonorensis.* Last record of almost all rodents of this biozone except Petauristidae, Sciuridae, Eomyidae and *Democricetodon.*

4) **Characterisation/most abundant rodents:** There is a significant change of rodent taxa from biozone C1 to D. The most abundant rodents are *Tachyoryctoides kokonorensis, Plesiosminthus, Heterosminthus, Parasminthus tangingoli* and Zapodidae n.g.n.sp.

5) **Localisation and lithostratigraphic position** (suppl. 1-3): Silt and Sand of the Loh Formation. There is no age control by basalts. Uppermost part of section in Tavan Ovoony Deng (RHN-A/12), Luugar Khudag (LOG-A/1) and Unkheltseg (UNCH-A/3).

Biozone D 1 (including D1/1 and D1/2): (Fig. 21/5-11)

Biozone D1 is characterized by some very small faunas which show no clear relationships among each other. Provisionally, biozone D1 is grouped in subgroup D 1/1 and D 1/2. The first is restricted to the NW, the second to the NE of the investigated area.

1) **Integrated rodent list from D1/1:**
Democricetodon sp. 2
Megacricetodon sp. 1
Heterosminthus cf. *orientalis*

2) **Characteristic species:** No characteristic species known yet.

3) **First record** of *Megacricetodon* and *Heterosminthus* cf. *orientalis.*

4) **Characterisation/most abundant rodents:** Very small fauna.

5) **Localisation and lithostratigraphic position** (suppl. 1-3): Red, silty sand of the Loh Formation. Above basalt II and below basalt III. Luugar Khudag (LOG-A/1), Olon Ovoony Khurem (ODO-A/1-6, ODO-B/1).

1) **Integrated rodent list from D 1/2:**
Saimys ? sp.
Democricetodon cf. *lindsayi*
Democricetodon cf. *tongi*
Megacricetodon cf. *sinensis*

Fig. 21
Rodent fossils from the Loh Formation representing biozones D, D1 and E. The localities are situated within the Valley of Lakes / Central Mongolia. The magnification is approximately 20 times. Coll. Naturhistorisches Museum Wien, Geolog.-Paläontol. Abt.

21/1 *Prodistilomys* sp., M sup.; LOG-A/1; locality Luugar Khudag; biozone D; Oligocene-Miocene transition.
21/2 *Heterosminthus* sp. 1; M 1 l, M 2 r, m 1-3 r; UNCH-A/3; locality Unkheltseg; biozone D; Oligocene-Miocene transition.
21/3 Petauristidae indet.; m 3 l; UNCH-A/3; locality Unkheltseg; biozone D; Oligocene-Miocene transition.
21/4 *Democricetodon* sp.; M 1 r; UNCH-A/3; locality Unkheltseg; biozone D; Oligocene-Miocene transition.
21/5 Sciuridae indet.; M 1/2 r, m 1/2 l; UTO-A/5; locality Ulaan Tolgoi; biozone D1; Early to Middle Miocene.
21/6 *Megacricetodon* cf. *sinensis;* M 1 l; UTO-A/5; locality Ulaan Tolgoi; biozone D1; Early to Middle Miocene.
21/7 *Democricetodon* cf.; M 1 l; UTO-A/5; locality Ulaan Tolgoi; biozone D1; Early to Middle Miocene.
21/8 *Heterosminthus orientalis;* M 1 l; UTO-A/5; locality Ulaan Tolgoi; biozone D1; Early to Middle Miocene.
21/9 Gliridae indet.; M 1/2 r; UTO-A/6; locality Ulaan Tolgoi; biozone D1; Early to Middle Miocene.
21/10 *Leptodontomys* sp.; M 1/2 r; UTO-A/5; locality Ulaan Tolgoi; biozone D1; Early to Middle Miocene.
21/11 *Keramidomys* sp.; D 4 l; UTO-A/5; locality Ulaan Tolgoi; biozone D1; Early to Middle Miocene.
21/12 *Lophocricetus* cf. *gansus;* M 1 l, M 2 r; M 3 l; BUK-A/ 12+14; locality Builstyn Khudag; biozone E; Late Miocene.
21/13 *Megacricetodon* sp.; M 1 l; BUK-A/ 12+14; locality Builstyn Khudag; biozone E; Late Miocene.
21/14 *Paralactaga* sp.; m 1 l, m 2 l; BUK-A/12+14; locality Builstyn Khudag; biozone E; Late Miocene.
21/15 *Allocricetus*? sp.; M 1 l, m 1 l; BUK-A/12+14; locality Builstyn Khudag; biozone E; Late Miocene. →

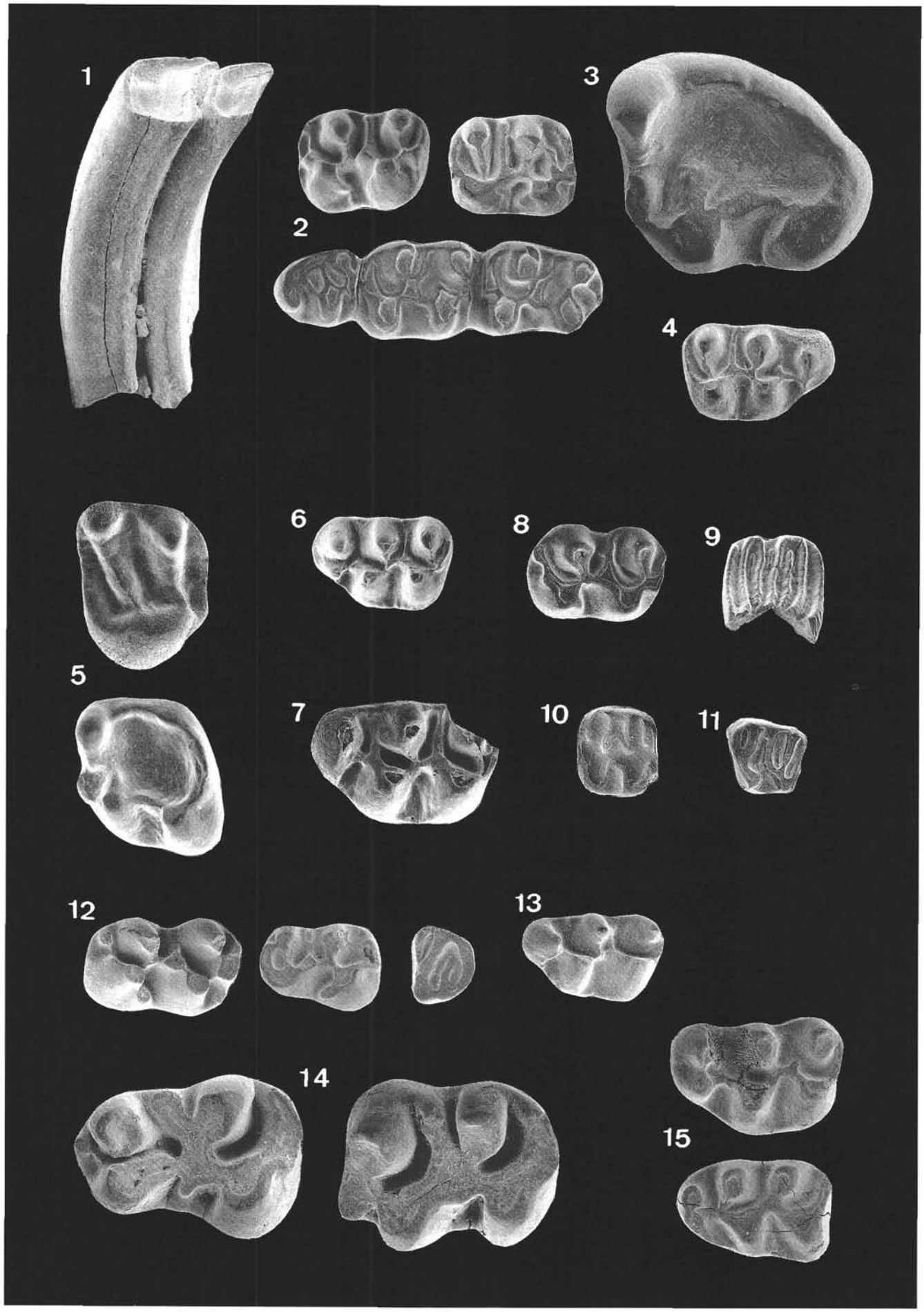

Plesiodipus sp.
Heterosminthus orientalis
Zapodidae indet.
Protalactaga ? sp.
Leptodontomys sp.
Keramidomys sp.
Ansomys ? sp.
Tachyoryctoides sp. 2
Sciuridae indet.
Atlantoxerus ? sp.
Gliridae indet.

2) **Characteristic species:** *Heterosminthus orientalis, Democricetodon* cf. *lindsayi, D.* cf. *tongi, Megacricetodon* cf. *sinensis.*

3) **First/last record:** First record: *Leptodontomys, Keramidomys, Plesiodipus* and others. Last record: all listed species.

4) **Characterisation/most abundant rodents:** There is a significant change in rodent taxa from D to D1. The rodents are associated with *Gomphotherium* and *Anchitherium.*

5) **Localisation and lithostratigraphic position** (suppl. 1-3): White to brownish silt and sand of the Loh Formation. In the NE of the investigated area there is no age control by basalts. Loh (LOH-A/2-8), Ulaan Tolgoi (UTO-A/ 3-6).

Biozone E: (Fig. 21/12-15)

1) **Integrated rodent list:**
Democricetodon sp.
Megacricetodon sp.
Allocricetus ? sp.
Prosiphnaeus sp. = (Rodentia indet. in: DAXNER-HÖCK et al. 1997)
Lophocricetus cf. *gansus*
Paralactaga sp.
Zapodidae indet.
Leptodontomys sp.
Eomyidae indet.
Sciuridae indet.

2) **Characteristic species:** *Lophocricetus* cf. *gansus, Paralactaga, Prosiphnaeus*

3) **First record:** All in 1) listed rodents.

4) **Characterisation/most abundant rodents:** There is a significant change of rodent taxa from biozone D1 to E. The most abundant rodent is *Lophocricetus* cf. *gansus.*

5) **Localisation and lithostratigraphic position** (suppl. 1-3): Red silt of the Loh Formation. There is no age control by basalts. Uppermost part of section BUK-A. Builstyn Khudag (BUK-A/12+14)

9. Biochronology

(Fig. 22, suppl. 3)

Based on earlier paleontological expeditions, fossil descriptions and faunal lists from famous localities within the Valley of Lakes as well as stratigraphic schemes have been published (MELLET 1968, DASHZEVEG 1970, SHEVYREVA 1972, KOWALSKI 1974, BADAMGARAV et al. 1975, DASHZEVEG 1970, RUSSEL & ZHAI 1987, and others). Recently BRYANT & MCKENNA (1995), VISLOBOKOVA (1996, 1997) and DASHZEVEG (1996) presented new ideas on biochronology and correlation based mainly on large mammal and large-sized small mammal fossils collected from the surface. The wide variety of field methods we applied allows to substantially enlarge the present knowledge with new paleontological, sedimentological, geological and geochronological data. The result is a biochronology based on seven biozones (A-E) of clear lithostratigraphic positions within the sediment sequences of the Hsanda Gol and the Loh Formations. The ages of the informal biozones are controlled by $^{40}Ar/^{39}Ar$ dating (see chapter 6 and Fig. 22) of three interlayered basalts (I-III).

For many years paleontologists considered the fossils of the Hsanda Gol Formation to be primarily of Middle and Late Oligocene age and assigned fossils from the Ergilin Dzo formation to the Early Oligocene (YANOVSKAYA et al. 1977, RUSSELL & ZHAI 1987). They based this conclusion on a correlation of the Ergilin Dzo mammals with those of the Chadronian land mammal age, which was at that time thought to be Early Oligocene. Since there is an international agreement on the Eocene/Oligocene boundary around 34 Ma (PREMOLI-SILVA & JENKINS, 1993) and since new $^{40}Ar/^{39}Ar$ datings terminate the Chadronian at about 34 Ma, the Chadronian mammals are now considered to be Late Eocene, as are the correlative mammals of the Ergilin Dzo formation (EMRY et al. 1998). Thus, according to EMRY et al. (1998), the oldest Oligocene mammals from Asia are represented by assemblages from the lower part of the Hsanda Gol Formation from Mongolia. In contrast DASHZEVEG (1996) considers only the lower Ergilin Dzo faunas from Mongolia to be of Late Eocene age, and the higher Ergilin Dzo faunas to be of Early Oligocene age. He correlated faunas of the higher parts of the Ergilin Dzo formation from Mongolia with European mammal faunas of the Early Oligocene (MP 21) based on the occurrences of *Stenoplesictis, Ronzotherium, Entelodon* and *Bothriodon* in both areas (DASHZEVEG 1996; Fig. 8).

To our knowledge after three seasons of fieldwork in the Valley of Lakes, there are no fossiliferous sediments below the Hsanda Gol sediments indicating an Oligocene age, but sediments of the Hsanda Gol Formation and the Loh Formation and the included fossils can be dated as follows (Fig. 22):

- Rodents representing biozone A were recovered from Hsanda Gol sediments below basalt I and are therefore at least of Early Oligocene age (older than 31.5 Ma).
- Rodents of biozone B are very well documented from Hsanda Gol sediments above basalt I and between two lava flows of basalt I. They were not observed in Loh sediments close to or above basalt II, which is restricted to the Loh Formation. Therefore, biozone B is assigned to the Early Oligocene (between 31.5 and 28 Ma).
- Rodents of biozone C are known from both the upper levels of the Hsanda Gol sequences (TGR-C) and sediments of the Loh Formation below (ABO-A) and above (TAR-A) basalt II. Thus, fossils of biozone C immediately below and above basalt II indicate a maximum age around 28 million years, which is early Late Oligocene. Major differences in rodent taxa point to a time gap between B and C, and/or to a significant change of the environment.
- In the Loh sequence of section TGW-A, biozone C is followed by C1. The most abundant rodents of C1 are *Yindirtemys deflexus* and *Yindirtemys gobiensis,* which serve as excellent stratigraphic markers. According to the close spatial relation of biozone C1 above C and below D the former indicates an age of Late Oligocene (younger than 28 Ma). Fossils of C1 are present in both the Hsanda Gol and the Loh Formations.
- Fossils of biozone D were only recovered in silts of the Loh Formation. *Tachyoryctoides kokonorensis* is the most characteristic rodent of this biozone as well as for the Chinese

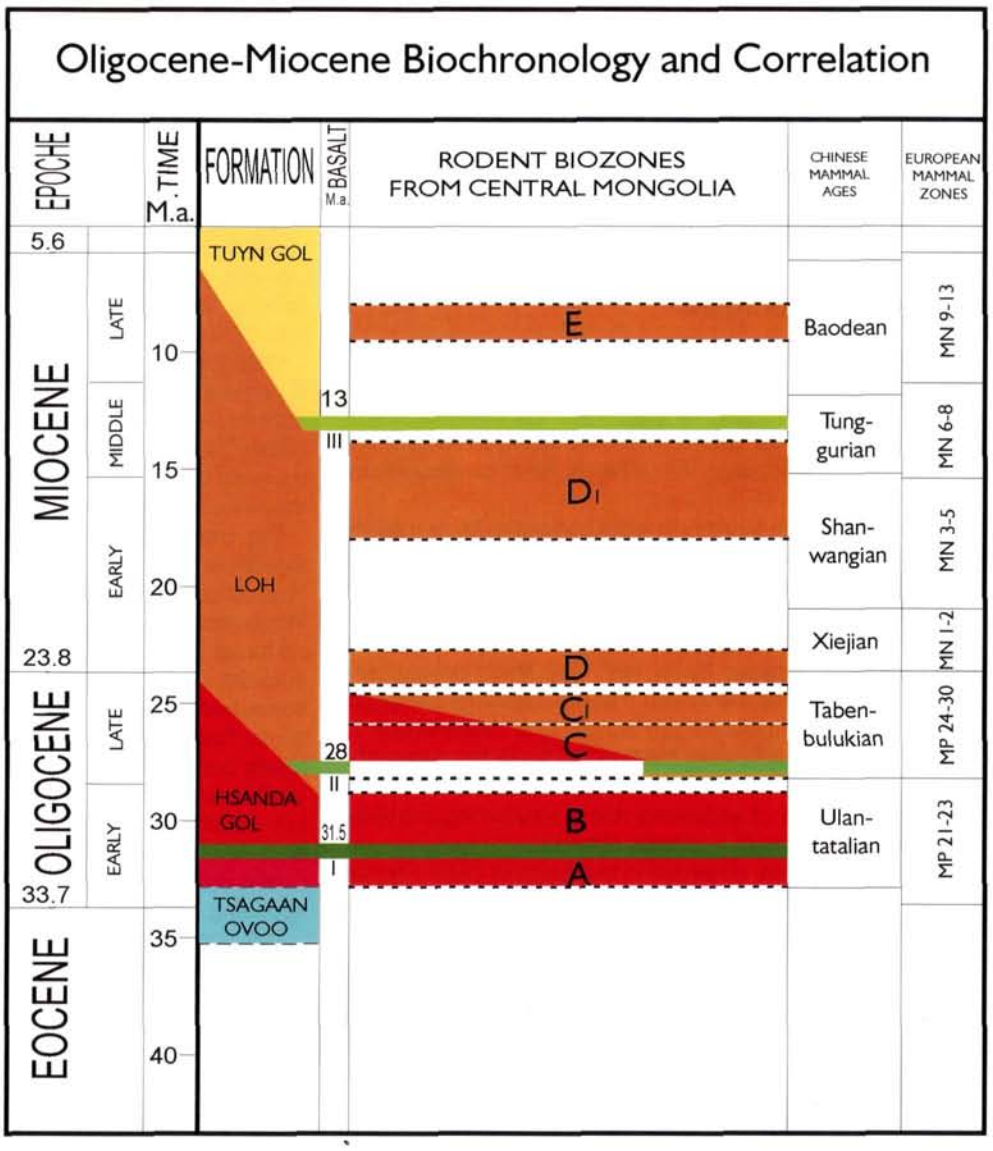

Fig. 22
Oligocene-Miocene biochronology of Central Mongolia based on informal biozones and on basalt datings. Tentative correlation with Chinese and European biochronologies. The boundaries between epochs are drawn according to BERGGEEN et al. (1995). Chinese mammal ages after TONG et al. (1995)

Xiejian (see also Chapter 10), which after LI & QIU (1980) marks the beginning of the Miocene. From our point of view there is no evidence for a marked Oligocene/Miocene boundary.

- Rodents of biozone D1 were collected from Loh sediments, from the area of Loh and Ulaan Tolgoi in the east, and from the northwestern part of the investigated area. The Early to Middle Miocene age is controlled by basalt datings in section LOG-B, where fossils of biozone D1 are sandwiched between basalt II and basalt III. The accompanying large mammals *Gomphotherium* and *Anchitherium* indicate an Early to Middle Miocene age.
- Rodents which characterize biozone E were recovered from the uppermost part of section BUK-A within silts of the Loh Formation. Major differences in fauna indicate a significant change of the environment and/or a long time gap between biozone D1 and E. Biostratigraphic data such as the first occurrences of *Paralactaga, Lophocricetus* cf. *gansus* and *Prosiphnaeus* (QIU 1996) indicate a Late Miocene age.

10. Correlation

In the correlation chart (Fig. 22) boundaries between epoches are drawn according to BERGGREN et al. (1995): Eocene/Oligocene = 33.7 Ma; Early / Late Oligocene = 28.5 Ma; Oligocene / Miocene = 23.8 Ma. We follow here the Chinese mammal ages given by TONG et al. (1995): Ulantatalian, Tabenbulukian for the Oligocene and Xieijan, Shanwangian, Tunggurian and Baodean for the Miocene.

- In Mongolia the Early Oligocene Hsanda Gol faunas from below and above basalt I are characterized by rodents of biozones A and B. They may be correlated with the Chinese vertebrate faunas Wulanbulage (WANG 1997) and Ulantatal (TONG et al. 1995) within the Ulantatalian. In Kasachstan the Buran Svita (EMRY et al. 1998) is thought to be partly Eocene, partly Early Oligocene. It remains to be shown in the future whether the Kasach fauna K 15 from the higher Buran Svita is correlative with biozone A and/or B from Mongolia.
- The biozones C and C1 are to be correlated with the Chinese Tabenbulukian, which includes the faunas from Shargaltein, Taben Buluk and Yikebulak (WANG 1997). There are some similiarities with the Altyn Chokysu fauna from Kasachstan (BENDUKIDZE 1993). The age is Late Oligocene.
- Based on the characteristic rodents *Tachyoryctoides kokonorensis* and *Plesiosminthus* as well as on the first occurrences of Sciuridae indet., the Mongolian biozone D is to be correlated with the Chinese Xiejian, which was thought to be Early Miocene by LI & QIU (1980). As there is no geochronologic evidence, we for the time being assign the Mongolian biozone D to the Oligocene-Miocene transition.
- The Early to Middle Miocene age of biozone D1 is predominantely based on paleontological data *(Gomphotherium, Anchitherium, Keramidomys, Heterosminthus orientalis),* which provide a correlation with the Late Shanwangian or Early Tunggurian Chinese mammal age.
- Rodents of the Mongolian biozone E are of Late Miocene

age. They point to an intermediate position between the Chinese faunas of Amuwusu and Ertemte, which are situated within the Chinese Baodean (QIU & QIU 1990).

Correlations of European and Mongolian vertebrate faunas and mammal zones, already drawn by DASHZEVEG (1996), VISLOBOKOVA (1997), will be evaluated as soon as all the rodents, insectivores and lagomorphs from the investigated area have been studied in detail.

11. Paleoenvironment

Sedimentological, paleontological, geological and tectonic data from three formations – the Tsagaan Ovoo, Hsanda Gol and Loh Formations – provide insight into the development of landscape and life conditions in Central Mongolia during the Paleogene and Neogene. We attempt here to reconstruct paleoenvironments.

The Tsagaan Ovoo sediments were generated by two different kinds of alluvial fan types. The stratigraphically lower parts, predominantly deposited by flash floods, reflect a transition from a "debris flow dominated fan" to a "braided fluvial fan". The finer-grained upper parts show a morphology best described by a "braided fluvial fan". The fining upward sequence within this formation can most probably be assigned to a combination of different processes. One interpretation is a response to the equilibrium the braided fluvial fan eventually reached with the hinterland. Another explanation could be the changing availability of sediments due to weathering processes as a consequence of a climatic change.

The sediment types observed in the Tsagaan Ovoo Formation require an accentuated paleorelief needed for relatively energy-rich ephemeral streams. The N-S direction of the paleocurrents indicates a mountainous landscape in the same area of the recent Khangai Mtns. Towards the end of the Tsagaan Ovoo sedimentation, the paleorelief diminished and gave rise to flat braided fluvial plains. The complete lack of fossils prohibits any inferences of plant and animal associations in the fluvial environment of the Tsagaan Ovoo Formation.

These braided fluvial plains acted as source rocks for the Hsanda Gol sediments. They are interpreted primarily as dust deposits containing reworked fluvial and/or lacustrine sediments. Within the broadly monotonous aeolian transported silts and clays of the Hsanda Gol Formation, only rare sand and gravel lenses occur. Caliche horizons, which were built under arid or semiarid conditions, are impermeable and could have formed shallow pans within the flat area. During occasionally heavy rainfalls they were filled with water and changed to oases supporting animals with food.

In Hsanda Gol sediments the fossil record is very good. The fossil accumulation could be interpreted in two ways or by a combination of both:

1. Episodic droughts and accompanying dust/sand storms forced animals to concentrate at those places, offering the last opportunity to find water and food. The bodies of dead animals were covered by fine dust and thus preserved. A recent example for comparable occurrences would be the most recent drought in Southern Africa in the Okawango delta, which lasted 7 years and culminated in a disaster in 1987 (JERSYKIEWITZ 1998).

2. Heavy rainfalls, which occasionally follow long dry periods in the desert, caused floods, and carcasses of dead animals were covered by mud in temporary shallow lakes.

Fossil plants were not preserved, but plant eaters in high diversity give evidence of the existence of a rich vegetation. Frequently, artiodactyls (*Miomeryx, Lophiomeryx, Gobiomeryx, Eumeryx* and others), rhinos (*Indricotherium* and *Eggysodon*), rodents *(Cricetops, Selenomys, Karakoromys, Tsaganomys* and others), and lagomorphs *(Desmatolagus, Sinolagomys, Procaprolagus)* occur. We assume that the large plant eaters migrated within a huge area of bush and tree savanna to pans and rivers to find protection, water and food supply. All these large and small mammals provided potential prey for carnivores such as *Amphicynodon, Nimravus, Stenogale, Stenoplesictis, Palaeoprinodon* and *Hyaenodon.* These animals are listed in VISLOBOKOVA 1997, RUSSELL and ZHAI 1987, DASHZEVEG 1996 and the present paper, Chapter 9.

Within the Hsanda Gol Formation, a basalt layer (31.5 Ma) is embedded in many areas. The sediments in faunas below and above basalt I are almost identical. This indicates that neither the volcanic eruption nor the basalt flows themselves, covering large parts of the Hsanda Gol beds, disturbed life or the environment considerably (comp. chapters 4 and 5).

The lower boundary of the Loh Formation is defined by a significant coarsening of the sediments compared with the Hsanda Gol Formation. The main part of the Loh sediments is interpreted to be the product of a transition between a "braided fluvial fan" and a "low sinuosity/meandering fluvial fan". In contrast to the upper parts of the Tsagaan Ovoo Formation some features of the Loh Formation point to a more permanently flowing river. For example, well-defined flood plain deposits occur relatively frequently. They show features of paleosoil horizons. Sporadically during the deposition of the total Loh sediment pile, dust sedimentation occurred; its appearance is comparable to the Hsanda Gol sediments, causing confusion in the assignment of these sediments to the corresponding formation.

The Loh sedimentation started earlier in the northernmost parts of the area where the Hsanda Gol Formation is thin or even missing, and progressed with time towards the south. This is evidenced by rodents from biozone C and C1 occurring in the Hsanda Gol Formation in the south and southeast (TGR-C, LOH-C) and in the Loh Formation in the north and west (TAR-A, TGW-A). The gradual change from the Hsanda Gol to the Loh Formation occurs at the transition from Early to Late Oligocene and within the Late Oligocene. The progressive coarsening of sediments associated with the change from aeolian to fluvial sediments requires a reactivation of the paleorelief comparable to that of the Tsagaan Ovoo Formation. Again, paleocurrent directions point from north to south, i. e. from the Khangai Mtns. towards the Valley of Lakes.

The reactivation of the paleorelief is accompanied by faulting processes along the Del fault and in the northwest (Abzag Ovoo) by faults separating the Baidrag crystalline basement from the Loh sediments. These faults cause a dip-slip of the southern block. As discussed in chapter 7, "Tectonics", the timing of the faulting is given by the inclined Hsanda Gol sediments and the horizontally bedded Loh sediments. Age dating on basalts from their eruption centers Barun Hsir and Dzun Hsir indicates a reactivating of volcanic eruptions around 28 Ma. The respective lavas never sealed the Del fault, which indicates that the latter was active at least until the 27-28 Ma eruptions. Further fault activity occurred during the Late Oligocene and the Miocene and was associated with a relief uplift of the crystalline mountains in the north relative to the basin in the south. Similar processes (BERKEY & MORRIS 1927, SCHLUPP 1996) clearly took place in the Gobi Altai and the Valley of Lakes in the south.

The existence of braided fluvial fans with widespread floodplains and ephemeral lakes – as indicated by pillow-like structures at the bottom of basalt flow II (TAR-A) – points towards

higher availability of water at the beginning of the Loh sedimentation. The change in environments could be one reason for the significant faunal change from biozone B to C (chapter 8.2). This is indicated by the first occurrence of *Tachyoryctoides* and by the replacement of the small ctenodactylid *Tataromys minor* by *T. sigmodon* and *T. parvus* in biozone C, and by the large ctenodactylid *Yindirtemys gobiensis* and *Y. deflexus* in biozone C1.

It should be noted that in the Late Oligocene, both the desert and semidesert sediments of the Hsanda Gol Formation coexisted with a "braided fluvial fan" of the Loh Formation within a few kilometres of each other. From the Oligocene to the Miocene the sedimentation of the Loh Formation remained constant, indicating similar environments over 15 to 20 Ma. The variation of the biozone C to E is probably the result of rodent evolution with time.

12. Acknowledgements

The research was supported by the Austrian Science Foundation (FWF), grant Nr. P 10505-GEO and the IGCP project Nr. 326. Our fieldwork was carried out in cooperation with local authorities and people, and a team of Mongolian drivers, cooks, and helpers. O. Fejfar, Th. Bolliger, E. Öttl, M. Haas, H. Zauner, T. Englert were members of the European team in 1995 and/or 1996. For a thorough introduction into the geology of this area we thank E. V. Devyatkin, who also made accessible to us new unpublished age data from the Valley of Lakes (together with E. Dudich). D. Topa carried out the microprobe analyses of the basalts and H. Brinkerink, D. Döppes, K. Huttunen, E. Preis and F. Topka sorted the washing remains. The REM-photos were taken by D. Gruber and the prints were made by A. Schumacher. E. Höck helped with computer graphics. The geochemical analyses were carried out in the laboratories of the Petrological Institute in Vienna. We would like to thank W. Richter, K. Petrakakis and P. Nagl for their continuous help with the analyses of the trace elements. The preparation of fossils was carried out in the laboratory of the Museum of Natural History, Vienna. All these individuals and institutions are gratefully acknowledged. We specially thank W. Richter, N. Schmidt-Kittler, W. Piller and F. F. Steininger for thorough reviews, critical discussions and corrections of the manuscript and M. Stachowitsch for correcting the English.

References

ASTM: U.S.A. Standard Testing Sieve, International Standard ISO 565, table 2. – W. S. Tyler Inc. Mentor, Ohio.

BADAMGARAV, D. 1993: A brief lithologo-genetic characteristics of Eocene-Oligocene and Miocene deposits of the Valley of Lakes and Begger depression. In BARSBOLD, R. and AKHMETIEV, M. A.: International Geological Correlation Programm, Project 326 Oligocene-Miocene Transitions in the Northern Hemisphere, Excursion Guide-Book Mongolia: Oligocene-Miocene Boundary in Mongolia, 36-39.

BADAMGARAV, D., DASHZEVEG, D., DEVYATKIN, E. V., ZHEGALLO, V. I., LISKUN, I. G. 1975: The stratigraphy of the Paleogene and Neogene in the Valley of Lakes (on the question of separations of stratotypical regions of Paleogene and Neogene in Central Asia). The Joint Soviet-Mongolian Paleontological Expedition, Transactions, 2, 250-268 (In Russian).

BALJINNYAM, I., BAYASGALAN, A., BORISOV, B. A., CISTERNAS, A., DEM'YANOVICH, M. G., GANBAATAR, L., KOCHETKOV, V. M., KURUSHIN, R. A., MOLNAR, P., PHILIP, H., VASHCHILOV, Yu.Ya. 1993: Ruptures of Major Earthquakes and Active Deformation in Mongolia and Its Surroundings. Geological Society of America Memoir, 181, 62 p.

BARRY, T. L. and KENT, R. W. 1998: Cenozoic Magmatism in Mongolia and the Origin of Central and East Asian Basalts. – In: FLOWER, M. F. J., CHUNG, S.-L., LO, C.-H., , LEE, T.-Y. (eds.): Mantle Dynamics and Plate Interactions in East Asia. – Geodynamic Series 27, 347-364, AGU.

BATES, R. L. and JACKSON, J. A. (eds.) 1987: Glossary of geology. – 3rd ed. American Geological Institute, Alexandria.

BAYARSAYHAN, C., BAYASGALAN, A., ENHTUVSHIN, B., HUDNUT, K. W., KURUSHIN, R. A., MOLNAR, P. and ÖLZIYBAT, M. 1996: 1957 Gobi-Altay, Mongolia, earthquake as a prototype for southern California's most devastating earthquake. Geology, 24, 579-582.

BENDUKIDZE, O. G. 1993: Miocene Small Mammals of Southwestern Kazakhstan and Turgai. 143 p., Tiblisi, Metsniereba (in Russian).

BERGGREN, W. A., KENT, D. V., SWISHER III, C. C. and AUBRY, M.-P. 1995: A revised Cenozoic geochronology and Chronostratigraphy. In: BERGGREN, W. A., KENT, D. V. and HARDENBOL, J. (ed.): Geochronology, Time Scale, and Global Stratigraphic Correlations: A Unified Temporal Framework for an Historical Geology. Society of Economic Paleontologists and Mineralogists Special Publication, 54, 129-212.

BERKEY, C. P., GRANGER, W. 1923: Later sediments of the desert basin of Central Mongolia. American Museum Novitates, 77, 1-16.

BERKEY, C. P. MORRIS F. K. 1927: Geology of Mongolia. – In: Natural History of Central Asia, 2, American Museum of Natural History, New York, 475 p.

BERKEY, C. P., GRANGER, W., MORRIS, F. K. 1929: Additional new formations in the later sediments of Mongolia. American Museum Novitates, 385, 1-12.

BRYANT, J. D. and MCKENNA, M. 1995: Cranial Anatomy and Phylogenetic Position of Tsaganomys altaicus (Mammalia Rodentia) from the Hsanda Gol Formation (Oligicene), Mongolia. American Museum Novitates, 3156, 1-42.

BURGHELE, A. 1987: Propagation of error and choice of standard in the ^{40}Ar-^{39}Ar technique. – Chem. Geol., 66, 17-19.

DALRYMPLE, G. B., ALEXANDER, E. C., LANPHERE, M. A. & KRAKER, G. P. 1981: Irradiation of samples for ^{40}Ar-^{39}Ar dating using the Geological Survey, TRIGA reactor. – U.S. – Geol. Surv. Prof. Paper, 1176, 55 p.

DASHZEVEG, D. 1970: Stratigraphy and fauna of the Upper Paleogene of Mongolian People's Republic. Bulletin Geological Institute of the Mongolian Academy of Sciences, 1, 45-56. (In Russian).

DASHZEVEG, D. 1996: Some Carnivorous Mammals from the Paleogene of the Eastern Gobi Desert, Mongolia, and the Application of Oligocene Carnivores to Stratigraphic Correlation. American Museum Novitates, 3179, 1-14.

DAXNER-HÖCK, G., HÖCK V., BADAMGARAV, D., FURTMÜLLER, G., FRANK, W., MONTAG, O. & SCHMID H.-P. 1997: Cenozoic Stratigraphy based on a sediment-basalt association in Central Mongolia as Requirement for Correlation across Central Asia. – in: AGUILAR, J.-P., LEGENDRE, S. & MICHAUX, J. (eds.): Biochronologie mammalienne du Cénozoique en Europe et domaines reliés. – Mém. Trav. E.P.H.E., Inst. Montpellier, 21, 163-176.

DEVYATKIN, E. V. 1981: The Cenozoic of Inner Asia. (Stratigraphy, geochronology and correlation). In: NIKIFOROVA (ed.): The Joint Soviet-Mongolian Scientific-Research Geological Expedition, Transactions, 27, 196 p. (in Russian).

DEVYATKIN, E. V. 1993a: An essay on the studies of Oligocene and Miocene deposits of the Prealtai zone of depressions (the Valley of Lakes and Begger Depression). – In: BARSBOLD, R. and AKHMETIEV, M. A.: International Geological Correlation Programm, Project 326 Oligocene-Miocene Transitions in the Northern Hemisphere, Excursion Guide-Book Mongolia: Oligocene-Miocene Boundary in Mongolia, 2-7.

DEVYATKIN, E. V. 1993b: Paleomagnetic and geochronological studies of Paleogene and Miocene deposits of Mongolia. – In: BARSBOLD, R. and AKHMETIEV, M. A.: International Geological Correlation Programm, Project 326 Oligocene-Miocene Transitions in the Northern Hemisphere, Excursion Guide-Book Mongolia: Oligocene-Miocene Boundary in Mongolia, 28-35.

DEVYATKIN, E. V. 1993c: The age and correlation of boundary horizons from the Oligocene-Miocene of Mongolia and adjacent regions of the Inner Asia. – In: BARSBOLD, R. and AKHMETIEV, M. A.: International Geological Correlation Programm, Project 326 Oligocene-Miocene Transitions in the Northern Hemisphere, Excursion Guide-Book Mongolia: Oligocene-Miocene Boundary in Mongolia, 39-53.

DEVYATKIN, E. V. 1994: Magnetostratigraphic Scheme of the Cenozoic in Mongolia. Stratigraphy and Geological Correlation, 2, No. 2, 33-45.

DEVYATKIN, E. V., BADAMGARAV, D. 1993: Geological essay on Paleogene and Neogene deposits of the Valley of Lakes and Prealtai depressions. – In: BARSBOLD, R. and AKHMETIEV, M. A.: International Geological Correlation Programm, Project 326 Oligocene-Miocene Transitions in the Northern Hemisphere, Excursion Guide-Book Mongolia: Oligocene-Miocene Boundary in Mongolia, 7-27.

DEVYATKIN, V., LISKUN, I. G., PEVZNER, M. A., BADAMGARAV, D. 1973: On the Stratigraphy of the Central Mongolia Cenozoic basalts. In: ZAITSEV, N. S. & LUTSHITSY, I. V. (eds.): Volcanic Associations of Mongolian People's Republic, their Composition and the Stratigraphic Position. The Joint Soviet-Mongolian Scientific-Research Geological Expedition, Transaction, 7, 13-46 (in Russian).

EMRY, R. J. , LUCAS, S. G., TYUTKOVA, L., WANG, B. 1998: The Ergilian – Shandgolian (Eocene-Oligocene) transition in the Zaysan Basin, Kazakstan. – In: Beard and Dawson (eds.): Dawn of the Age of Mammals in Asia. – Bulletin of Carnegie Museum of Natural History, 34, 298-312.

EVERNDEN, J. F., SAVAGE, D. E., CURTIS, G. H. and JAMES, G. T. 1964: Potassium-argon dates and the Cenozoic mammalian chronology of North America. American Journal of Sciences, 262, 145-198.

FRASER, G. S. 1989: Clastic Depositional Sequences. Processes of Evolution and Principles of Interpretation. Prentice Hall, Englewood Cliffs, New Jersey 0732, 459 p.

FRIEDMAN, G. M. and SANDERS, J. E. 1978: Principles of Sedimentology. John Wiley & Sons, New York Chichester Brisbane Toronto, 791 p.

GENSHAFT, U. S. and SALTYKOVSKY, A.Y. 1990: The Catalogue of Inclusions of Deep-seated Rocks and Minerals in Mongolian Basalts. – The Joint Soviet-Mongolian Scientific-Research Geological Expedition, Transaction, 46, 71 p (in Russian).

GENSHAFT, U. S., KLIMENKO, G. V., SALTYKOVSKY, A.Y., Agejeva, L. I. 1990: New data on the composition and age of Cenozoic volcanites in Mongolia. Doklady Akademia Nauk, 311 No. 2, 419-424 (in Russian).

GODDARD E. N., TRASK P. D., FORD DE R. K., ROVE O. N., SINGEWALD J. T. JR. & OVERBECK R. M. 1951: Rock-color chart. – Geol. Soc. Am., New York.

GRADZINSKI, R., KAZIERCZAK, J. and LEFELD, J. 1968: Geographical and geological data from the Polish-Mongolian Palaeontological Expeditions. – in: KIELAN-JAWOROWSKA, Z. (ed.): Results of the Polish-Mongolian Palaeontological Expeditions, Pt. I. – Palaeont. Polonica 19, 33-82.

HOFMANN, A. W. 1997: Mantle geochemistry: the message from oceanic volcanism. – Nature, 385, 219-229.

HUNT, C. B. 1972: Geology of Soils – Their Evolution, Classification, and Uses. – Freeman and Company, San Francisco, 344 p.

JERZYKIEWICZ, T. 1998: Okavango Oasis, Kalhari Desert: A Contemporary Analogue of the Late Cretaceous Vertebrate Habitat of the Gobi Basin, Mongolia. Geoscience Canada, 25(1), 15-25.

KEPEZHINSKAS, V. V. 1979: Cenozoic Alkaline Basaltoids of Mongolia and related deep inclusions. The Joint Soviet-Mongolian Scientific-Research Geological Expedition, Transactions, 25, 311 p. (in Russian).

KIELAN-JAWOROWSKA, Z. and DOVCHIN, N. 1968: Narrative of the Polish-Mongolian Palaeontological Expeditions 1963-1965. In: KIELAN-JAWOROWSKA, Z. (ed.): Results of the Polish-Mongolian Palaeontological Expeditions, Pt. I. – Palaeont. Polonica, 19, 7-30.

KOWALSKI, K. 1974: Middle Oligocene Rodents from Mongolia. Palaeontologia Polonica, 30, 147-178.

KRUMBEIN, W. C. 1934: Size frequency distributions of sediments. – J. Sediment. Petrol., 4, 65-77.

KURIMOTO, C., TUNGALAG, F., BAYARMANDAL, L. and ICHINNOROV, N. 1998: K-Ar ages of white micas from pelitic schists of the Bayanhongor area, west Mongolia. Bull. Geol. Soc. Japan, 49(1), 19-23.

KURUSHIN, R. A., BAYASGALAN, A., ÖLZIYBAT, M., ENHTUVISHIN, B., MOLNAR, P., BAYARSAYHAN, Ch., HUDNUTH, K. W., LIN, J. 1997: The Surface Rupture of the 1957 Gobi-Altay, Mongolia, Earthquake. Geol. Soc. Am. Special Paper, 320, 143 p.

LE MAITRE, R. W. 1989: A Classification of Igneous Rocks and Glossary of Terms. Blackwell Scientific Publications, Oxford London Edinburgh Boston Melbourne, 193 p.

LETTNER, H. 1988: NAAHPGE-Computerprogramm zur Verrechnung von Gammaspektrometridaten für die Neutronenaktivierungsanalyse. Unveröff. PC-Programm am Inst. f. Geowiss., Univ. Salzburg.

LI, C. and QIU, Zd. 1980: Early Miocene mammalian fossils of Xining Basin, Quinghai. (in Chinese. – extended English summary). – Vertebrata Palasiatica, 18(3), 198-214.

LISKUN, I. G. and BADAMGARAV, D. 1977: Lithology of the Cenozoic of Mongolia. – The Joint Soviet-Mongolian Scientific-Research Geological Expedition, Transactions, 20, 159 p. (in Russian).

MAIZELS, J. 1989: Sedimentology, paleoflow dynamics and flood history of jökulhlaup deposits: paleohydrology of Holocene sediment sequences in southern Iceland sandur deposits. J. of Sediment. Petrol., 59, 204-223.

MELLET, J. S. 1968: The Oligocene Hsanda Gol Formation, Mongolia: A Revised Faunal List. American Museum Novitates, 2318, 1-16.

MIALL, A. D. 1990: Principles of sedimentary basin analysis. – 2nd ed. Springer, Berlin Heidelberg New York, p. 668.

MIALL, A. D. 1996: The Geology of Fluvial Deposits. Springer Verlag, Berlin Heidelberg New York, 582 p.

NICKLING, W.G. 1994: Aeolian sediment transport and deposition. In: PYE, K. (ed.): Sediment transport and depositional processes. Blackwell, Oxford: 293-350.

NORTON, L. D. 1984: The relationship of present topography to preloess deposition topography in east – central Ohio. Soil Sci. Soc. Am. J., 48, 147-151.

OLLIER, C. and PAIN, C. 1996: Regolith, Soils and Landforms. John Wiley & Sons, Chichester New York Brisbane Toronto Singapore, 316 p.

PEARCE, J. A. and NORRY, M. J. 1979: Petrogenetic implications of Ti, Zr, Y and Nb variations in volcanic rocks. – Contr. Mineral. Petrol. 69, 33-47.

PREMOLI-SILVA, I. & D. C., JENKINS, D. C. 1993: Decision on the Eocene-Oligocene boundary stratotype. – Episodes, 16, 379-382.

PYE, K. 1987: Aeolian Dust and Dust Deposits. Academic Press (London), 334 p.

QIU, Zd. 1996: Middle Miocene Micromammalian Fauna from Tuggur, Nei Mongol. – Beijing (Chinese – extended English summary). – 1-216.

QIU, Zx. and QIU, Zd. 1990: Neogene local mammalian faunas: association and ages. (in Chinese). – Journal of Stratigraphy, 14 (4), 241-26o.

READING, H. G. 1996: Sedimentary Environments: Processes, Facies and Stratigraphy. – 3 ed., Blackwell Science, London Edinburgh Cambridge, 688 p.

RUSSELL, D. E. and ZHAI, R. 1987: The Paleogene of Asia: mammals and stratigraphy. Memoires du Museum National d'Histoire Naturelle, 52, 488 p.

SALVADOR, A. (ed.) 1994: International Stratigraphic Guide: a guide to stratigraphic classification, terminology, and procedure. – 2. ed., International Subcommission on Stratigraphic Classification of IUGS International Commission on Stratigraphy, Boulder, p. 214.

SAMSON, S. D. & ALEXANDER, E. C. 1987: Calibration of the labratory ^{40}Ar-^{39}Ar dating standard, Mmhb-1. – Chemical Geology, 66, 27-34.

SCHLUPP, A. 1996: Neotectonique de la Mongolie Occidentale Analysee a partir de Donnees de Terrain, Sismologiques et Satellitaires. These L'Université Louis Pasteur de Strasbourg, 172 p.

SCHULTZ, L. G. 1964: Quantitative interpretation of mineralogical composition from X-ray and chemical data for the Pierre Shale. – Geological Survey Professional Paper 391-C.

ŞENGÖR, A. M. C., NATAL'IN, B. A. and BURTMAN, V. S. 1993: Altaids, evolution of the Altaid tectonic collage and Palaeozoic crustal growth in Eurasia. Nature, 364, 299-307.

ŞENGÖR, A. M. C. & NATAL'IN, B. A. 1996: Paleotectonics of Asia: fragments of a synthesis. – In: An YIN & Mark HARRISON (eds.): The Tectonic Evolution of Asia, 486-640. Cambridge University Press.

SHEVYREVA, N. S. 1972: New Rodents from the Paleogene of Mongolia and Kasakhstan. Paleontological Journal Moskwa, 6, 399-408 (in Russian).

SINDOWSKI, K.-H. 1957: Die synoptische Methode des Kornkurven-Vergleichs zur Ausdeutung fossiler Sedimentationsräume. Geol. Jb., 73, 235-275.

STANISTREET, I. G. and MCCARTHY, T. S. 1993: The Okavango fan and the classification of subaerial fan systems. Sedimentary Geology, 85, 115-133.

STEEL, R. J., MÆHLE, S., NIELSEN, H., RØE, S. L. and SPINNANGR, Å. 1977: Coarsening-upward cycles in the alluvium of Hornelen Basin (Devonian), Norway: Sedimentary response to tectonic events. – Geo. Soc. Amer. Bull., 88, 1124-1134.

STEININGER, F. F. and PILLER, W. 1999: Empfehlungen (Richtlinien) zur Handhabung der stratigraphischen Nomenklatur. Courier Forschungsinst. Senckenberg, 209, 19 p.

SUESS, E. 1901: Das Antlitz der Erde. Bd. 3 (erste Hälfte), Tempsky, Wien, 508 p.

SUN, S. S. and MCDONOUGH, W. F. 1989: Chemical and isotopic systematics of oceanic basalts: implications for mantle composition and processes. In: SAUNDERS, E. D. & NORRIS, M. J. (eds): Magmatism in the Ocean Basins. Geol. Soc. Spec. Publ., 42, 313-345.

SWINEFORD, A. and FREY, J. C. 1945: A mechanical analysis of wind-blown dust compared with analysis of loess. Am. Jour. Sci., 243, 249-255.

TAKAHASHI, Y., OYUNGEREL, S., NAITO, K. and DELGERTSOGT, B. 1998: The granitoid series in Bayankhongor area, central Mongolia. Bull. Geol. Soc. Japan, 49(1), 25-32.

TERAOKA, Y., SUZUKI, M., TUNGALAG, F., ICHINNOROV, N. and SAKAMAKI, Y. 1996: Tectonic framework of the Bayankhongor area, west Mongolia. Bull. Geol. Soc. Japan, 47(9), 447-455.

TOMURTOGOO, O. 1997: A New Tectonic Scheme of the Paleozoides in Mongolia. In: Xu Zhiqin, Rem Yufeng and Qiu Xiaoping (Eds): Proc. 30th Intern. Geol. Congr. Vol 7, 75-82.

TONG, Y., ZHENG, S. and QIU, Z. 1995: Cenozoic Mammal Ages of China. – Vertebrata Palasiatica, 33, 290-314.

TSOAR, H. and PYE, K. 1987: Dust transport and the question of desert loess formation. Sedimentology, 34, 139-153.

VISHER, G. S. 1969: Grain size distributions and depositional processes. – Journal of Sediment Petrol., 39, nr. 3, 1074-1106, Tulsa, Oklahoma.

VISLOBOKOVA, I. A. 1996: Age of the Shand Gol Fauna and Evolution of Central Asia Mammals in the Oligocene. Stratigraphy and Geological Correlation, 4, 156-165.

VISLOBOKOVA , I. A. 1997: Eocene – Early Miocene Ruminants in Asia. – In: AGUILAR J.-P., LEGENDRE, S. and MICHAUX, J. (eds.): Biochronologie mammalienne du Cénozoique en Europe et domaines reliés. – Mém. Trav. E.P.H.E., Inst. Montpellier, 21, 215-223.

WALKER, G. R. (ed.) 1980: Facies Models. Geoscience Canada Reprint Series 1, Anisworth Press Limited, Kitchener, Ontario.

WANG, B. 1997: The Mid-Tertiary Ctenodactylidae (Rodentia, Mammalia) of Eastern and Central Asia. – Bulletin of the American Museum of Natural History, 234, 1-88.

WHITFORD-STARK, J. L. 1987: A survey of Cenozoic volcanism on mainland Asia. – Geol. Soc. America, Spec. Paper, 213, 74 p.

YANOVSKAYA, N. M., KUROCHKIN, E. N., DEVYATKIN, E. V. 1977: Ergilin Dzo locality – the stratotype of the lower Oligocene in South-East Mongolia. The Joint Soviet-Mongolian Scientific-Research Geological Expedition, Transactions, 4, 14-33. (In Russian).

YARMOLUK, V. V., IVANOV, V. G., SAMOILOV, V. S., ARAKELIANZ, M. M. 1995: Stages of formation of late Mesozoic and Cenozoic intraplate volcanism of South Mongolia. Doklady Akademia Nauk, 344 Nr. 5, 673-676 (in Russian).

ZORIN, Yu. A., BELICHENKO, V. G., TURUTANOV, E. Kh., KOZHEVNIKOV, V. M., RUZHENTSEV, S. V., DERGUNOV, A. B., FILIPPOVA, I. B., TOMURTOGOO, O., ARVISBAATAR, N., BAYASGALAN, Ts., BIAMBAA, Ch., KHOSBAYAR, P. 1993: The South Siberia – Central Mongolia transsect. Tectonophysics, 225, 361-378.

Manuskript eingegangen am: 24. 02. 1999 ●
Revidierte Fassung eingegangen am: 16. 07. 1999 ●
Manuskript akzeptiert am: 30. 07. 1999 ●

Supplement 1

Geological map of the Taatsiin Gol area / Valley of Lakes / MONGOLIA

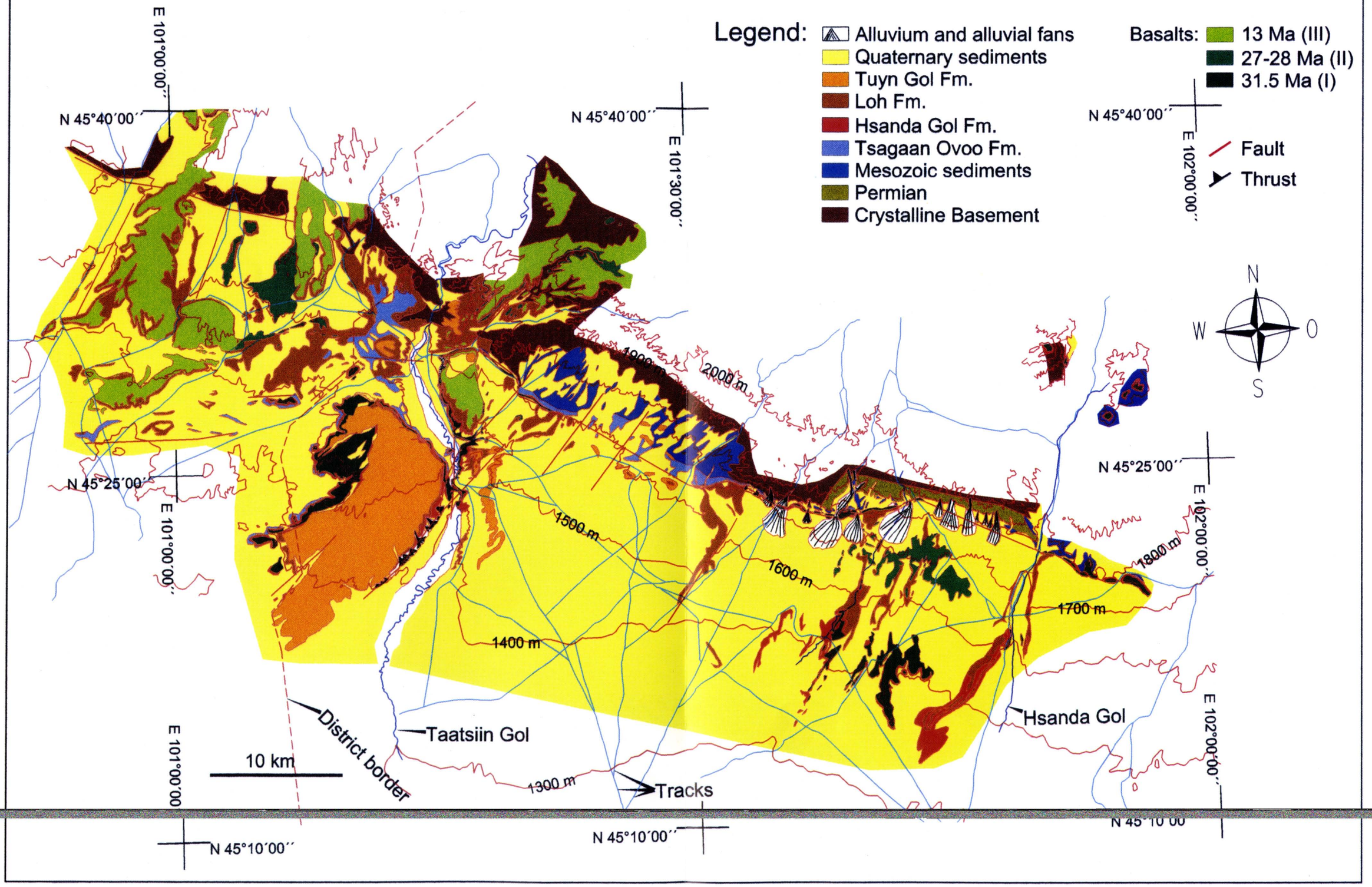

Geological map of the Taatsiin Gol area / Valley of Lakes / MONGOLIA

Position of the profiles and denotation of areas

Legend:
- Alluvium and alluvial fans
- Quaternary sediments
- Tuyn Gol Fm.
- Loh Fm.
- Hsanda Gol Fm.
- Tsagaan Ovoo Fm.
- Mesozoic sediments
- Permian
- Crystalline Basement

Basalts:
- 13 Ma (III)
- 27-28 Ma (II)
- 31.5 Ma (I)

- Fault
- Thrust

E 101°00´00´´
N 45°40´00´´
N 45°40´00´´
E 101°30´00´´
N 45°40´00´´
E 102°00´00´´
N 45°25´00´´
E 101°00´00´´
N 45°25´00´´
E 102°00´00´´
E 101°00´00´´
N 45°10´00´´
N 45°10´00´´
E 102°00´00´´
N 45°10´00´´

Luugar Khudag
Abzag Ovoo
ABO-A
LOG-A
LOG-B
Olon Ovoony Khurem
ODO-B
ODO-A
Tavan Ovoony Deng
Tarimalyn Khurem
TAR-A
RHN-A
DEL-A
UNCH-A
TGR-1564
TGL-A
HL
Khongil
Unkheltseg
Del
DEL-B
Taatsiin Gol left
TGR-A
TGR-B
TGR-AB
TGR-ZO
TGR-C
TGW-A
Khunug
Taatsiin Gol right
BUK-D
BUK-C
BUK-B
BUK-A
Builstyn Khudag
Barun Hsir
Mt. Ushgoeg
Andai Sair
UTO-A
Ulaan Tolgoi
Dzun Hsir
TAT-C
TAT-D
Tatal Gol
Loh
LOH-A
LOH-C
LOH-B
SHG-B
SHG-AB
SHG-A
SHG-C
Hsanda Gol
Hsanda Gol

1500 m
1600 m
1700 m
1400 m
1300 m
2000 m

District border
Taatsiin Gol
Tracks
10 km

N
W
O
S

Supplement 3

Correlation of Oligocene - Miocene continental sediments on base of lithological, geochronological and paleontological data

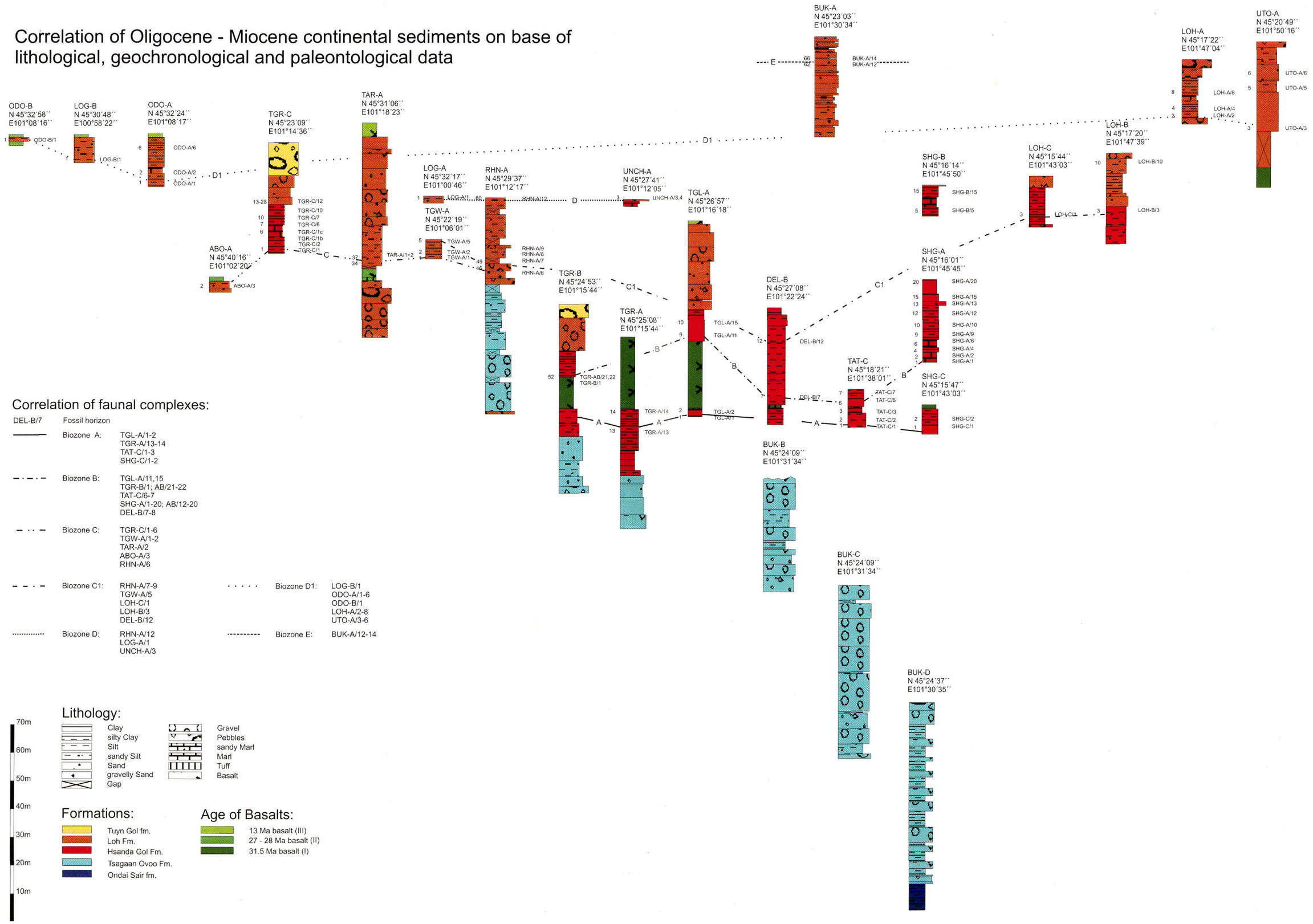

Correlation of faunal complexes:

DEL-B/7 Fossil horizon

———	Biozone A:	TGL-A/1-2 TGR-A/13-14 TAT-C/1-3 SHG-C/1-2
– · – · –	Biozone B:	TGL-A/11,15 TGR-B/1; AB/21-22 TAT-C/6-7 SHG-A/1-20; AB/12-20 DEL-B/7-8
– ·· –	Biozone C:	TGR-C/1-6 TGW-A/1-2 TAR-A/2 ABO-A/3 RHN-A/6
– – · –	Biozone C1:	RHN-A/7-9 TGW-A/5 LOH-C/1 LOH-B/3 DEL-B/12
·····	Biozone D1:	LOG-B/1 ODO-A/1-6 ODO-B/1 LOH-A/2-8 UTO-A/3-6
·····	Biozone D:	RHN-A/12 LOG-A/1 UNCH-A/3
----------	Biozone E:	BUK-A/12-14

70m
60m
50m
40m
30m
20m
10m

Lithology:

- Clay
- silty Clay
- Silt
- sandy Silt
- Sand
- gravelly Sand
- Gap
- Gravel
- Pebbles
- sandy Marl
- Marl
- Tuff
- Basalt

Formations:

- Tuyn Gol fm.
- Loh Fm.
- Hsanda Gol Fm.
- Tsagaan Ovoo Fm.
- Ondai Sair fm.

Age of Basalts:

- 13 Ma basalt (III)
- 27 - 28 Ma basalt (II)
- 31.5 Ma basalt (I)

Supplement 4

Legend

lithology

Clay (Cl)
silty Clay (siCl)
Silt (Si)
sandy Silt (sSi)
Sand (S)
gravelly Sand (grS)
Gravel (Gr)
gravelly boulder (grBd)
Boulder (Bd)
Marl (M)
Tuff
Basalt

symbols for sedimentary structures - abbreviations

structures

rip up clasts (ruc)
ripples (R)
trough cross-bedding (T)
planar cross-bedding (P)
Imbrication (I)
laminated (l)
normal grading (n.G)
inverse grading (inv.G)
sandy lense (sL)
gravelly lense (grL)
root traces (rt)
"manganese incrustations" (Mn)

boundaries

erosive
wavy
not clear

further abbreviations

(B) … taken on the top
(T) … taken at the base
m … massive, structureless

Type section: **TGR-B** GPS: N 45°24′53″ E 101°15′44″ thickness: 64,6 m altitude of base: 1440 m exposed formations: Tsagaan Ovoo, HsandaGol, Loh, Tuyn Gol

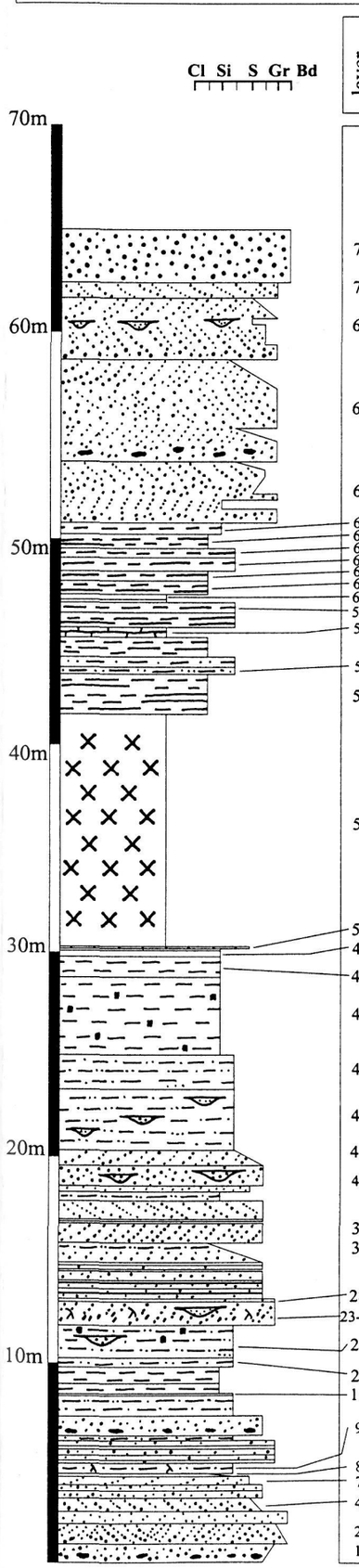

layer	thick-ness (in cm)	lithology colour	sedimentary structures	sedimentolo. sample (gravelsample) **paleontolo. sample**	remarks
				(TGR-B/Tuyn Gol 1)	
71	485	grBd; light brown	m		Tuyn Gol fm.
70	85	sGk; light greenish gray	m; T	(TGR-B/Tuyn Gol 2) 29 (B), 30 (T)	
69	290	sbdGr; dusky yellow	m; I; T; sL	28 (B)	Layer 69 reflects a channel.
68	500	sGr; moderate brown	m; T; ruc; grL	27 (T) (TGR-B/Loh 2)	Layer 68 reflects a channel.
67	300	sGr; light greenish gray	T; P; n.G; inv.G		Layer 67 reflects a channel.
66	55	Si; light olive brown		25	
65	70	siCl		24	
64	45	siCl		23	
63	65	siCl; light olive brown		22	
62	50	siCl	m	21	
61	65	siCl		20	
60	25	M		19	Layer 60 is compacted.
58	50	siCl		18 (B)	
56	20	M; pale reddish brown			
53	50	sSi; pale reddish brown	m		
52	230	siCl; moderate reddish orange	m	17 (T); **TGR-B/1, TGR-AB /21,22**	
51	1130	Basalt I			
50	10	tuff horizon	l	16	
48	30	Si; moderate reddish brown	m	15	Layer 48 is a baked horizon.
47	100	Si; moderate reddish brown	m	14	
46	380	Si; moderate reddish brown	m; Mn	13	
45	170	sSi; pale reddish brown	m	12	
44	300	sSi; dark reddish brown	m; sL; grL	9 (B), 10, 11	
43	75	sisGr; dark reddish brown	T; P; n.G		Layer 37-41: interbedding of sandy/gravelly (T, R) and silty/clayey (m) beds.
42	25	sGr; dark reddish brown	m; grL		
36	95	Gr	T	8	
35	95	sisGr; grayish yellow green	m; n.G	7	
28	25	Gr; yellowish gray	T	(TGR-B/Tsagaan Ovoo XY)	
23-27	170		T; I; sL; rt		Layer 29-34: interbedding of S and Gr (T).
22	160	sSi; light olive brown	m; Mn; grL		
21	45	sSi; pale olive	m	6	
18	10	sSi; light olive brown	m; Mn	5	
9	50	sSi; dark reddish brown	m; n.G; rt	4 (B)	Layer 10-17: interbedding of gravelly and sandy beds (T; n.G; inv.G; rt; ruc; grL).
8	15	siS	m; n.G	3	
7	40	S	T; grL	2 (B)	
4	65	sGr; grayish yellow green	T; n.G		
2	100	sGr; yellowish gray	I; T; n.G.	2: (TGR-B/Tsagaan Ovoo 1)	
1	90		m; ruc; inv.G	1 (B)	

Tuyn Gol fm.
Loh Fm.
Hsanda Gol Fm.
Tsagaan Ovoo Fm.